

POLYSTYRENE / BORON NITRIDE NANOTUBE COMPOSITES:
SYNTHESIS, PROCESSING AND CHARACTERIZATION

A THESIS SUBMITTED TO
THE GRADUATE SCHOOL OF NATURAL AND APPLIED SCIENCES
OF
MIDDLE EAST TECHNICAL UNIVERSITY

BY

ERDEM BALIK

IN PARTIAL FULFILLMENT OF THE REQUIREMENTS
FOR
THE DEGREE OF MASTER OF SCIENCE
IN
CHEMICAL ENGINEERING

JANUARY 2015

Approval of the thesis:

**POLYSTYRENE / BORON NITRIDE NANOTUBE COMPOSITES:
SYNTHESIS, PROCESSING AND CHARACTERIZATION**

submitted by **ERDEM BALIK** in partial fulfillment of the requirements for the degree of **Master of Science in Chemical Engineering Department, Middle East Technical University** by,

Prof. Dr. Gülbin Dural Ünver
Dean, Graduate School of **Natural and Applied Sciences**

Prof. Dr. Halil Kalıpçılar
Head of Department, **Chemical Engineering**

Prof. Dr. Göknur Bayram
Supervisor, **Chemical Engineering Dept., METU**

Assoc. Prof. Dr. Naime Aslı Sezgi
Co-Supervisor, **Chemical Engineering Dept., METU**

Examining Committee Members:

Prof. Dr. Cevdet Kaynak
Metallurgical and Materials Engineering Dept., METU

Prof. Dr. Göknur Bayram
Chemical Engineering Dept., METU

Assoc. Prof. Dr. Naime Aslı Sezgi
Chemical Engineering Dept., METU

Assoc. Prof. Dr. Ayşen Yılmaz
Chemistry Dept., METU

Assist. Prof. Dr. Erhan Bat
Chemical Engineering Dept., METU

Date: 29.01.2015

I hereby declare that all information in this document has been obtained and presented in accordance with academic rules and ethical conduct. I also declare that, as required by these rules and conduct, I have fully cited and referenced all material and results that are not original to this work.

Name, Last name: Erdem Balık

Signature:

ABSTRACT

POLYSTYRENE / BORON NITRIDE NANOTUBE COMPOSITES: SYNTHESIS, PROCESSING AND CHARACTERIZATION

Balık, Erdem

M.S., Department of Chemical Engineering

Supervisor: Prof. Dr. Göknur Bayram

Co-Supervisor: Assoc. Prof. Dr. Naime Aslı Sezgi

January 2015, 177 pages

In recent years, boron nitride nanotubes (BNNTs) have been added to polystyrene (PS) which is a widely used thermoplastic polymer in order to improve its thermal and mechanical properties. Solution mixing and melt blending techniques are commonly used methods to prepare polymer-boron nitride nanotube (BNNT) composites. However, these two composite preparation methods have a common problem about the dispersion of fillers in the polymer matrix.

In this study, PS-BNNT composites were prepared using masterbatch with extrusion method at 0.5, 1, and 3 wt % BNNT loadings in order to disperse the nanotubes in the polymer matrix homogeneously. The composites with 0.5 wt% BNNTs were also obtained from in-situ polymerization and extrusion method, separately. Neat PS and all the composites were characterized in terms of their morphology, mechanical and thermal properties.

PS was synthesized using solution and bulk polymerization techniques. The effect of polymerization time and initiator concentration in bulk polymerization on the

molecular weight of PS was studied in order to find the best synthesis conditions for PS production. The best synthesis conditions were determined as a polymerization reaction time of 3 hrs, an initiator concentration of 0.01 mol/L and a reaction temperature of 95 °C. Fourier Transform Infrared (FTIR), X-ray diffraction (XRD), viscosity average molecular weight (M_v), Melt Flow Index (MFI) and Gel Permeation Chromatography (GPC) characterization methods were used to compare the properties of synthesized PS with commercial PS. The results of all the characterization methods revealed that PS was successfully synthesized and its molecular weight was close to that of commercial PS.

BNNTs used in the polymer composite were successfully synthesized from the reaction of ammonia gas with a powder mixture of elemental boron and iron oxide. The formation of hexagonal boron nitride was proved by XRD analysis.

Results of SEM analyses indicated that the nanotubes were dispersed homogeneously for the composites with 0.5 wt% BNNTs prepared by masterbatch with extrusion method. The tensile and impact strengths of these composites were improved remarkably with respect to neat polymer and the composites prepared using the other methods. The agglomeration of BNNTs in the polymer matrix increased with an increase in BNNT addition.

Differential Scanning Calorimetry analysis showed that the glass transition temperature of the composites prepared by masterbatch with extrusion method was decreased with respect to the synthesized PS. Also, no significant change in terms of glass transition temperature of the composites was observed with the addition of BNNTs. Thermal gravimetric analysis (TGA) of the composites prepared by masterbatch with extrusion method showed that the thermal stability of composites remained unchanged with the addition of BNNTs.

Keywords: Bulk Polymerization, Polystyrene, Boron Nitride Nanotubes, In-situ polymerization, Composite.

ÖZ

POLİSTİREN / BOR NİTRÜR NANOTÜP KOMPOZİTLERİ: SENTEZİ, PROSESİ VE KARAKTERİZASYONU

Balık, Erdem

Yüksek Lisans, Kimya Mühendisliği

Tez Yöneticisi: Prof. Dr. Göknur Bayram

Ortak Tez Yöneticisi: Assoc. Prof. Dr. Naime Aslı Sezgi

Ocak 2015, 177 sayfa

Son yıllarda bor nitrür nanotüpler (BNNTs), mekanik ve termal özellikleri geliştirmek için yaygın olarak kullanılan bir termoplastik polimer olan polistiren'e (PS) eklenmektedir. Çözelti içinde ve eriyik halde karıştırma metotları PS-BNNT kompozitlerinin hazırlanmasında sıkça kullanılmaktadır. Fakat, bu iki hazırlama metodunun ortak problemi, dolgu malzemesinin polimer matriksi içerisinde dağılmasıdır.

Bu çalışmada, PS-BNNT kompozitleri ağırlıkça % 0,5, 1 ve 3 BNNT oranlarındaki nanotüpleri polimer matriksi içerisinde homojen olarak dağıtmak amacıyla, yoğun bileşimli karışım ve sonrasında eriyik halde karıştırma metoduyla hazırlanmıştır. Ayrıca, ağırlıkça % 0,5 BNNT içeren kompozitler yerinde polimerizasyon ve ekstrüzyon metotlarından ayrı ayrı elde edilmiştir. Saf PS'in ve bütün kompozitlerin morfoloji, mekanik ve termal özellikler açısından karakterizasyonu yapılmıştır.

Polistiren çözelti ve yığın polimerizasyon yöntemleri kullanılarak sentezlenmiştir. Polistiren üretiminde en iyi sentez koşullarını bulmak için, yığın polimerizasyon zamanının ve başlatıcı konsantrasyonunun molekül ağırlığı üzerindeki etkisi

çalışılmıştır. En iyi sentez koşulları; 3 saatlik polimerizasyon reaksiyon zamanı, 0,01 mol/L'lik başlatıcı konsantrasyonu ve 95 °C'lik reaksiyon sıcaklığı olarak belirlenmiştir. Fourier Transform Infrared (FTIR), X-ışını kırınım ölçümü (XRD), viskozite ortalama molekül ağırlığı ölçümü (M_v), akış indeksi (MFI) ve büyüklükçe ayırma kromatografisi (GPC) gibi karakterizasyon metotları, sentezlenen PS'nin özelliklerinin ticari PS ile karşılaştırılması için kullanılmıştır. Bütün karakterizasyon yöntemlerinin sonuçları, polistirenin başarılı bir şekilde sentezlendiğini ve molekül ağırlığının ticari PS'nin molekül ağırlığına yakın olduğunu göstermiştir.

Polimer kompozitlerinde kullanılan bor nitrür nanotüpler amonyak gazının bor ve demir oksit toz karışımıyla tepkimeye girmesi sonucunda başarılı bir şekilde sentezlenmiştir. XRD analizi ile hekzagonal bor nitrürün oluştuğu ispatlanmıştır.

SEM analiz sonuçları, yoğun bileşimli karışım (Masterbatch) ve sonrasında eriyik halde karıştırma metodu kullanılarak hazırlanan, ağırlıkça %0,5 BNNT içeren kompozitlerde bor nitrürün homojen bir şekilde dağıldığını ortaya koymuştur. Bu kompozitlerin çekme ve darbe dayanımı saf polimere ve farklı metotlar ile hazırlanan kompozitlere göre ciddi bir artış göstermiştir. Daha yüksek oranda BNNT eklenmesinde, bor nitrürlerin polimer matrisi içerisinde kümelenmeleri artmıştır.

Diferansiyel Taramalı Kalorimetre analizleri, yoğun bileşimli karışım ve sonrasında eriyik halde karıştırma metodu kullanılarak hazırlanan kompozitlerin camsı geçiş sıcaklıklarının sentezlenen PS'e göre azaldığını göstermiştir. Ayrıca, bor nitrür nanotüp oranı arttıkça, kompozitlerin camsı geçiş sıcaklığı değerlerinde önemli bir artış olmadığı gözlemlenmiştir. Yoğun bileşimli karışım ve sonrasında eriyik halde karıştırma metodu kullanılarak hazırlanan PS-BNNT kompozitlerinin termal gravimetrik analizi (TGA), bor nitrür nanotüp oranı arttıkça kompozitlerin ısıl dayanımının sabit kaldığını göstermiştir.

Anahtar Kelimeler: Yığın Polimerizasyon, Polistiren, Bor Nitrür Nanotüpler, Yerde Polimerizasyon, Kompozit.

To my lovely family

ACKNOWLEDGMENTS

I would like to express my gratitude to my supervisor, Prof. Dr. Gökür Bayram, for her guidance, encouragement, understanding and continuous support throughout this thesis. I also present my sincere gratitude to my co-supervisor Assoc. Prof. Dr. Naime Aslı Sezgi for her valuable advice, encouragement and guidance at all levels of my study. I am very grateful to both of her for giving me all possibilities to complete this thesis study.

I would like to thank Selin Noyan for introducing me the boron nitride nanotubes experimental system at the beginning of the study. I would also like to thank Miray Yaşar for valuable help throughout this study. I want to thank my dear lab friends Tülay Bursalı, Elif Yürekli and Saeed Khan for their contributions and friendship throughout this study. I sincerely thank Kerime Güney, Mihrican Açıkgöz and Yavuz Güngör from METU Chemical Engineering Department for sharing their experience throughout this study. I would also like to thank METU Chemical Engineering Department for providing opportunity to complete this thesis.

I want to thank my dear friends, Cemre Aşar, Gülçin Kaltalı, Burçin İkizer, Tuğçe Kırbaş, Fırat Ozanırk, İlhan Ayas for their valuable friendship. I would like to thank Büşra Akınalan for her endless support and encouragement.

Finally, my sincere thanks go to my family, Yasemin, Yaşar and Ecem Balık for their endless love, guidance and patience.

TABLE OF CONTENTS

ABSTRACT	v
ÖZ	vii
ACKNOWLEDGMENTS.....	x
LIST OF TABLES.....	xvi
LIST OF FIGURES	xix
NOMENCLATURE	xxv
CHAPTERS.....	1
1. INTRODUCTION	1
2. BACKGROUND	5
2.1 Composites	5
2.1.1 Classification of Composites	5
2.1.2 Polymer Matrix Composites (PMCs)	6
2.2 Polymer Nanocomposites	6
2.3 Preparation of Polymer-Nanotube Composites	8
2.3.1 Solution Dispersion Method	8
2.3.2 In-Situ Polymerization Method	9
2.3.3 Melt Mixing Method	10
2.4 Properties and Synthesis of Polystyrene.....	11
2.4.1 Properties of Polystyrene	11
2.4.2 Polystyrene Synthesis	12
2.5 Boron Nitride Nanotubes (BNNTs)	15
2.5.1 Properties of Boron Nitride Nanotubes	15
2.5.2 Application of Boron Nitride Nanotubes.....	16
2.5.3 Synthesis Methods of Boron Nitride Nanotubes.....	16
2.5.3.1 Arc Discharge Method	16
2.5.3.2 Laser-Based Method	17
2.5.3.3 Chemical Vapor Deposition	17
2.5.3.4 Other Synthesis Techniques	18
2.6 Polymer Processing Techniques	19

2.6.1 Screw of Extruder	20
2.6.2 Twin Screw Extrusion	21
2.7 Injection Molding	22
2.8 Characterization Methods	23
2.8.1 Fourier Transform Infrared (FTIR) Spectroscopy	23
2.8.2 Measurement of Molecular Weight	24
2.8.2.1 Viscosity Average Molecular Weight (M_v)	24
2.8.2.2 Gel Permeation Chromatography (GPC).....	26
2.8.3 Melt Flow Index (MFI) Measurement	27
2.8.4 X-ray Diffraction (XRD) Analysis	28
2.8.5 Surface Area Measurement	29
2.8.6 Scanning Electron Microscopy (SEM) Analysis	29
2.8.7 Mechanical Characterization	30
2.8.7.1 Tensile Test.....	30
2.8.7.2 Impact Test.....	33
2.8.8 Thermal Characterization	34
2.8.8.1 Differential Scanning Calorimetry (DSC) Analysis.....	34
2.8.8.2 Thermal Gravimetric Analysis (TGA)	35
2.9 Previous Studies	36
2.9.1 Polystyrene Synthesis.....	36
2.9.2 Production of Boron Nitride Nanotubes.....	37
2.9.3 Polymer-Nanotube Composites	39
2.10 Motivation of the Study	44
3. EXPERIMENTAL.....	47
3.1 Materials.....	47
3.1.1 Polystyrene	47
3.1.2 Styrene.....	48
3.1.3 Azobisisobutyronitrile	49
3.2 Polymerization of Styrene	50
3.2.1 Experimental Procedure	50
3.2.1.1 Solution Polymerization	50
3.2.1.2 Bulk Polymerization.....	51

3.2.1.3 Polystyrene Synthesis Parameters	52
3.2.1.3.1 Optimization of Synthesis Parameters for Solution Polymerization	52
3.2.1.3.2 Optimization of Synthesis Parameters for Bulk Polymerization	52
3.3 Production of BNNTs.....	53
3.3.1 Experimental Set-Up	53
3.3.2 Experimental Procedure.....	54
3.3.3 Purification of BNNTs.....	55
3.4 Preparation of PS-BNNT Nanocomposites	56
3.4.1 Melt Blending Method.....	57
3.4.2 In-Situ Polymerization Method.....	58
3.4.3 Masterbatch with Extrusion Method	58
3.5 Sample Preparation for Characterization.....	60
3.5.1 Injection Molding	60
3.6 Characterization Studies	61
3.6.1. Characterization of Polymerization of Styrene	61
3.6.1.1 Fourier Transform Infrared (FTIR) Spectroscopy	62
3.6.1.2 Measurement of Molecular Weight	62
3.6.1.2.1 Viscosity Average Molecular Weight (M_v).....	62
3.6.1.2.2 Gel Permeation Chromatography (GPC)	62
3.6.1.3 Melt Flow Index (MFI) Measurement	63
3.6.2 Characterization of Purified BNNTs	63
3.6.2.1 X- Ray Diffraction (XRD)	63
3.6.2.2 Surface Area Measurement	63
3.6.2.3 Scanning Electron Microscopy (SEM)	64
3.6.3 Characterization of PS-BNNT Composites	64
3.6.3.1 Morphological Analysis	64
3.6.3.1.1 Scanning Electron Microscopy (SEM)	64
3.6.3.2 Mechanical Analysis	64
3.6.3.2.1 Tensile Test.....	64
3.6.3.2.2 Impact Test	65
3.6.3.3 Thermal Analysis.....	66

3.6.3.3.1 Differential Scanning Calorimetry (DSC)	66
3.6.3.3.2 Thermal Gravimetric Analysis (TGA).....	67
4. RESULTS AND DISCUSSION	69
4.1 Polystyrene Synthesis and Characterization	70
4.1.1 Effect of Synthesis Parameters in Solution Polymerization Technique on Molecular Weight of PS.....	70
4.1.2 Effect of Synthesis Parameters in Bulk Polymerization Technique on Molecular Weight of PS.....	72
4.1.2.1 Effect of Polymerization Reaction Time on Molecular Weight of PS	72
4.1.2.2 Effect of Initiator Concentration on Molecular Weight of PS	74
4.1.3 Characterization of Synthesized PS	77
4.1.3.1 Fourier Transform Infrared (FTIR) Analysis.....	77
4.1.3.2 X-Ray Diffraction (XRD) Analysis	78
4.2 Synthesis, Purification and Characterization of BNNTs	79
4.2.1 X-Ray Diffraction (XRD) Analysis	80
4.2.2 Surface Area Measurement	81
4.2.3 Scanning Electron Microscopy (SEM) Analysis	83
4.3 Preparation and Characterization of PS-BNNTs Composites.....	85
4.3.1 Scanning Electron Microscopy (SEM) Analysis	85
4.3.2 Mechanical Analysis	94
4.3.2.1 Tensile Test.....	94
4.3.2.2 Impact Test.....	104
4.3.3 Thermal Analysis	107
4.3.3.1 Differential Scanning Calorimetry (DSC)	107
4.3.3.2 Thermal Gravimetric Analysis (TGA)	109
5. CONCLUSIONS	113
REFERENCES.....	115
APPENDICES.....	127
A. CALCULATION OF VISCOSITY AVERAGE MOLECULAR WEIGHT OF POLYMER SYNTHESIZED USING SOLUTION POLYMERIZATION TECHNIQUE.....	127

B. CALCULATION OF VISCOSITY AVERAGE MOLECULAR WEIGHT OF POLYMER SYNTHESIZED USING BULK POLYMERIZATION TECHNIQUES	141
C. MOLECULAR WEIGHT DISTRIBUTION CURVES.....	155
D. FTIR SPECTRA AND XRD RESULTS	159
E. TENSILE AND IMPACT TEST RESULTS.....	165
F. REPRESENTATIVE STRESS-STRAIN CURVES	167
G. DIFFERENTIAL SCANNING CALORIMETRY RESULTS	173

LIST OF TABLES

TABLES

Table 3.1 Properties of polystyrene (Styrolution PS 116 N/L)	47
Table 3.2 Properties of styrene	49
Table 3.3 Properties of AIBN.....	49
Table 3.4 Tested parameters in polystyrene synthesis for solution polymerization ..	52
Table 3.5 Tested parameters in polystyrene synthesis for bulk polymerization	53
Table 3.6 Composition of all composites and their synthesis parameters	60
Table 3.7 Dimensions of the tensile test specimen.....	65
Table 4.1 Viscosity average molecular weight of SOL-sPS with respect to polymerization reaction time at a polymerization reaction temperature of 95 °C and initiator concentration of 0.03 mol/L.....	71
Table 4.2 The best synthesis conditions for PS production via solution polymerization.....	71
Table 4.3 Viscosity average molecular weight and MFI test results of both cPS and BULK-sPS synthesized using an initiator concentration of 0.03 mol/L at a reaction temperature of 95 °C and at different reaction times.....	73
Table 4.4 Viscosity average molecular weight and MFI test results of both cPS and BULK-sPS synthesized at different initiator concentrations at constant reaction temperature of 95 °C and time of 3 hrs.....	75
Table 4.5 GPC results of both cPS and BULK-sPS synthesized at different initiator concentrations and at constant polymerization reaction temperature of 95 °C and time of 3 hrs.	76
Table 4.6 The best synthesis conditions for PS production via bulk polymerization.	77
Table 4.7 Synthesis conditions for BNNT synthesis.	80
Table 4.8 Tensile properties of cPS, BULK-sPS, and E-cPS.	95
Table 4.9 DSC results of pure PS and the PS-BNNT composites.....	109
Table A.1 Flow times of SOL-sPS synthesized at 1.5 hrs polymerization reaction time in the presence of solvent.....	127

Table A.2 Flow times of SOL-sPS synthesized at 3 hrs polymerization reaction time in the presence of solvent.	128
Table A.3 Flow times of SOL-sPS synthesized at 6 hrs polymerization reaction time in the presence of solvent.	128
Table A.4 Flow times of SOL-sPS synthesized at 9 hrs polymerization reaction time in the presence of solvent.	129
Table A.5 Flow times of PS synthesized at 3 hrs polymerization reaction time in the absence of solvent.	129
Table A.6 Calculated viscosities of SOL-sPS synthesized at 1.5 hrs polymerization reaction time in the presence of solvent.	131
Table A.7 Calculated viscosities of SOL-sPS synthesized at 3 hrs polymerization reaction time in the presence of solvent.	132
Table A.8 Calculated viscosities of SOL-sPS synthesized at 6 hrs polymerization reaction time in the presence of solvent.	133
Table A.9 Calculated viscosities of SOL-sPS synthesized at 9 hrs polymerization reaction time in the presence of solvent.	134
Table A.10 Calculated viscosities of PS synthesized at 3 hrs polymerization reaction time in the absence of solvent.	135
Table B.1 Flow times of BULK-sPS synthesized at a polymerization reaction time of 1.5 hrs.	141
Table B.2 Flow times of BULK-sPS synthesized at a polymerization reaction time of 3 hrs.	142
Table B.3 Flow times of BULK-sPS synthesized at a polymerization reaction time of 6 hrs.	142
Table B.4 Flow times of cPS.	143
Table B.5 Calculated viscosities of BULK-sPS synthesized at a polymerization reaction time of 1.5 hrs.	144
Table B.6 Calculated viscosities of BULK-sPS synthesized at a polymerization reaction time of 3 hrs.	144
Table B.7 Calculated viscosities of BULK-sPS synthesized at a polymerization reaction time of 6 hrs.	145
Table B.8 Calculated viscosities of cPS.	145

Table E.1 Tensile test results of neat PS and PS-BNNT composites..... 165
Table E.2 Impact strength values of neat PS and PS-BNNT composites..... 166

LIST OF FIGURES

FIGURES

Figure 2.1 Preparation of polymer-nanotube composites using solution dispersion method.....	9
Figure 2.2 Preparation of polymer-nanotube composites by means of in-situ polymerization method.	10
Figure 2.3 Preparation of polymer-nanotube composites with the help of melt mixing method.....	11
Figure 2.4 Molecular model of a single-wall boron nitride nanotube	15
Figure 2.5 CVD method for production of BNNTs	18
Figure 2.6 Schematic illustration of the extrusion process	19
Figure 2.7 A schematic representation of single screw extruder	20
Figure 2.8 Major parts of extruder screw	20
Figure 2.9 Different types of twin-screw extruders	21
Figure 2.10 Motion of twin-screw extruders	22
Figure 2.11 Stages of injection molding process.....	23
Figure 2.12 Typical plots of inherent and reduced viscosities with respect to concentration to find intrinsic viscosity	25
Figure 2.13 Schematic of MFI apparatus	27
Figure 2.14 Diffraction of X-ray beam by planes of atoms	28
Figure 2.15 Tensile test apparatus and tensile test specimen	31
Figure 2.16 Typical stress-strain curves	32
Figure 2.17 Different forms of stress-strain plots	33
Figure 2.18 Charpy impact test	34
Figure 2.19 Typical DSC plot	35
Figure 3.1 Chemical structure of polystyrene	48
Figure 3.2 Chemical structure of styrene	48
Figure 3.3 Chemical structure of AIBN	49
Figure 3.4 Schematic view of solution polymerization.	50
Figure 3.5 Schematic representation of bulk polymerization experimental set-up. ..	51

Figure 3.6 BNNT production system	54
Figure 3.7 Purification of BNNTs.	56
Figure 3.8 Thermoprism TSE 16 TC twin screw extruder.	57
Figure 3.9 DSM Xplore injection molding.	61
Figure 3.10 Tensile Test Specimen.	65
Figure 3.11 Ceast Resil Impactor.	66
Figure 4.1 FTIR spectra of polystyrene synthesized at the optimum conditions using solution and bulk polymerization methods.	78
Figure 4.2 XRD patterns of polystyrene synthesized at optimum conditions using solution and bulk polymerization methods.	79
Figure 4.3 XRD pattern of the purified BNNTs.	81
Figure 4.4 Adsorption/desorption isotherms of purified BNNTs.	82
Figure 4.5 Desorption pore size distribution of purified BNNTs.	83
Figure 4.6 SEM images of the purified BNNTs (a) 10,000x magnification, (b) 20,000x magnification, (c) 50,000x magnification, (d) 100,000x magnification, and (e) another view of the sample at 50,000x magnification.	84
Figure 4.7 SEM images of the BULK-sPS under the best synthesis conditions (a) 1,000x magnification, and (b) 10,000x magnification.	86
Figure 4.8 SEM images of the cPS (a) 1,000x magnification, and (b) 10,000x magnification.	86
Figure 4.9 SEM images of neat PS prepared by masterbatch with extrusion method (a) 1,000x magnification, and (b) 10,000x magnification.	87
Figure 4.10 SEM images of PS-BNNT composites prepared by masterbatch with extrusion method at 0.5 wt% BNNTs (a) 1,000x magnification, (b) 10,000x magnification, (c) 20,000x magnification, and (d) 50,000x magnification.	88
Figure 4.11 SEM images of PS-BNNT composites prepared by masterbatch with extrusion method at 1.0 wt% BNNTs (a) 1,000x magnification, (b) 10,000x magnification, (c) 20,000x magnification, and (d) 50,000x magnification.	89
Figure 4.12 SEM images of PS-BNNT composites prepared by masterbatch with extrusion method at 3.0 wt% BNNTs (a) 1,000x magnification, (b) 10,000x magnification, (c) 20,000x magnification, and (d) 50,000x magnification.	90

Figure 4.13 SEM images of PS-BNNT composites prepared by in-situ polymerization method at 0.5 wt% BNNT (a) 10,000x magnification, (b) 20,000x magnification, (c) 50,000x magnification, and (d) 100,000x magnification.	92
Figure 4.14 SEM images of PS-BNNT composites prepared by extrusion method at 0.5 wt% BNNT (a) 1,000x magnification, (b) 10,000x magnification, (c) 20,000x magnification, and (d) 50,000x magnification.	93
Figure 4.15 Tensile strengths of PS samples. (cPS: commercial PS, BULK-sPS: synthesized via bulk polymerization, E-cPS: extruded commercial PS).	95
Figure 4.16 Young's moduli of PS samples. (cPS: commercial PS, BULK-sPS: synthesized via bulk polymerization, E-cPS: extruded commercial PS).	96
Figure 4.17 Elongation at break of PS samples. (cPS: commercial PS, BULK-sPS: synthesized via bulk polymerization, E-cPS: extruded commercial PS).	96
Figure 4.18 Tensile strengths of neat PS and PS-BNNT composites containing 0.5, 1 and 3 wt% BNNTs. (BULK-sPS: synthesis via bulk polymerization, E-cPS: Extrusion, ME-PS: Masterbatch with extrusion).....	98
Figure 4.19 Young's moduli of PS and PS-BNNT composites containing 0.5, 1 and 3 wt% BNNTs. (BULK-sPS: synthesis via bulk polymerization, E-cPS: Extrusion, ME-PS: Masterbatch with extrusion).....	99
Figure 4.20 Elongation at break of PS and PS-BNNT composites containing 0.5, 1 and 3 wt% BNNTs. (BULK-sPS: synthesis via bulk polymerization, E-cPS: Extrusion, ME-PS: Masterbatch with extrusion).....	100
Figure 4.21 Tensile strengths of PS-BNNT composites prepared by three different methods at 0.5 wt% BNNTs loading. (ME-PS+0.5: composite prepared by masterbatch with extrusion method, ISP-PS+0.5: composite prepared by in-situ polymerization, E-cPS+0.5: composite prepared by extrusion).	102
Figure 4.22 Young's moduli of PS-BNNT composites prepared by three different methods at 0.5 wt% BNNTs loading. (ME-PS+0.5: composite prepared by masterbatch with extrusion method, ISP-PS+0.5: composite prepared by in-situ polymerization, E-cPS+0.5: composite prepared by extrusion).	103
Figure 4.23 Elongation at break of PS-BNNT composites prepared by three different methods at 0.5 wt% BNNTs loading. (ME-PS+0.5: composite prepared by	

masterbatch with extrusion method, ISP-PS+0.5: composite prepared by in-situ polymerization, E-cPS+0.5: composite prepared by extrusion).	104
Figure 4.24 Impact strengths of PS samples. (cPS: commercial PS, BULK-sPS: Synthesis via bulk polymerization, E-cPS: extruded commercial PS).....	105
Figure 4.25 Impact strengths of PS-BNNT composites prepared by masterbatch with extrusion method. (BULK-sPS: synthesis via bulk polymerization, E-cPS: Extrusion, ME-PS: Masterbatch with extrusion).	106
Figure 4.26 Impact strengths of PS-BNNT composites prepared by three different methods at 0.5 wt% BNNTs loading. (ME-PS+0.5: composite prepared by masterbatch with extrusion method, ISP-PS+0.5: composite prepared by in-situ polymerization, E-cPS+0.5: composite prepared by extrusion).	107
Figure 4.27 TGA plots of PS samples. (cPS: commercial PS, BULK-sPS: Synthesis via bulk polymerization, E-cPS: extruded commercial PS, ME-PS: neat PS prepared through masterbatch with extrusion method).....	110
Figure 4.28 TGA plots of the composites prepared by masterbatch with extrusion method at different BNNTs loading. (ME-PS: composite prepared by masterbatch with extrusion method).	111
Figure 4.29 TGA plots of the composites prepared by three different methods at 0.5 wt% BNNTs. (ME-PS+0.5: composite prepared by masterbatch with extrusion method, ISP-PS+0.5: composite prepared by in-situ polymerization, E-cPS+0.5: composite prepared by extrusion).	112
Figure A.1 Variation of reduced and inherent viscosities of SOL-sPS synthesized at 1.5 hrs polymerization reaction time in the presence of solvent with respect to concentration.	136
Figure A.2 Variation of reduced and inherent viscosities of SOL-sPS synthesized at 3 hrs polymerization reaction time in the presence of solvent with respect to concentration.	137
Figure A.3 Variation of reduced and inherent viscosities of SOL-sPS synthesized at 6 hrs polymerization reaction time in the presence of solvent with respect to concentration.	137

Figure A.4 Variation of reduced and inherent viscosities of SOL-sPS synthesized at 9 hrs polymerization reaction time in the presence of solvent with respect to concentration.	138
Figure A.5 Variation of PS synthesized at 3 hrs polymerization reaction time in the absence of solvent with respect to concentration.	138
Figure B.1 Variation of reduced and inherent viscosities of BULK-sPS synthesized at a reaction time of 1.5 hrs with respect to concentration.	146
Figure B.2 Variation of reduced and inherent viscosities of BULK-sPS synthesized at a reaction time of 3 hrs with respect to concentration.	146
Figure B.3 Variation of reduced and inherent viscosities of BULK-sPS synthesized at reaction time of 6 hrs with respect to concentration.	147
Figure B.4 Variation of cPS with respect to concentration.	147
Figure B.5 Variation of reduced and inherent viscosities of BULK-sPS synthesized using 0.03 mol/L initiator concentration with respect to concentration.	152
Figure B.6 Variation of reduced and inherent viscosities of BULK-sPS synthesized using 0.02 mol/L initiator concentration with respect to concentration.	152
Figure B.7 Variation of reduced and inherent viscosities of BULK-sPS synthesized using 0.01 mol/L initiator concentration with respect to concentration.	153
Figure C.1 Molecular weight distribution of BULK-sPS synthesized using an initiator concentration of 0.03 mol/L.	155
Figure C.2 Molecular weight distribution of BULK-sPS synthesized using an initiator concentration of 0.02 mol/L.	156
Figure C.3 Molecular weight distribution of BULK-sPS synthesized using an initiator concentration of 0.01 mol/L.	157
Figure C.4 Molecular weight distribution of cPS.	158
Figure D.1 FTIR spectra of SOL-sPS synthesized at different polymerization reaction times and temperature of 95 °C.	159
Figure D.2 FTIR spectra of SOL-sPS synthesized with and without solvent at 3 hrs polymerization reaction time and temperature of 95 °C.	160
Figure D.3 FTIR spectra of BULK-sPS synthesized at different polymerization reaction times.	160

Figure D.4 FTIR spectra of BULK-sPS synthesized at different initiator (AIBN) concentrations.	161
Figure D.5 FTIR spectrum of styrene monomer.	161
Figure D.6 XRD patterns of SOL-sPS synthesized at different polymerization reaction time and at temperature of 95 °C.	162
Figure D.7 XRD patterns of SOL-sPS synthesized with and without solvent at 3 hrs polymerization reaction time and at temperature of 95 °C.	162
Figure D.8 XRD patterns of BULK-sPS synthesized at different polymerization reaction times.	163
Figure D.9 XRD patterns of BULK-sPS synthesized at different initiator (AIBN) concentrations.	164
Figure F.1 Representative stress-strain curve for cPS.	167
Figure F.2 Representative stress-strain curve for BULK-sPS.	168
Figure F.3 Representative stress-strain curve for E-cPS.	168
Figure F.4 Representative stress-strain curve for ME-PS.	169
Figure F.5 Representative stress-strain curve for ME-PS+0.5.	169
Figure F.6 Representative stress-strain curve for ME-PS+1.0.	170
Figure F.7 Representative stress-strain curve for ME-PS+3.0.	170
Figure F.8 Representative stress-strain curve for ISP-PS+0.5.	171
Figure F.9 Representative stress-strain curve for E-cPS+0.5.	171
Figure G.1 DSC thermogram of cPS.	173
Figure G.2 DSC thermogram of BULK-sPS.	174
Figure G.3 DSC thermogram of E-cPS.	174
Figure G.4 DSC thermogram of ME-PS.	175
Figure G.5 DSC thermogram of ME-PS+0.5.	175
Figure G.6 DSC thermogram of ME-PS+1.0.	176
Figure G.7 DSC thermogram of ME-PS+3.0.	176
Figure G.8 DSC thermogram of ISP-PS+0.5.	177
Figure G.9 DSC thermogram of E-cPS+0.5.	177

NOMENCLATURE

A_0	Cross-sectional area of tensile specimen, mm ²
D	Distance between grips of tensile specimen, mm
E	Modulus of elasticity, MPa
F	Force, N
K'	Constant of Huggins' equation
K''	Constant of Kramer's equation
L	Overall length of tensile specimen, mm
L_0	Initial gauge length of tensile specimen, mm
L_i	Gauge length of tensile specimen, mm
M_n	Number average molecular weight
M_p	Molecular weight at peak maximum
M_v	Viscosity average molecular weight
M_w	Weight average molecular weight
M_z	Z-average molecular weight
T	Thickness of tensile specimen, mm
T_c	Crystallization temperature, °C
T_g	Glass transition temperature, °C
t_{mix}	Mixing time, hrs
t_{rxn}	Polymerization reaction time, hrs
T_{rxn}	Polymerization reaction temperature, °C
V_{styrene}	Volume of styrene, mL
W_{AIBN}	Amount of AIBN, g

W Width of narrow portion of tensile specimen, mm

Greek Letters

ε Engineering Strain
 θ Scattering angle, °
 η Intrinsic viscosity, dl/g
 η_{red} Reduced viscosity, dl/g
 η_{inh} Inherent viscosity, dl/g
 η_r Relative viscosity
 η_{sp} Specific viscosity
 λ Wavelength, nm
 σ Engineering stress, MPa

Abbreviations

AIBN Azobis Isobutyronitrile
ASTM American Society for Testing and Materials
BET Brunauer, Emmett and Teller
BNNTs Boron Nitride Nanotubes
BULK-sPS Synthesized PS via Bulk Polymerization
cPS Commercial PS
CNTs Carbon Nanotubes
CMCs Ceramic Matrix Composites
CTE Coefficient of Thermal Expansion
CVD Chemical Vapor Deposition
DIN Deutsches Institut für Normung
DSC Differential Scanning Calorimetry

DTA	Differential Thermal Analysis
E	Extrusion
ELSD	Evaporative Light Scattering Detector
FTIR	Fourier Transform Infrared
GPC	Gel Permeation Chromatography
HIPS	High Impact PS
IEC	International Electrotechnical Commission
ISP-PS	In-Situ Polymerization
ISO	International Organization for Standardization
ME	Masterbatch with Extrusion
MFI	Melt Flow Index
MWD	Molecular Weight Distribution
MWNTs	Multi-walled Carbon Nanotubes
OPV	Organic Photovoltaic
PANI	Polyaniline
PDI	Polydispersity Index
PE	Polyethylene
PEVA	Poly(ethylene vinyl alcohol)
PMCs	Polymer Matrix Composites
PMMA	Poly(methylmethacrylate)
PP	Polypropylene
PS	Polystyrene
PU	Polyurethane
PVB	Poly(vinylbutyral)
PVF	Polyvinyl Formal
SEC	Size Exclusion Chromatograph

SEM	Scanning Electron Microscopy
SOL-sPS	Synthesized PS via Solution Polymerization
SWNTs	Single Walled Carbon Nanotubes
TEM	Transmission Electron Microscope
THF	Tetrahydrofuran
TGA	Thermal Gravimetric Analysis
XRD	X-Ray Diffraction

CHAPTER 1

INTRODUCTION

A composite material is the combination of two or more materials to obtain a new material with unique properties. The history of composites dates back to 1940's to solve technological problems for a long time. However, in the 1960's the attention has been turned into polymeric based composites for various applications such as automotive components, consumer goods and aerospace parts [1].

The composites can be divided into three categories such as metals, ceramic and polymer. Today polymer based composites are widely preferred due to extensive properties offered by polymeric materials. Polymers are commonly used as a main matrix because of light weight, easy production and often ductile nature. On the other hand, polymers have lower modulus and strength relative to metals and ceramics. In order to improve their mechanical, thermal or electrical properties, polymeric materials have been filled with reinforcements which are in the form of fibers, whiskers or platelets [2].

Nanotechnology is one of the most popular areas for technological development in the 21st century. Nanocomposite technology is a prominent branch of material science. The nano-sized reinforcements are described as at least one dimension of those fillers in the nanometer (10^{-9}) range [3].

Manufacturing of polymer nanocomposites has been started in the early 1980s. Composite from Nylon 6 and nanostructure clay was firstly developed by researchers of Toyota Central Research laboratories in 1986 [4]. Today, nanocomposite technology is appropriate for all polymer types from thermoset to thermoplastics. Layered silicates and carbon nanotubes are the most investigated nanoparticles in the development of polymer nanocomposite field [3].

Carbon nanotubes (CNTs) are basically defined as rolled-up sheets of graphite which have dimensions in nanometer range. Since the discovery of carbon nanotubes by Iijima in 1991 [5], many investigators have worked on the preparation of CNT based composite materials because CNTs provide great improvement in the physical properties of polymer [6]. In polymer nanocomposite field, boron nitride nanotubes (BNNTs) are the another type of nanotubes that have been used as a filler in polymer matrix.

BNNTs were firstly synthesized using arc-discharge method in 1995. The inner diameters of synthesized boron nitride nanotubes are on the order of 1 to 3 nanometers and the lengths of BNNTs are up to 200 nanometers. BNNTs containing boron and nitrogen atoms have similar nanostructure with CNTs [7]. In addition to that, thermal and mechanical properties of BNNTs are similar to those of CNTs. On the other hand, BNNTs show the significant resistance to thermal oxidation rather than CNTs at high temperatures [8]. BNNTs have a constant and wide band gap which indicates electrically isolating property [9]. Therefore, BNNTs are expected to be good candidate to fabricate polymer composite because of their unique properties. Many studies have been conducted to synthesize BNNTs due to their great mechanical and thermal properties. However, remarkable effort has been made to purify the as-synthesized BNNTs that always contain impurities coming from their synthesis.

There have been many studies about polymer-BNNT nanocomposites over the last years. The effects on BNNT addition into polymer matrix have been investigated through thermal and mechanical properties of BNNT-reinforced composites [10, 11, 12, 13, 14]. Most of studies have been conducted using solution-mixing with evaporation techniques and melt mixing method in order to fabricate the polymer-BNNT composites [10, 11, 12, 13, 14]. Solution mixing method is a good approach for research purpose. In this technique, the composites are prepared by dispersion of nanotubes into polymer matrix using appropriate solvent. Melt mixing is a common use method especially in industry due to its easy of processing and environmentally friendly. Based on the scientific studies, the homogeneous dispersion of fillers

throughout the polymer matrix had not been achieved even if both solution mixing and melt mixing method were used.

The objective of this study is to introduce a new approach which is the preparation of polystyrene (PS)-BNNTs nanocomposites with the help of in-situ polymerization and then use them in melt mixing method. Before preparing masterbatch, PS was synthesized using two different polymerization techniques: solution and bulk polymerization and then characterized by Fourier Transform Infrared (FTIR) spectroscopy, viscosity average molecular weight (M_v), Gel Permeation Chromatography (GPC) and Melt Flow Index (MFI). The second aim is to synthesize PS having same structure, molecular weight, morphology, mechanical and thermal properties with commercial PS. Production of BNNTs was carried out through ammonia gas with a powder mixture of boron and iron oxide. Synthesized BNNTs were also purified before being used in the polymer composites. The purified material was characterized by X-Ray Diffraction (XRD), surface area measurement and Scanning Electron Microscopy (SEM) analyses. A concentrated mixture of PS-BNNTs (Masterbatch) was first prepared by polymerizing styrene monomer containing a high amount of BNNTs loading. Masterbatch was mixed with commercial PS at different desired compositions using a twin-screw extruder. Melt blending and in-situ polymerization methods were also applied separately for the fabrication of the polymer nanocomposites at a selected composition. The properties of the composites with the same BNNTs loadings, which are prepared by three different methods; namely melt mixing, in-situ polymerization, and masterbatch with extrusion were compared with one another. Before characterization, all of specimens were prepared using injection molding machine according to standards of test methods.

For the characterization of the composites, SEM analyses were used to investigate the dispersion of the fillers within the polymer matrix. Tensile and impact tests were performed to determine the effect of BNNT loading on the mechanical properties of neat PS. Differential scanning calorimetry (DSC) and thermal gravimetric analysis (TGA) were performed to investigate thermal behavior of the prepared composites.

CHAPTER 2

BACKGROUND

2.1 Composites

Basic definition of the word “composite” is that combination of two or more different parts [15]. In engineering manner, composite is a material created by combining two or more materials. The constituents can combine at macroscopic level but they are not soluble in each other. A typical composite material usually consists of at least two different phases. One constituent is named as a continuous part or matrix. The other one is reinforcing phase which is embedded in matrix. The material of reinforcing phase should be in the form of fibers, particles or sheets [16]. The main advantage of composite material is that, if well prepared, they usually show the best qualities of their components or constituents. Several properties such as strength, stiffness, fatigue life, temperature dependent-behavior, thermal insulation, and conductivity can be improved by forming a composite material [17].

2.1.1 Classification of Composites

Composites can be classified according to matrix materials which are metals, ceramics and polymers. Metal matrix composite consists of continuous metallic matrix with reinforcement. Reinforced metal matrix composite has some advantages relative to their matrix. Addition of reinforcement improves the stiffness, hardness, wear resistance, and thermal conductivity with reducing thermal expansion of materials [18]. For ceramic matrix composites (CMCs), ceramic fibers are embedded in a ceramic matrix. The most important advantage of CMCs compared to metal based matrix is that they have a extremely smaller density which is important for many applications and a much higher processing temperature [19]. This study gives broad information about polymer matrix composites.

2.1.2 Polymer Matrix Composites (PMCs)

A polymer is a long-chain molecule which is composed of repeating identical structure units. Carbon, hydrogen and other nonmetallic elements are the main organic compounds of polymers. All polymers can be divided into two main groups that are thermoplastics and thermosets. Both types of polymers can be used as a matrix in composite preparation. Thermoplastics are polymers that would be heat softenable and meltable in order to process into a desired shape. When cooled again, they can reversibly regain their solid state form. Thermosetting polymers are crosslinked networks where chains have been chemically linked by covalent bonds during synthesis [20]. When they are heated, curing reaction is occurred. Further heating of these types of polymer causes to degradation of polymer [21]. PMCs are the combination of polymer matrix and reinforcing agent dispersed into polymer phase. By the way, reinforcing agent is generally called as filler. Polymer matrix composites are commonly used because of their low cost and easy fabrication methods.

As compared to neat polymers, reinforced polymers offer some improvements in terms of properties such as tensile strength, fracture toughness, stiffness, corrosion resistance, thermal conductivity, temperature resistance, and flammability. Properties, orientation and concentration of the fillers in polymer matrix and properties of polymer matrix phase are the main factors to determine the properties of PMCs [22].

2.2 Polymer Nanocomposites

The field of nanotechnology is the most promising area for current research and developments in all disciplines [23]. Polymer-based nanocomposite materials have become a notable area in nanotechnology and material research due to the increasing availability and improvement of nanomaterials. They have been used in several applications such as electronics, pharmaceuticals and through studies in material science [23, 24, 25].

Nanocomposite is defined as two-phase material in which one of the phases is dispersed in the second one at nanometer (10^{-9}) level [26]. In other words, two-phase material consists of matrix phase and a reinforcing phase (filler). Matrix phase can be metal, ceramic or polymer. The fillers are the nanostructure materials that have to be at least one dimension in nanometer range [2]. Due to its structure, the fillers can be expressed as nanofillers in the preparation of nanocomposites.

Polymeric nanocomposites are mainly polymers that have been filled with low level of nanofillers. Either thermoplastic or thermosetting materials can be used as polymer matrix. Different types of nanofillers such as nanotubes, fibers, whiskers can be chosen as reinforcement in the composite according to the properties expected in the final composite [3].

Nanocomposites can be distinguished in terms of how many dimensions of the dispersed particles are in nanometer level. Isodimensional, two-dimensional and one-dimensional are the main types of nanocomposites. Isodimensional nanocomposite can be defined as three dimensions of nanoparticle which are in the order of nanometers. Spherical silica nanoparticles are one of the commonly used materials of this class. When two dimensions are in nanometer range and third one is in the range larger than nanometer, it is identified as two-dimensional nanoparticle. It forms an elongated structure like nanotubes, fibers or whiskers. Carbon nanotubes and cellulose whiskers are the widely used materials of this group. One-dimensional nanoparticles are expressed as only one dimension in nanometer scale. Graphites, clays and layered silicates are some examples of this group [27]. These fillers are used in polymer matrixes in order to produce stronger, tougher and lighter-weight materials by considering the low cost and material availability. It is also an important point that nanofillers enhance the properties of neat polymers remarkably at lower filler loading rather than conventional fillers [24].

Based on Collister's study [2001], some of the properties such as thermal endurance, flame retardance, abrasion resistance, liquid and gas barrier, reduction in shrinkage and residual loss, electrical, electronic and optical properties can be improved by dispersion of nanofillers into the polymer matrixes [28].

Polymer-nanotube composites are the commonly studied polymeric nanocomposites type for research purpose. Significant attention has been turned into nanotubes because of their unique mechanical, thermal, chemical, and electrical properties. Therefore, nanotubes have become preferable reinforcements to be used in polymer matrixes. However, there are some problems about usage of polymer-nanotube composites effectively. Large scale production of purified nanotubes and dispersibility of nanotubes in polymer matrix can be considered as main difficulties in the composite preparation [10]. Today, main intention in recent studies focuses on these two main problems in polymer-nanotube composites.

2.3 Preparation of Polymer-Nanotube Composites

The process of polymer-nanotube composite preparation is significant for dispersing nanotubes into the polymer matrix homogeneously. Several methods are known to fabricate polymer nanocomposites. These are; solution dispersion, in-situ polymerization and melt mixing (extrusion).

2.3.1 Solution Dispersion Method

Solution dispersion method is mainly focused on the dispersion of nanotubes within a polymer matrix by using an adequate solvent. In this method, nanotubes are firstly dispersed in the solvent and then polymer is formed in this mixture. The solution is mixed in order to allocate the agglomerated nanotubes throughout the mixture. After sonication is completed, composite is cast into glass plate and the solvent is removed using evaporation technique. Composite film is peeled off from glass plate and then pressed in order to give a final shape [10]. Figure 2.1 shows the flowchart of solution dispersion method. It is commonly preferred method for researchers in order to obtain homogeneously dispersed polymer-nanotube composites.

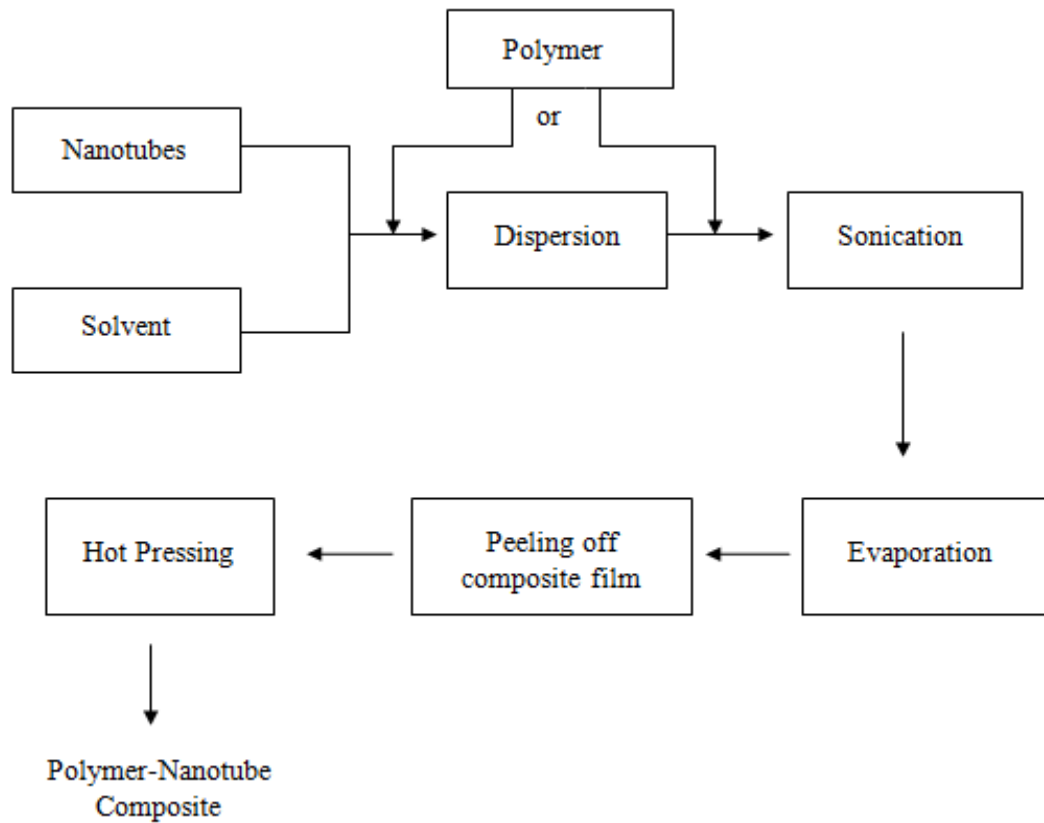


Figure 2.1 Preparation of polymer-nanotube composites using solution dispersion method.

2.3.2 In-Situ Polymerization Method

Preparation of polymer-nanotube composites can be achieved by allocation of nanotubes in the liquid monomer followed by polymerization. In this technique, the nanotubes are dispersed into liquid monomer or a monomer solution. Polymerization can be initiated by suitable initiator, heat or radiation [28]. The polymer composites containing allocated nanotubes inside polymer matrix are obtained by the end of the polymerization. Figure 2.2 demonstrates the steps of in-situ polymerization method.

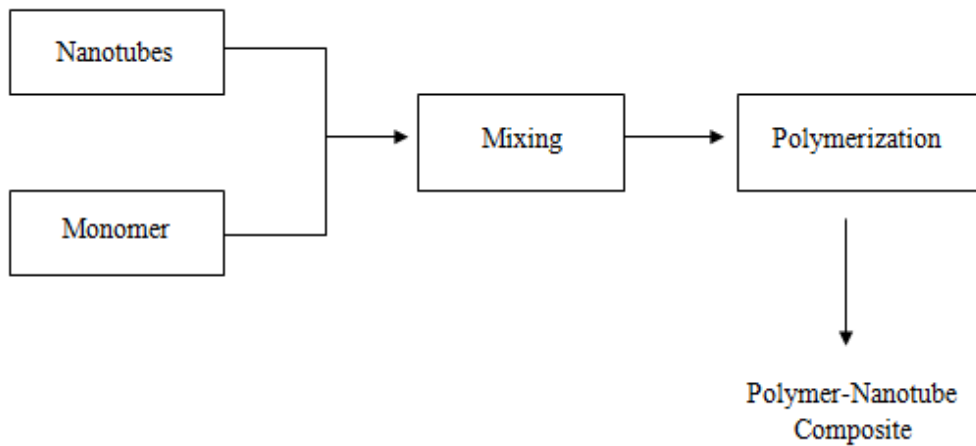


Figure 2.2 Preparation of polymer-nanotube composites by means of in-situ polymerization method.

2.3.3 Melt Mixing Method

Although solution dispersion method is a convenient technique for both nanotube dispersion and composite preparation, it is completely inappropriate for many polymer types which are insoluble in solvent. Therefore, melt mixing is a common alternative method for mixing of nanotubes with polymers especially for thermoplastic materials [29]. This route also refers to melt blending or mixing through extrusion process. In melt mixing method, melted polymer is blended with nanotubes or other additives in order to prepare polymer-nanotube composites. Figure 2.3 illustrates the flowchart representation of melt mixing method.

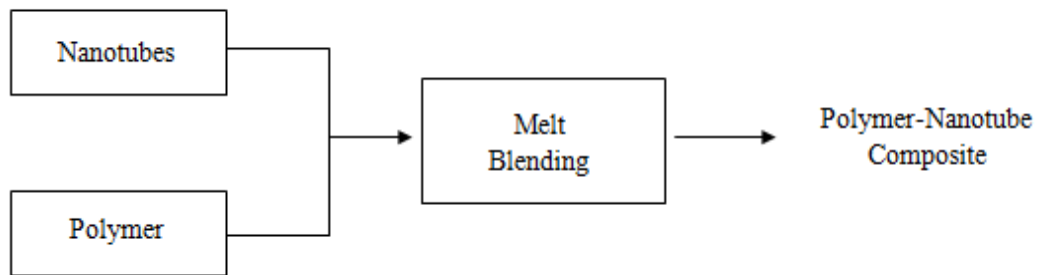


Figure 2.3 Preparation of polymer-nanotube composites with the help of melt mixing method.

2.4 Properties and Synthesis of Polystyrene

2.4.1 Properties of Polystyrene

Polystyrene (PS) is one of the important materials of standard thermoplastic group like polyethylene, polypropylene, and polyvinylchloride. Due to its unique properties, polystyrene can be preferred in a wide range of applications [30]. Characteristic properties of polystyrene can be described in terms of its stiffness, transparency, brittleness and being chemically inert and good electrical insulator. It can be easily converted into desirable products by means of extrusion, injection molding, blow molding, and thermoforming [31]. Polystyrene has excellent flow characteristics leading to easy processing. These advantages can be meaningful with its low cost property. Polystyrene is commercially available in three forms: General-Purpose PS (also known as the crystal PS), high impact PS (HIPS) and expandable PS [32].

Chemical structure of all commercial polystyrene is in atactic form where aromatic ring of styrene monomer is randomly attached to chain [33]. The atactic form of polystyrene prevents the crystallization. In other words, it is in an amorphous solid structure at room temperature which is below its glass transition temperature [31]. Polystyrene with high refractive index make it favorable in optical applications. On

the other hand, PS has several disadvantages, including its brittleness, low heat-deflection temperature, and poor UV resistance.

The applications of polystyrene involve many areas such as transparent food packaging, refrigerator and freezer equipment, housewares, electronics, appliances, and furniture [32].

2.4.2 Polystyrene Synthesis

The kinetics of polymerization can be classified into two main groups which are step-growth and chain-growth polymerizations [20]. Chain-growth polymerization is generally preferred for polymer synthesis. Styrene which is also known as vinylbenzene is a significant industrial unsaturated aromatic monomer. Polymerization of styrene is the most important reaction of styrene monomer [30]. Polystyrene was first produced commercially by the Dow Chemical company in 1938. The first polymerization process was occurred by loading cans of styrene into oven and allowing them to polymerize spontaneously to high conversion [34]. Today, several polymerization methods including free radical, cationic, anionic and coordination polymerization are used to produce polystyrene. Free radical polymerization is the most common technique used for producing polystyrene [31]. Initiation, propagation and termination are the main steps of free radical polymerization. Initiation of active monomer and then propagation of this active chain (free radical) by sequential addition monomers and finally termination of this active chain in order to obtain the polymer are the important points of free radical polymerization respectively [20].

Free radical polymerization is initiated by dissociation of the initiator to form radical species. In order to generate radical species, free radical initiators such as organic peroxides or azo compounds are thermally decomposed. The labile bonds of these organic compounds can be broken by heat, UV visible light and γ -irradiation. Benzoyl peroxides and 2,2'-azobis(isobutyronitrile) (AIBN) are commonly used initiators in free radical polymerization [20].

The reaction mechanism of free radical polymerization is as follows; [21]



In the first step, the initiator (I-I) is dissociated to form free radical initiator species denoted by R· (Reaction 2.1). It is also called as initiation step.

The formed free radical (R·) is attached to monomer molecule (M) (Reaction 2.2).



P₁· is the growing chain with 1 repeating unit. The chain propagates by adding another monomer unit (Reaction 2.3).



The free radical still exists in the product of addition reaction (P₂·). Another monomer unit is added to propagating chains (Reaction 2.4).



The propagation reaction is maintained by adding the monomer unit to propagating chain. Therefore, the general form of propagation reaction is given below (Reaction 2.5):



The chain growth is terminated either combination or disproportionation. In termination by combination step (Reaction 2.6), two propagating chains can combine each other to form a covalent bond between them in order to a single terminated polymer (P_(x+y)).



Termination by disproportionation (Reaction 2.7) leads to obtain two different polymer chains (P_x, P_y).



Different polymerization techniques are used to synthesize polystyrene. Solution, bulk, suspension and emulsion are the popular techniques for the polymerization of styrene. This study focuses on the solution and bulk polymerization techniques.

Reaction of solution polymerization takes place in the aqueous medium (solvent). There are several criteria for selecting appropriate solvent. Firstly, the monomer and initiator must be soluble in it. Also, melting and boiling points of solvent should be suitable for polymerization reaction temperature. The solvent selection may be affected by other factors such as toxicity, cost and flash point. The main advantage is that better heat control and removal is done with the presence of the solvent. Solvent must be evaporated or removed in order to obtain pure polymer [20, 35].

The bulk polymerization is the easiest one among the other techniques to synthesize polystyrene. It requires only monomer and monomer-soluble initiator, and chain transfer agent needed for molecular weight control. Polymer yield is higher than solution polymerization technique. There is an option about casting the polymerization mixture into final product form. Heat dissipation during the polymerization is the main problem of this technique. Free radical polymerization reactions are highly exothermic. When reaction proceeds, the rxn temperature will increase and additional heat will be generated. Therefore, heat must be removed during the reaction but heat removal becomes difficult at the near end of polymerization [20, 35].

2.5 Boron Nitride Nanotubes (BNNTs)

Nanotubes have been intensively studied over the last decades with the invention of carbon nanotubes (CNTs). BNNTs are structurally analogues of CNTs. BNNTs are formed by rolling of boron and nitrogen atoms [36]. Figure 2.4 represents the molecular model of boron nitride nanotube.

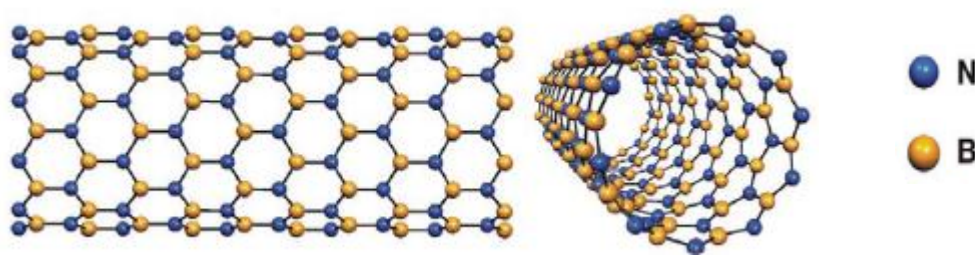


Figure 2.4 Molecular model of a single-wall boron nitride nanotube [37].

2.5.1 Properties of Boron Nitride Nanotubes

BNNTs are remarkable materials especially in terms of their mechanical, thermal and electrical characteristics. Mechanical properties of BNNTs are very similar to CNTs. BNNTs have extremely high Young's modulus which is around 1.22 TPa [38].

Besides mechanical properties, BNNTs have many advantages about thermal properties. Based on the theoretical and experimental studies, BNNTs are good thermal conductors because of effective phonon heat transfer [39]. Ishigami et al. have revealed that thermal conductivity of BNNT was determined as 600 W/m.K. [40]. BNNTs possess excellent thermal stabilities which is very important for specific applications. According to thermal gravimetric analysis (TGA), BNNTs start to oxidize nearly at 800 °C. In other words, BNNTs have higher resistance to oxidation than CNTs which is approximately 400 °C [8].

BNNTs have uniform electronic properties. They have large band gap of 5 eV. Even if their diameter and chiralities are changed, the electrical properties of BNNTs will not be affected due to their wide band-gap [41]. It can be easily said that BNNTs are isolating materials. Therefore, BNNTs have become a good choice for insulation of polymer composite materials [42].

2.5.2 Application of Boron Nitride Nanotubes

In the literature, applications of BNNTs or potential uses are not at expected level. Today, limitations about production of BNNTs have already existed. The main reason is that BNNTs are produced only in gram quantities. However, recent publications have shown that BNNTs can be used in some potential applications [41].

For example, BNNTs can be preferable for high temperature applications because of their high oxidation resistance [8]. BNNTs are the electrically insulating materials. For that reason, this kind of nanofillers can be used as reinforcement in order to prepare isolating composite materials [42]. Furthermore, BNNTs have become semiconductors by doping with other materials. For instance, carbon-doped or metal-doped BNNTs can be very attractive for hydrogen storage [41].

2.5.3 Synthesis Methods of Boron Nitride Nanotubes

As it is mentioned before, mass production of BNNTs is very difficult. Hence, several growth techniques have been tried in order to synthesize BNNTs in a large amount. In general, three popular approaches are mainly used. These are: arc discharge, laser-based and chemical vapor deposition [41].

2.5.3.1 Arc Discharge Method

BNNTs were first successfully synthesized by arc-discharge method. This synthesis method was similar to growth of CNTs [7]. In conventional arc discharge method, electrodes which are anode and cathode are used as reactants and vaporization take place between these two electrodes by means of electric energy. Vacuum chamber, gas-flow controllers and two electrodes with a DC power supply are the main instruments of conventional arc discharge method [43].

For BNNTs synthesis, the anode contains pure BN which is inserted into hollow tungsten electrode. The copper cathode electrode is rapidly cooled. Arc discharge is applied between these two electrodes. During the discharge, helium gas is fed to the vacuum chamber and dc current is applied between two electrodes with a constant

voltage. After the arc discharge completed, the grey product is formed on the copper cathode [7]. Nanotubes are deposited on the cathode electrode.

2.5.3.2 Laser-Based Method

Besides electrical energy, the photonic energy can also be converted to heat in order to evaporate reactants into ion gas form. Laser based technique can be defined as the light which is either continuous beam or discrete pulses is sent to source materials. Incident light increases the temperature of irradiated zone to high degree within a short period of time. If the temperature exceeds the sublimation point of the source material, the local explosion may occur and the source material may effuse from the surface. The reactants which are in ion form are generated by using this technique [43].

For BNNTs synthesis, continuous beam or discrete pulses of light are sent to boron source and the carrier gas is used for carrying the target material to the collector. The target material is collected from collector [44]. The laser method needs high amount of energy and temperature like in the arc discharge method. Low amount of BNNTs which have a perfect cylindrical structure with small defects is produced [43]. The main disadvantage of this technique is that synthesized BNNTs contain a high amount of impurities like undesired BN particles or flakes [37].

2.5.3.3 Chemical Vapor Deposition

Chemical vapor deposition (CVD) is the most popular technique that the reaction takes place between volatile reactants at elevated temperature in order to be deposited [43]. For example, Lourie et al. reported the synthesis of BNNTs by using borazine ($B_3N_3H_6$) and catalyst particles. The catalyst was centered in tubular furnace reactor and heated to high temperatures. Then, borazine vapor was decomposed and deposited on the catalyst as a white solid material [43, 45]. Typical set-up for the synthesis of BNNTs using CVD method is shown in Figure 2.5 [11].

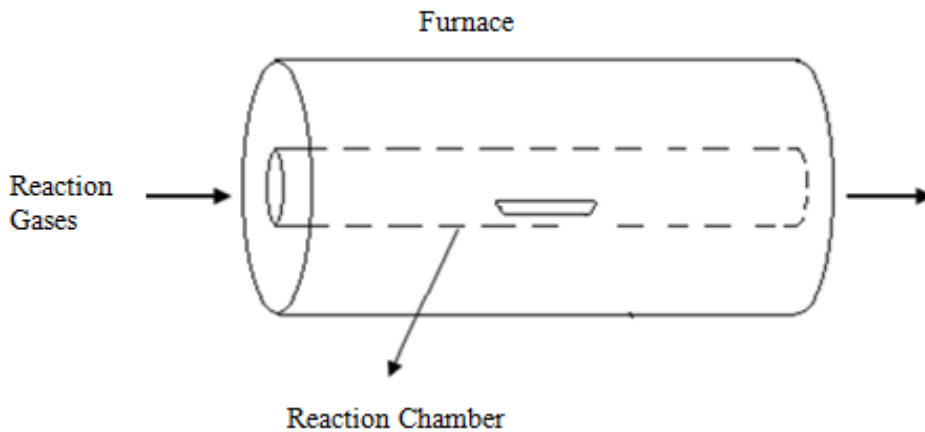


Figure 2.5 CVD method for production of BNNTs [11].

2.5.3.4 Other Synthesis Techniques

Ball milling and annealing method is one of the alternative technique to produce BNNTs. This technique contains two steps that are the ball milling of elemental boron in NH_3 at room temperature and thermal annealing at $1000\text{ }^\circ\text{C}$. High yield of BNNTs, low cost and ease of the control are the main advantages of this technique relative to the others. In the first step of this technique, high-energy ball milling leads to structural changes of elemental boron and chemical reaction at room temperature. The reaction which is called as nitriding reactions takes place between boron powder and ammonia gas. Disorder BN and nanocrystalline boron is formed during high-energy ball milling procedure. After ball-milling, the boron based material is annealed at high temperature. Boron nitride nanostructures are grown up from this metastable and chemically activated during thermal annealing [46].

The other thermal method is the reaction of ammonia gas with a powder mixture of boron and iron oxide. The boron and iron oxide powder mixture is homogeneously mixed at room temperature by taking into account the weight ratio of reactants. The homogenized mixture is placed into the center of horizontal tubular reactor. The reaction is carried out between ammonia gas and this powder mixture at high temperatures. High yield of BNNTs with low cost can also be synthesized by using this method. The reactant gas composition, reaction temperature and weight ratio of powder reactants are very important on the structure of BNNTs [44].

2.6 Polymer Processing Techniques

Several polymer processing techniques such as extrusion, injection molding and blow molding etc. are used to fabricate plastic products. In this study, extrusion and injection molding techniques are carried out in order to prepare materials. Therefore, these processing techniques are examined thoroughly.

In extrusion process, a molten polymer is continuously forced through the die in order to be shaped into desired items [32]. This method allows several processes taking place in a single machine. These include melting, metering, mixing, reacting, side-stream addition, and venting. In Figure 2.6, the schematic representation of the extrusion process is given.

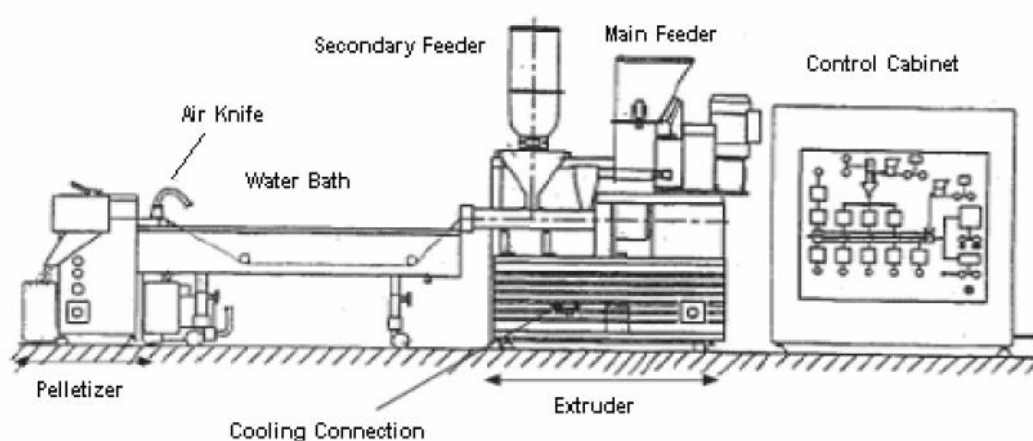


Figure 2.6 Schematic illustration of the extrusion process [47].

Extruder has a horizontally placed barrel. Inside the barrel, either single or double screw is used for mixing. In a typical extrusion process, thermoplastic materials in powder or granular form are fed from main feeder to the screw. After feeding, they are heated by controllable heaters and conveyed with the rotation of screw which helps to create mixing regime inside the barrel. Molten polymer is blended with their additives and transmitted to the die section by means of shear forces created by motion of screw.

At the end of the extruder, the viscous forms of polymer exits from die to form extrudate of the desired shape [48]. Typical single screw extruder is shown in Figure 2.7.

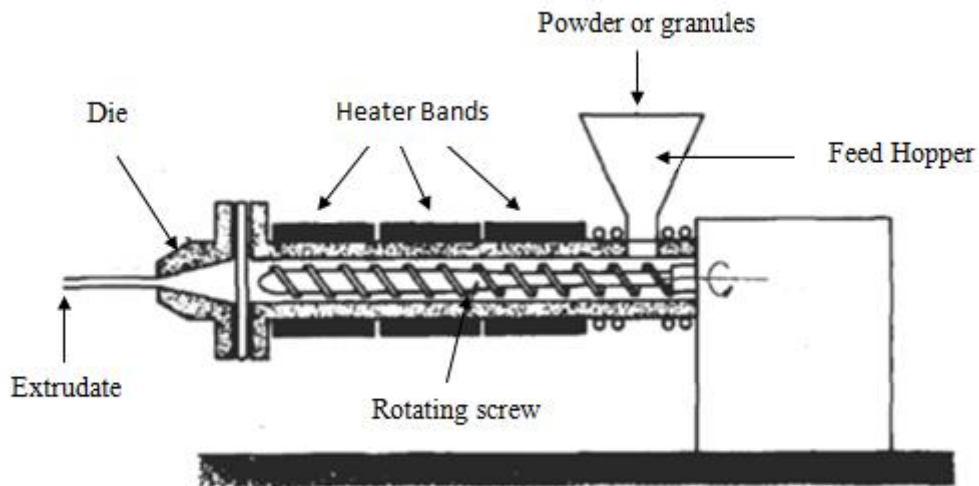


Figure 2.7 A schematic representation of single screw extruder [48].

2.6.1 Screw of Extruder

The screw inside the barrel is the most important part of the extruder. The main purpose is to maintain homogeneous mixing inside the barrel. For that reason, a screw is divided into three major sections which are feed, compression or transition and metering zones. Three distinct sections of screw are given in Figure 2.8.

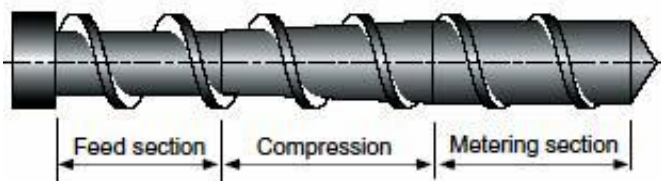


Figure 2.8 Major parts of extruder screw [48].

The extrusion process begins with the feeding of raw polymer from the hopper or feeding hole. After feeding, the raw polymer is preheated to a proper temperature and conveyed to the compression zone.

In the compression zone, the raw polymer is melted and mixed. Then, the melt mixed polymer is pressurized by the rotational motion of screw. The main purpose of this section is to compress the molten polymer and create the shear forces inside the material for better mixing. Additionally, the screw depth of this section decreases in order to ensure compactness of material. This squeezing part prevents the formation of air bubbles inside polymer melt. If they are formed into polymer melt, they will send to feed zone again.

In the metering section, the screw depth is again constant but it becomes much less than feeding section. The metering section provides homogenization of the polymer melt. The polymer melt is sent to the die at a constant rate, temperature and under sufficient pressure [48].

2.6.2 Twin Screw Extrusion

The use of twin screw extruders has been increased rapidly in recent years. The main reason is that the twin screw extruder has two co-operating screws in its heated barrels. These types of machines are allowed to improve operational parameters of extrusion. For example, output rates, mixing efficiency and heat generation parameters of the extrusion process can be enhanced with respect to single screw extruders. The arrangement of the double screw and the rotation direction inside the barrel are the two main considerations for determining the types of twin-screw extruders. These types are shown in Figure 2.9.

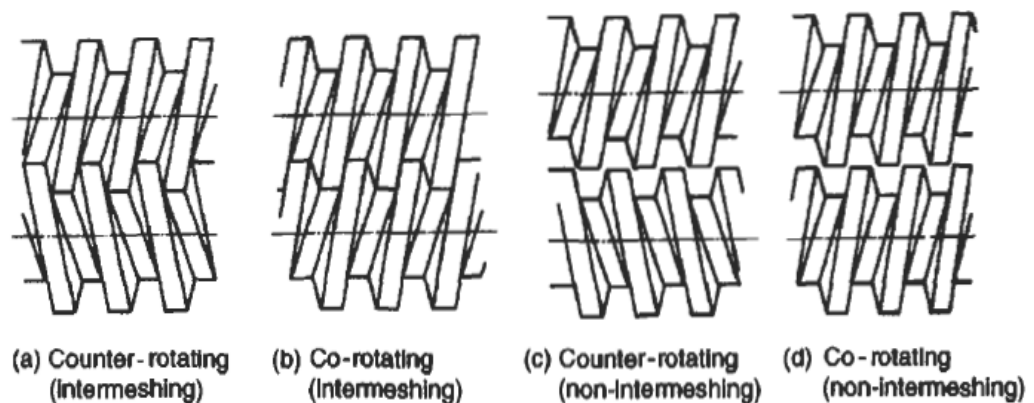


Figure 2.9 Different types of twin-screw extruders [48].

Based on Figure 2.9, different arrangements can be used for twin-screw extruders. In counter-rotating motion, the molten polymer is sheared, pressurized and effectively squeezed between these screws. In co-rotating motion, the polymer is conveyed from one screw to another [48]. The motion of counter-rotating and co-rotating twin screw extruders are represented in Figure 2.10.

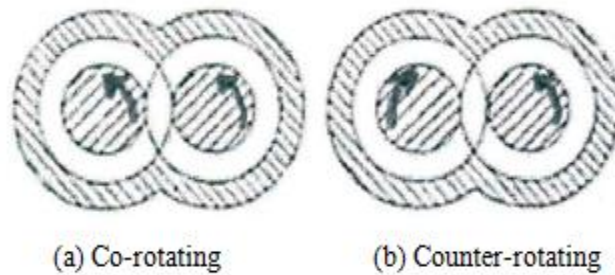


Figure 2.10 Motion of twin-screw extruders [49].

2.7 Injection Molding

Injection molding is most frequently used processing technique for plastics. The powder or pellet form of thermoplastic materials, recently thermosets, is converted to finished articles with the help of this method [32]. This process is carried out by injection molding machine. The basic stages of this process are given in Figure 2.11.

The polymer is heated until it melts. Then, the melted polymer is injected into a cold mold under high pressure. The polymeric material is solidified inside the mold. At the last stage, the mold is opened and the product is ejected from the mold [50].

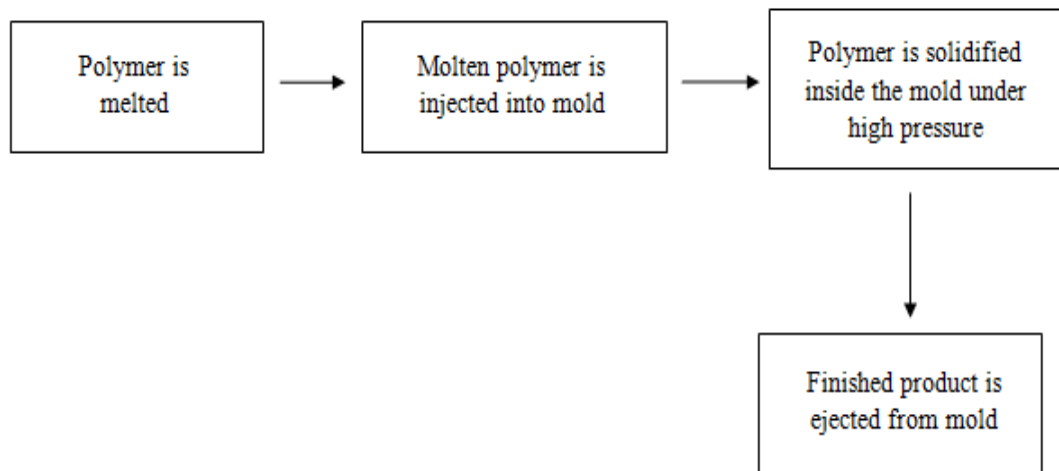


Figure 2.11 Stages of injection molding process.

The injection and the clamp unit are the two main parts of injection molding process in order to complete the cyclical steps in melt injection. Melting of polymer and then injection of this molten polymer into the mold is the main responsibilities of injection unit. In the clamping system, it has one main property: to keep the mold closed and to prevent any polymer from escaping the mold during the injection of molten polymer [51].

Appropriate process conditions such as temperature and pressure can be adjusted according to the polymer type which is used to be injected.

2.8 Characterization Methods

A large number of techniques are carried out in order to determine the properties of polymers, their nanocomposites and also fillers to be used. In the following subsections, these characterization techniques are explained in detail.

2.8.1 Fourier Transform Infrared (FTIR) Spectroscopy

Infrared spectroscopy is basically defined as the interaction of infrared light with material. It is very sensitive to detect functional groups or chemical bonds in materials. The most important feature of infrared spectroscopy is to determine unknowns in samples. Fourier Transform Infrared Spectroscopy is the most

commonly used type of spectrometer. Middle infrared radiation range (400 – 4000 cm^{-1}) is applied to characterize the materials. Absorption and transmission of infrared lights are the main approaches for identifying the chemical composition of unknown sample. When infrared radiation is interacted with sample in infrared spectrum, radiation is absorbed by material leading to vibration in their chemical bonds. The existence of chemical bonds in sample is the essential condition for infrared absorbance in order to occur. Transmittance is the ratio of light intensity with or without sample. Therefore, information about absorption and transmission of infrared lights is required to interpret the chemical bonds and functional groups of unknown material [52].

2.8.2 Measurement of Molecular Weight

Molecular weight distribution of commercial or synthesized polymers has to be known to use them in specific applications. Several techniques are used to determine the molecular weight distribution of polymers. Molecular weight determination methods are divided into two categories: absolute and relative ones. In this study, relative methods such as viscosity average molecular weight, Gel-Permeation Chromatography are explained in detail.

2.8.2.1 Viscosity Average Molecular Weight (M_v)

Viscosity average molecular weight method is based on the determination of intrinsic viscosity $[\eta]$ for polymer solution [20]. Intrinsic viscosity $[\eta]$ is defined as the fractional change in the viscosity of a solution per unit concentration of a polymer at infinite dilution. The mathematical expression of intrinsic viscosity is given below [53] :

$$[\eta] = \left(\frac{\eta_{sp}}{c} \right)_{c \rightarrow 0} = \left[\frac{\ln \eta_r}{c} \right]_{c \rightarrow 0} \quad (2.1)$$

(η_{sp}/c) is the expression of reduced viscosity (η_{red}). Also, inherent viscosity (η_{inh}) is expressed by $(\ln \eta_r/c)$.

Huggins and Kramer's equations are used to determine intrinsic viscosity. The mathematical expression of Huggins' equation which is the relation between reduced viscosity and concentration is given in Equation (2.2) [53]

$$\eta_{\text{red}} = \left(\frac{\eta_{\text{sp}}}{c}\right) = [\eta] + K'[\eta]^2 C \quad (2.2)$$

Also, Kramer's equation is expressed by the variation of $(\ln\eta_r/c)$ with concentration. The mathematical relation is given in Equation (2.3) [53]:

$$\eta_{\text{inh}} = \frac{(\ln\eta_r)}{c} = [\eta] + K''[\eta]^2 C \quad (2.3)$$

Reduced and inherent viscosities are plotted with respect to concentration to determine intrinsic viscosity. Both (η_{sp}/c) and $(\ln\eta_r/c)$ extrapolates to zero concentration (Figure 2.12). The intercept of the plots give the accurate value of intrinsic viscosity (Figure 2.12).

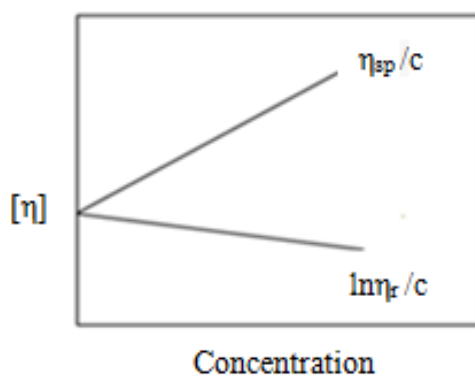


Figure 2.12 Typical plots of inherent and reduced viscosities with respect to concentration to find intrinsic viscosity [54].

After determining the intrinsic viscosity of polymer solution, Mark-Houwink-Sakurada equation is used to determine viscosity average molecular weight. This relation can be written as [20];

$$[\eta] = K \bar{M}_v^a \quad (2.4)$$

In this equation, both K and a are the empirical constants which are only appropriate for a given polymer, solvent and temperature. In other words, temperature, polymer-

solvent system and molecular weight of the polymer in solution are the main functions of intrinsic viscosity. If the measurements are carried out at constant temperature by using appropriate solvent for a specific polymer, the polymer's molecular weight can be estimated quantitatively [21].

2.8.2.2 Gel Permeation Chromatography (GPC)

Gel Permeation Chromatography (GPC) which is also called as Size Exclusion Chromatograph (SEC) is the most frequently used technique for determination of molecular weight and molecular-weight distribution of polymers [20]. The molecular weight of polymers starting from oligomers to 10^6 can be characterized by this method. Molecular-weight distribution of polymers in terms of number average (M_n), weight average (M_w), z-average (M_z) and polydispersity index (PDI or M_w/M_n) can also be determined by means of GPC technique.

The main principle of GPC method is the separation of polydisperse polymers according to their sizes. The separation process is occurred by passing a solution through a column packed with microporous gel particles. A dilute polymer solution is injected along with a solvent which is continuously pumped through the column with a constant flow rate. The size of polymer molecules is a key point for separation. This means that, the smaller molecules can easily penetrate the pores of the gel in column rather than the larger ones. During elution, the larger molecules come out first from the column and enter into the detector quickly. In other words, the larger molecules will spend less time to elute from the column with respect to smaller molecules [53]. This method helps to distinguish different size of polymer molecules which have been eluted from the column in descending order of molecular weight.

Polymer sensitive detectors such as infrared or ultraviolet devices are used in order to monitor the concentration of polymer molecules in each eluting fractions [20]. A typical GPC curve for a sample is plotted by detector signal to elution volume or elution time. The data of elution volume or elution time are recorded by detector signal in order to plot typical GPC curve [53].

GPC calibration curve is obtained by the known molecular weight samples. The calibration curve is the plot of molecular weight versus elution volume. Once the proper calibration is obtained, the molecular weight of any samples can be found from the elution volume which is obtained for the samples [53].

2.8.3 Melt Flow Index (MFI) Measurement

The melt index which is also called as melt flow rate measures the mass flow rate of polymer through a standard orifice under prescribed conditions of temperature and load [55]. The melt index value of molten polymers is determined by the weight of the polymer extruded during specified time under certain conditions. The melt index of polymers is expressed in grams per ten minutes [56].

The melt index machine resembles the simple ram extruder. The barrel is filled with polymer and heated to appropriate temperature. When the polymer is melted, the weight is applied to the piston in order to push forward the extrudate polymer through the die. As the extruded weight of polymer per unit time decreases, the viscosity or molecular weight of polymer will increase. In other words, high MFI value of polymers shows low viscosity and low molecular weight [57]. In Figure 2.13, schematic representation of MFI apparatus is given.

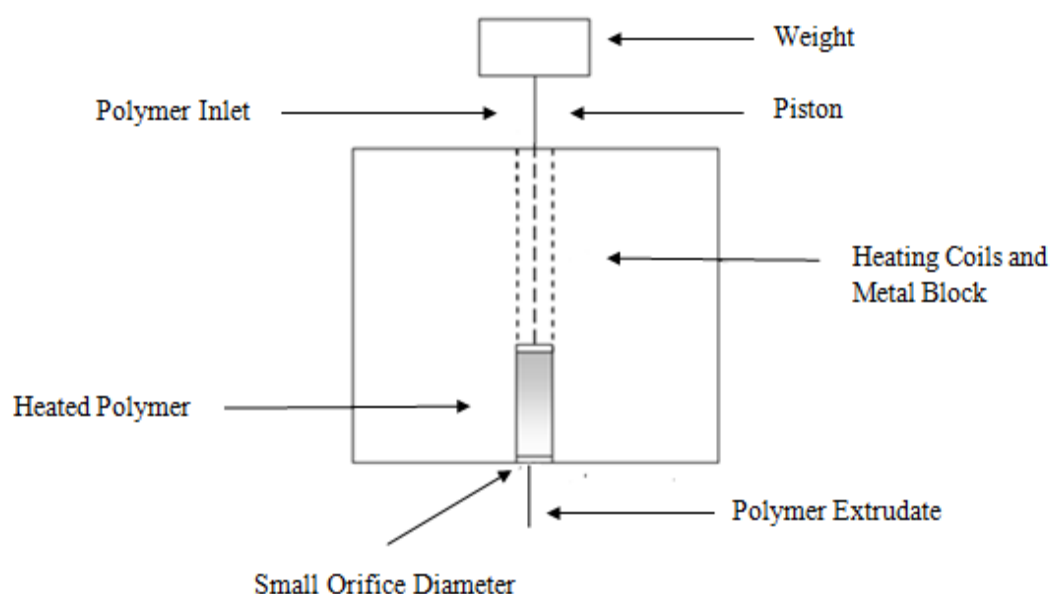


Figure 2.13 Schematic of MFI apparatus [58].

2.8.4 X-ray Diffraction (XRD) Analysis

X-ray diffraction (XRD) is commonly used method in order to determine crystallographic structure of materials. This method helps to investigate the arrangement of atoms or molecules through the interaction of electromagnetic radiation [55].

X-rays which are the form of electromagnetic radiation have high energies with short wavelength [59]. In XRD analysis, an X-ray beam with a given wavelength is sent to solid material. A beam of X-rays are diffracted only for certain specific orientations of the material [55]. The diffraction of X-rays is shown by Bragg's equation which is written as follows,

$$n\lambda = 2d\sin\theta \quad (2.5)$$

where, λ is the wavelength of the X-ray beam, d denotes the distance between planes, θ is the angle of incidence and n is an integer which shows the degree of diffraction [60]. Bragg's law gives a relationship between wavelength of X-ray beams, atomic distance between planes and angle of diffraction. The diffraction parameters of X-ray beam is given in Figure 2.14.

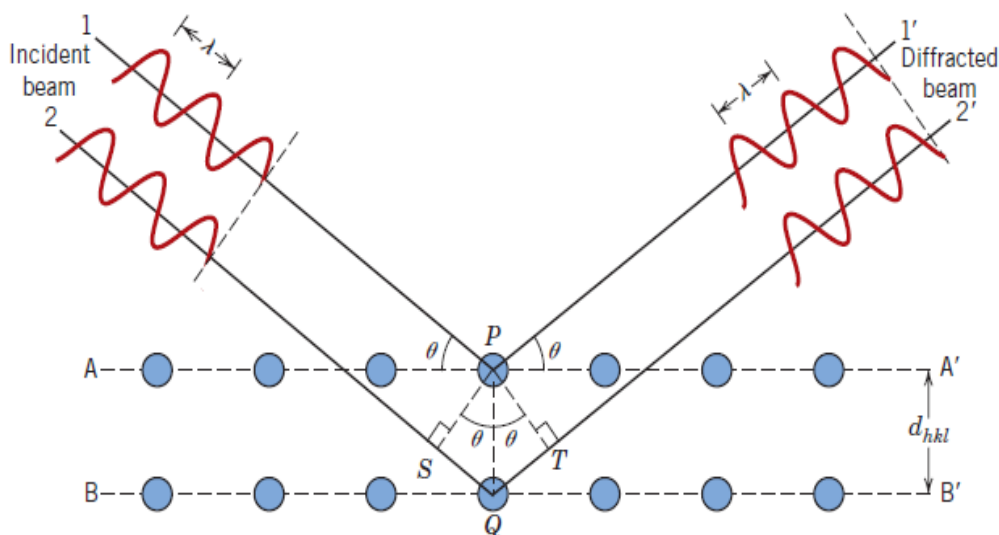


Figure 2.14 Diffraction of X-ray beam by planes of atoms [59].

X-ray diffraction apparatus which is called as diffractometer is used to determine the diffraction angle of the material. When the θ angle is slowly increasing, the recorder of diffractometer automatically plots the intensity of diffracted beam versus diffraction angle (2θ). Crystallinity of specimens can be determined by characteristics peaks which are indicated by 2θ values. Hence, XRD pattern gives information about which crystalline phase exists in the material and the proportionality of crystalline phase [59].

2.8.5 Surface Area Measurement

BET method is the initials of scientists who are Brunauer, Emmett and Teller. This technique which is related to surface characterization of porous materials was developed in 1938. BET surface analysis method is used to determine surface area, pore-size distribution of solid materials.

In multi-point BET surface analysis, the initial weight of sample is known and nitrogen gas with controlled pressure is applied to solid materials. When the nitrogen pressure is increased, nitrogen molecules are adsorbed by bulk free surface and pores of the sample. After covering the surface with nitrogen molecules, the pressure of nitrogen is decreased and nitrogen molecules are desorbed from material. Surface characteristics of the material can be identified by adsorption and desorption isotherms of the samples [11].

2.8.6 Scanning Electron Microscopy (SEM) Analysis

SEM is a microscopic analysis technique for scattering the pattern or profiles of the material. This method is very useful to gather information about material's surface morphology. In this technique, electron beam which is produced by electron gun is sent to specimen in order to scan the surface of the material. The material's surface has to be electrically conductive. For example, if the sample is electrically isolating, the surface of the material is coated with thin layer of conductive material such as gold or carbon in order to make it as a conductive sample [28].

When the electron beam is sent to specimen, the interaction is occurred between electron beam and atoms which produce the signals. These signals are detected by

detector and scanned images of the materials surface can be visible by the varying intensity of the signal. The variations in the intensity of signals lead to obtain visible scanned images of the samples on the screen [28]. More than 50,000 times magnification can be possible for SEM images in order to make accurate consequence about material's surface morphology [59].

2.8.7 Mechanical Characterization

Mechanical properties of materials are the most crucial properties among all physical and chemical properties. For most applications, polymers are commonly preferred because of their unique mechanical properties. Therefore, several test methods are used to investigate the mechanical performance of the polymers. Ductility, hardness, strength and toughness are some types of the mechanical properties. In this study, tensile and impact test are examined thoroughly.

2.8.7.1 Tensile Test

The purpose of tensile test is to get information about mechanical features of materials such as tensile strength, yield strength, modulus of elasticity and elongation at break. Based on tensile test standards, test specimens are generally in the form of dogbone shape or rectangular. In tensile testing machine, both ends of the specimen are clamped between a pair of jaws. The upper jaw is attached to a moveable crosshead. Before starting the experiment, the dimensions of specimen are measured and then clamped into the jaws. When the tensile test is started, the crosshead of testing machine is raised at a constant speed rate. During the test, the load which is applied to specimen is continuously recorded until the specimen breaks. Finally, force and elongation data of the specimens are offered for plotting by tensile test [31]. The schematic representation of tensile testing machine is given in Figure 2.15.

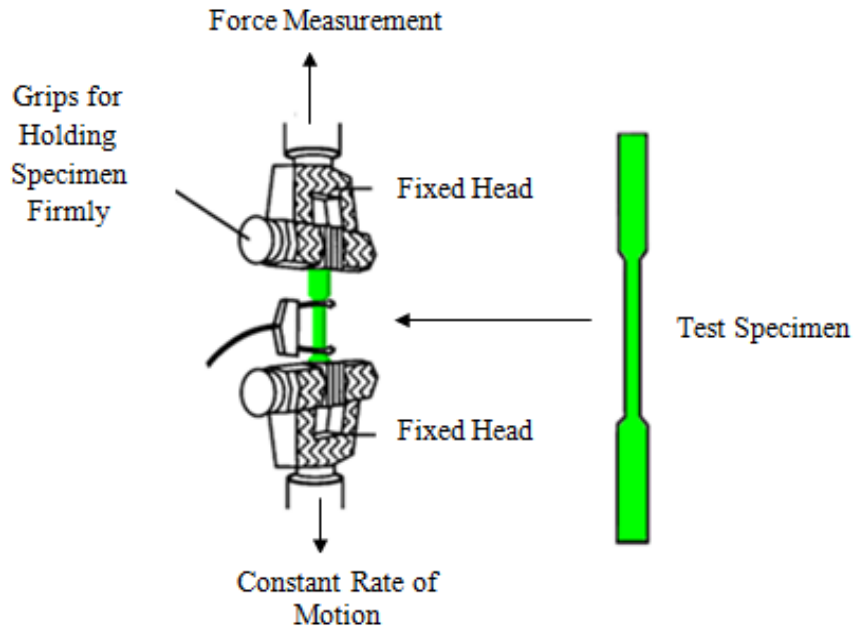


Figure 2.15 Tensile test apparatus and tensile test specimen [61].

As it is mentioned before, force versus elongation plot is obtained by tensile test. The raw data of tensile test can be converted into engineering stress vs. engineering strain plot by using the dimensions of specimen. The equation of engineering stress and strain is expressed by Equations (2.6) and (2.7) respectively [33].

$$\sigma = \frac{F}{A_0} \quad (2.6)$$

$$\varepsilon = \frac{L_i - L_0}{L_0} \quad (2.7)$$

In Equation 3.6, force applied on the specimen is denoted by F (N). A_0 (mm^2) is cross-sectional area of tensile specimen and σ is the engineering stress (MPa). In Equation 3.7, engineering strain (ε) which is the dimensionless quantity is defined as the ratio of the change in the gauge length (mm) to the initial gauge length (mm).

Young's modulus also called as modulus of elasticity is the one of tensile property of the materials. Young's modulus is directly related with stiffness of a material and obeys the Hooke's law [62]:

$$\sigma = E. \epsilon \quad (2.8)$$

Based on the Hooke's law, the modulus of elasticity is the slope of the initial and elastic region (linear region) of stress-strain curves.

Tensile strength is the maximum tensile stress that the material can sustain without fracture. Yield strength of a material is the maximum stress which is required to produce plastic deformation. Typical stress versus strain plot is given in Figure 2.16.

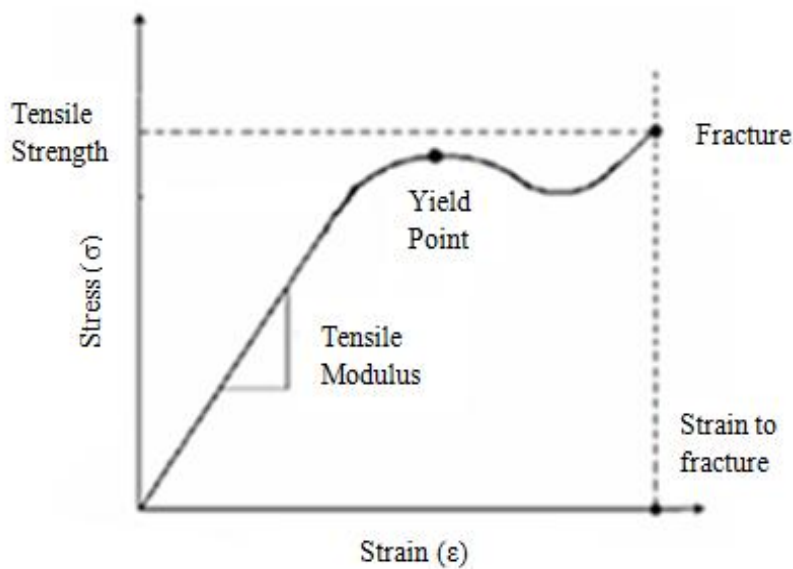


Figure 2.16 Typical stress-strain curves [63].

The stress-strain behavior of the materials shows a variety due to their material properties. In Figure 2.17, different types of stress-strain curves are represented.

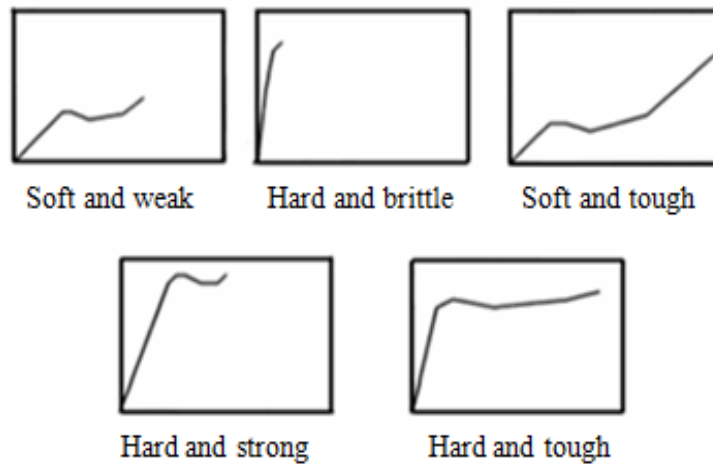


Figure 2.17 Different forms of stress-strain plots [63].

2.8.7.2 Impact Test

Impact strength is a measure of needed energy in order to break the sample. Impact strength gives information about toughness of the material. In general, impact-related tests are divided into two categories: falling-mass test and pendulum test. Izod and Charpy test techniques are generally used to determine the impact strength of the polymers. For both the Izod and Charpy test, the hammer is released from a specified height to break a sample under standard conditions. The energy is determined from the potential energy loss of the hammer. In Izod test, notched specimen is used to measure the energy of the sample. On the other hand, the material can be tested with unnotched or oppositely notched specimen [35]. Impact strength calculation can be done by dividing the absorbed energy to cross sectional area of the sample. In Figure 2.18, Charpy impact test apparatus is given.

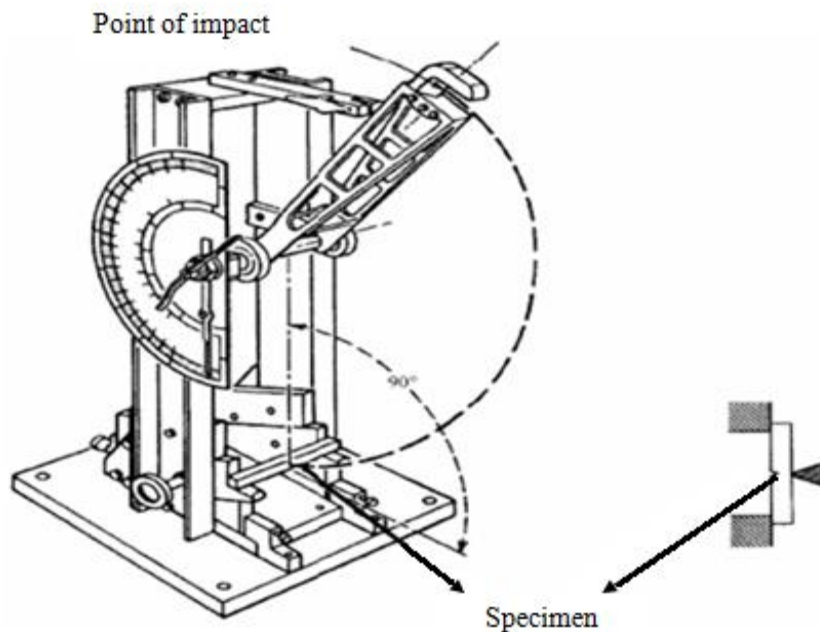


Figure 2.18 Charpy impact test [47].

2.8.8 Thermal Characterization

There are several techniques to detect the thermal response of the materials when it is subjected to a controlled temperature. Differential scanning calorimetry (DSC), thermo-gravimetric analysis (TGA) and differential thermal analysis (DTA) are the three main methods. In this study, DSC and TGA techniques are investigated for thermal behavior of the materials.

2.8.8.1 Differential Scanning Calorimetry (DSC) Analysis

DSC is frequently used to observe thermal transition of material under certain temperature program. Glass transition, crystallization and melting temperatures of materials can be interpreted by this technique. The flow of energy (heat) adsorbed or released by a sample is measured with the help of DSC analysis [64].

In the DSC analysis, two pans are used to analyze thermal behavior of sample. The material is placed into sample pan and other one is used as a reference pan which is empty one. Both pans are heated by heaters supplying thermal energy.

In a typical DSC program, the temperature of both pans are increased with a constant heat rate of 5 °C /min, or 10 °C /min or 20 °C /min [21]. During the analysis, heat flow difference between sample and reference pans is measured and data is collected in order to plot differential heat flow as a function of temperature.

When the temperature is increased, physical transformation such as melting, glass transition or crystallization can occur. During physical transformation, discontinuity in power signal is started. This means that, heat is needed for a sample pan in order to continue their physical changes [28]. A typical DSC curve is given in Figure 2.19.

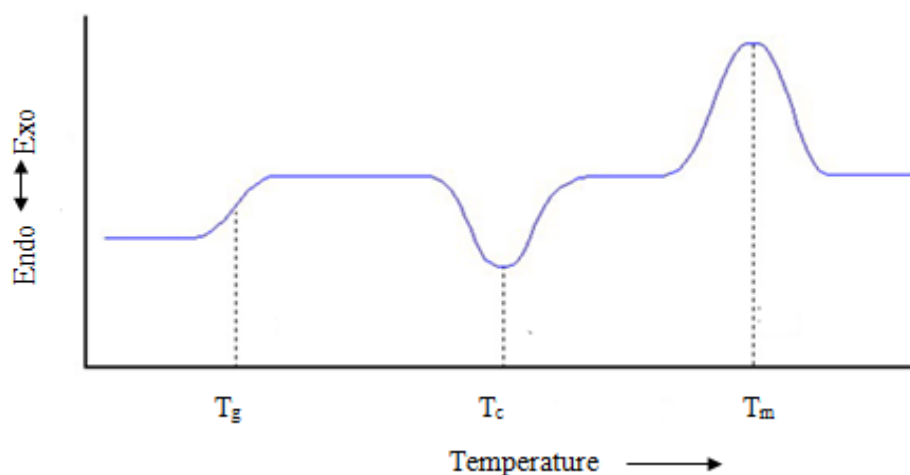


Figure 2.19 Typical DSC plot [28].

2.8.8.2 Thermal Gravimetric Analysis (TGA)

Thermogravimetric analysis is used to determine materials resistance towards heat. In this method, the weight of material is continuously recorded under the temperature program. Under the controlled atmosphere as air or nitrogen is supplied during the analysis.

When the material temperature is increased with a constant heating rate, the initial weight of sample starts to decrease due to evaporation or degradation of the material. As the temperature is enhanced further, the weight of residual is decreased. The filler content in composite is quantitatively analyzed with the help of this technique [28].

2.9 Previous Studies

In this study, PS synthesis, production of BNNTs and polymer-nanotube composites are generally taken into account in the literature survey.

2.9.1 Polystyrene Synthesis

Altares et al. [65] synthesized the low molecular weight polystyrene using anionic polymerization technique. All samples were polymerized under high vacuum in order to measure the molecular weight. Polymers were synthesized by changing the anionic initiator and styrene amount in terms of mole and weight, respectively. Intrinsic viscosity, viscosity average and number average molecular weight of polymers were determined using different techniques such as conventional solution fractionation, elution and gas chromatography. For example, elution chromatography was used to determine the low molecular weight of polymers which were less than 1500.

McIntyre et al. [66] synthesized the high molecular weight polystyrene samples and characterized them using light-scattering and equilibrium ultracentrifugation method. The solution polymerization method was used using a tetrahydrofuran (THF) as a solvent. Molecular constants of high molecular weight synthesized polystyrene samples were determined via a light-scattering and ultracentrifugation technique. Also, intrinsic viscosity as a function of weight average molecular weight (M_w) was plotted using a Mark-Houwink equation in order to determine theta solvent values at the theta temperature.

Choi et al. [67] synthesized the polystyrene using bulk styrene polymerization method in order to study the kinetics of styrene polymerization. Symmetrical bifunctional initiator (2,5-dimethyl-2,5-bis(benzoyl peroxy)) was used in order to initiate the reactions. The Gel Permeation Chromatography (GPC) technique with THF solvent was applied to determine molecular weight and its distribution. The effect of polymerization temperature changing from 90 °C to 110 °C on monomer conversion was determined at 0.025 mol/L initiator concentration. Molecular weight distributions of polymers were also determined at the same initiator concentration.

Effect of initiator concentration changing from 0.05 to 0.01 mol/L on monomer conversion was studied at the polymerization temperature of 100 °C. Also, the molecular weight distribution of synthesized polymers with respect to initiator concentration was determined. When the initiator concentration was decreased from 0.05 to 0.01 mol/L as a function of time at the same polymerization temperature, M_w and M_n determined from experimental data were increased remarkably.

Patra et al. [68] synthesized the high molecular weight polystyrene (PS) and poly(methyl methacrylate) using an emulsion polymerization technique. Metal metallocene compound (Cp_2ZrCl_2) catalyst with anionic surfactant as a emulsifier was used in order to polymerize the styrene or methylmethacrylate in aqueous medium. Polymerization was carried out by changing polymerization time between 3-20 hrs in order to determine polymer yield and molecular weight of polystyrene and PMMA. The highest yield and polydispersity index (M_w/M_n) of polystyrene was determined with the values of 84% and 1.9, respectively at the constant reaction temperature of 90 °C, monomer concentration of 0.5 mol/L and at 15 hrs polymerization time.

2.9.2 Production of Boron Nitride Nanotubes

Chopra et al. [7] synthesized boron nitride nanotubes using an arc-discharge method. The inner and outer diameter of synthesized nanotubes can be varied between 1-3 nm and 6-8 nm, respectively. The length of nanotubes was over 200 nm.

Tang et al. [69] synthesized boron nitride nanotubes by heating a mixture of amorphous boron powder and iron oxide to high temperatures inside an alumina tube. The ammonia gas was preferred as a reactant. The reaction temperature and the ratio of boron (B) to iron oxide (Fe_2O_3) played a vital role in order to determine diameter and morphology of the product.

Tang et al. [70] synthesized BNNTs from a mixture of boron and magnesium at reaction temperature of 1300 °C. Magnesium was evaporated from the final product. SEM images showed that diameter and length of one-dimensional nanostructure were ranged from several nanometers to about 70 nm and up to 10 micrometers, respectively. The broad distribution in terms of diameter of BNNT was obtained.

Tang et al. [71] synthesized multi-wall boron nitride nanotubes by using chemical vapor deposition method. The mixture of elemental boron and gallium oxide was reacted with ammonia. Based on the morphological analysis of synthesized multi-wall boron nitride nanotubes, wall deformation was observed and it was dependent upon tube diameter. The wall deformation was lead to stress relaxation of bond rotation.

Zhi et al. [72] synthesized boron nitride nanotubes using a mixture of iron oxide, magnesium oxide and elemental boron. This powder mixture was used as effective precursor for BNNTs synthesis. The reaction was carried out at a wide temperature range of 1100-1700 °C. Diameter and purity of BNNTs were not dependent upon the wide scale temperature reaction. Approximately 200 mg BNNTs were synthesized at the temperature of 1500 °C with 1 hour and also no significant impurity was detected in the synthesized material. They believed that the BNNTs were easily scaled up using a larger diameter of boats. XRD result revealed that crystalline h-BN phase was obtained.

Lee et al. [73] synthesized multi-wall boron nitride nanotubes in horizontal tubular furnaces within a hour. In this method, a mixture of boron, magnesium oxide and iron oxide was placed in alumina boat and this boat was centered into quartz test tube which was located in the center of furnace. The furnace was heated to 1200 °C and ammonia gas was fed to the system at this temperature. Ammonia was reacted with a mixture. Finally, clean and long BNNTs were collected from the wall of alumina boat.

Özmen et al. [44] synthesized the BNNTs from the reaction of ammonia gas with a powder mixture of elemental boron and iron oxide in horizontal tubular furnace. The powder mixture of elemental boron and iron oxide was placed inside the center of tubular furnace. Different boron to iron oxide ratios and reaction temperature were scaled in order to see the effect of synthesis parameters on the morphological properties of BNNTs and to investigate the reaction kinetics of BNNTs synthesized by the reaction of NH₃ with elemental boron and iron oxide. XRD results revealed that, the solid phases were iron, boron oxide, iron boride, hexagonal and rhombohedral. The outer and inner diameters of synthesized BNNTs were changed

between 64-136 and 7-28 nm respectively. It was observed that BNNTs were synthesized by the reaction of nitrogen which was formed from the NH_3 decomposition reaction with Fe_xB_y produced from the reaction of B with Fe_2O_3 . Finally, optimum reaction conditions were determined as a reaction temperature of 1300 °C and boron to iron oxide ratio of 15/1.

Noyan [74] synthesized the BNNTs from the reaction of ammonia gas with a powder mixture of elemental boron and iron in horizontal tubular furnace with connecting a mass spectrometer to analyze the effluent stream. The synthesized material was purified using acid treatment method in order to get rid of reaction impurities from the sample. Based on the XRD analysis, the solid phases which are hexagonal BNNTs, rhombohedral BNNTs, boron-iron compounds, and iron were observed in the unpurified synthesized material. The reaction kinetics of BNNTs was investigated in terms of decomposition of ammonia gas, formation of boron-iron compounds and boron nitride. The outer diameter ranges of synthesized BNNTs were changed between 10-550 nm. Physical properties of BNNTs especially surface area were decreased with an increase in temperature. Deposition rates of boron nitride with respect to temperature were scaled. Based on the parameter optimization, the synthesis conditions which were B/Fe ratio of 15/1 at 1300 °C were the optimum reaction conditions for the highest deposition rate of BNNTs.

2.9.3 Polymer-Nanotube Composites

Tong et al. [75] prepared modified polyethylene (PE) and single-wall carbon nanotubes (SWNTs) via in-situ Ziegler-Natta polymerization. Polymerization of ethylene was carried out using a synthesized catalyst which was a modified surface of SWNT/ $\text{MgCl}_2/\text{TiCl}_4$ at 50 °C within a glass reactor. Two different composites, SWNT/PE and modified-SWNT/PE were prepared in order to investigate the influence of surface modification of SWNT. Mechanical test results revealed that the mechanical properties of modified-SWNT/PE were better than SWNT/PE because of the strong interaction between in-situ polymerized SWNT and PE. For example, tensile test properties such as yield strength, tensile strength and modulus of

modified-SWNT/PE were enhanced to 25, 15.2 and 25.4% as compared to raw-SWNT/PE.

Park et al. [76] fabricated polystyrene (PS) and multi-wall carbon nanotubes (MWNTs) with modified surface using in-situ bulk polymerization method. The polymerization was initiated by AIBN at 70 °C for 48 hrs polymerization reaction time within a three-neck pyrex reactor. The prepared composite was characterized especially in terms of molecular weight, structural and morphological analysis. GPC analysis revealed that when the addition of CNT was increased up to 1.0 wt %, the polydispersity index (PDI) was increased as compared to neat polystyrene. SEM images of composite showed that dispersion of CNTs into polystyrene matrix was achieved with the help of in-situ polymerization method. In addition to that, rheological measurements were agreement SEM results because of the effective load transfer.

Mhetre et al. [77] prepared the nylon 6 and multi-wall carbon nanotubes (MWNTs) composite using a in-situ polymerization technique. Ultrasonication and quick polymerization was carried out in order to disperse carbon nanotubes in polymer matrix uniformly. The preparation of the composite using a quick polymerization and followed by ultrasonication was a very effective method to disperse nanotubes without using any solvent or chemical treatment of nanotubes. Mechanical results revealed that remarkable enhancement was observed at very low concentration of CNTs because of the high aspect ratio of carbon nanotubes. Molecular weight results showed that the viscosity average molecular weight of composites was decreased dramatically with increasing the addition of CNTs. This shows that polymer chain growth of prepared composites was reduced because of the better dispersion of CNTs.

Lahelin et al. [78] fabricated the composites polystyrene (PS), poly (methyl methacrylate) (PMMA) and carbon nanotubes (CNTs) separately using in-situ emulsion and emulsion/suspension polymerization method. The addition of CNTs varied from 0 to 15 wt%. Mechanical properties revealed that the significant improvement was obtained at low concentration. On the other hand, molecular weight of composites increased with the addition of CNTs. Therefore, it was very

difficult to evaluate which parameter had much more influence to improve the mechanical properties.

Annala et al. [79] prepared the composites of polystyrene (PS), poly (methyl methacrylate) (PMMA) and carbon nanotubes (CNTs) separately by using in-situ polymerized masterbatch or melt mixing method, respectively. When compared the interfacial adhesion between polymer and nanotubes with respect to composites and preparation methods, the better resistivity results of the PS/CNTs composites prepared by melt mixing method showed the good adhesion between polymer and nanotubes than the others.

Zhi et al. [14] fabricated the Polyaniline (PANI)-BNNT composite films using solution mixing method. BNNTs were synthesized from the mixture of boron and metal oxide using CVD method. Raman, UV/Vis absorption and XRD revealed that the strong interaction between BNNT and PANI was observed using the solution mixing method. On the other hand, SEM images of composites showed that the dispersion of BNNTs into the polymer matrix was not achieved due to shrink and broken of composite films. Long irradiation time caused to broken of composite films.

Zhi et al. [10] fabricated the Polystyrene (PS)-BNNT composite films using solution dispersion method. CVD method was again used to synthesize BNNTs. PS/BNNT composite films showed a perfect transparency as compared to polymer-CNT composites. The aim was to improve mechanical and thermal properties of composites. Tensile test was showed that Young's modulus of composite was increased by ~21% with the addition of 1 wt% BNNTs. TEM images confirmed that the dispersion of BNNTs and the strength interfacial between PS and BNNT improved using PmPV solvent. Thermal properties of composites were investigated in terms of DSC and TGA analysis. Oxidative temperatures of the composites were enhanced from 358 to 388 °C with addition of 1 wt% BNNTs. On the other hand, the glass transition temperature of PS was decreased by only 3.5 °C at 3.0 wt% BNNTs.

Harrison et al. [80] prepared extruded polyethylene (PE)-hexagonal boron nitride composites using melt mixing method. Mechanical and radiation shielding properties

of composites were examined. In order to improve the interfacial adhesion between boron nitride and PE, the powder surface of the boron nitride was functionalized using a trifunctional alkoxy silane coupling agent and those were mixed in water solution in order to obtain modified boron nitride. Based on mechanical results of composites, tensile modulus of neat PE was improved by the addition of 15 vol% of hexagonal boron nitride. The functionalized surfaces of boron nitride were induced to obtain this improvement especially in tensile modulus of composites. On the other hand, the tensile strength of composites was improved slightly as compared to tensile modulus. Addition of coupling agent was also increased tensile strength of the composites. The toughness of the material was not improved significantly with respect to neat resin because of the formation of voids by particles. When the surface modified composite with 1.0 wt% BNNT was used, the toughness was also increased.

Zhi et al. [12] fabricated the poly(methylmethacrylate) (PMMA)-BNNT composites using solution dispersion method. Mechanical and thermal behavior of composites was investigated in terms of elastic modulus, strength and elongation, thermal stability, glass transition temperature and thermal conductivity, respectively. Blank PMMA and two different sizes of composite films with a thickness of 27 and 52 μm at 1.0 wt% BNNTs were prepared in order to observe the improvement of mechanical and thermal composites. The modulus of PMMA was improved up to 19% with the addition of 1.0 wt% BNNTs. When the thickness of the composite was increased from 27 to 52 μm at 1.0 wt% BNNTs, modulus (GPa) and elongation (%) of composite was slightly improved from 2.47 to 2.51 and 3.93 to 4.21, respectively. Also, the strength (MPa) of composite films at 1.0 wt% BNNTs were obtained as 54.35 and 54.73 MPa with increasing of the thickness from 27 to 52 μm , respectively. TGA and DSC analysis revealed that the stability of PMMA-BNNT composite at 1.0 wt% BNNTs was increased slightly as compared to blank PMMA composite films and glass transition of composite was increased from 82.9 to 85.2 $^{\circ}\text{C}$ because of the mobility of chains. In order to investigate the thermal conductivity of PMMA/BNNT composites with 5 and 10 wt% BNNTs, thermal conductivity of PMMA/BNNT composites with 10 wt% BNNTs was increased three times as compared to neat PMMA.

Ravichandran et al. [81] produced polymer–BNNT composite in order to use a specific application of packaging of organic photovoltaic (OPV) device. Polymer matrix can be chosen as Saran (a co-polymer of vinylidene chloride and acrylonitrile). BNNTs were synthesized from the reaction of boron, iron oxide and magnesium oxide at 1200 °C. The BNNT loading in polymer matrix was increased up to 1.5 wt% of BNNTs. High transparency in visible region, good barrier properties and thermal stability were shown in resulting composites.

Zhi et al. [82] fabricated the composites of poly(methyl methacrylate) (PMMA), polystyrene (PS), poly(vinylbutyral) (PVB) and poly(ethylene vinyl alcohol) (PEVA) with purified BNNTs. Thermal, mechanical and electrical properties of composites were investigated. Thermal conductivity of polymers increased with the addition of 18-37 wt% BNNTs. The addition of BNNTs decreased the coefficient of thermal expansion (CTE) of polymer.

Terao et al. [83] produced the composite films which contains polyvinyl formal (PVF)/BNNTs. The improvement of thermal conductivity of composites was aimed. With 1 wt% and 10 wt% of BNNT loading, thermal conductivity of composites were dramatically increased.

Demir [11] prepared the polypropylene (PP)-BNNT composites with different BNNT loadings using a twin-screw extrusion. BNNTs were synthesized from the reaction of ammonia gas with a powder mixture of elemental boron and iron oxide. The effects of BNNT addition on the thermal and mechanical properties of the composites were investigated in terms of crystallization temperature, thermal stability and coefficient of linear thermal expansion, tensile strength, yield strength, elongation at break and Young's modulus. Characterization of composite in terms of thermal behavior revealed that thermal stability of the all composites was improved as compared to neat resin. Also, a significant enhancement was observed in terms of crystallization temperature (T_c) of composites with BNNT addition. The mechanical test results were shown that the addition of 0.5 and 1.0 wt% BNNTs slightly improved the yield strength and Young's modulus with respect to neat PP. The tensile strength and elongation at break values of composites were decreased with the addition of BNNTs.

Li et al. [13] produced the polyurethane (PU)-BNNT composites at different volume contents. The solution dispersion method was used to prepare the composites. Mechanical test results revealed that with the addition of 0.5 vol% and 2.0 vol% of BNNTs, the compressive modulus of composites was improved at the percentage of 38.2 and 6.3, respectively. Rockwell hardness values (HRR) of composites decreased with an increasing volume fraction. The Rockwell hardness value of neat polyurethane was determined as 80.7 ± 2.1 HRR. When the hardness of BNNTs composites was measured at 0.5 vol% and 2.0 vol%, it was found as 79.1 ± 1.9 HRR and 76.2 ± 4.2 HRR, respectively.

2.10 Motivation of the Study

According to the studies on polymer-nanotube composites, the effect of BNNTs on mechanical and thermal properties together with preserving the electrically isolating nature has been verified. However, during these studies most of polymer-BNNT composites were prepared using solution dispersion or melt blending technique. Even though solution mixing method can be considered as an appropriate method for research purpose in order to disperse nanotubes in polymer matrix, it has the disadvantage of using solvent. The melt mixing method, on the other hand, is a widely used technique due to easy processing and low cost. Even if these methods are applied to prepare the composites, homogeneous dispersion of BNNT fillers in the polymer matrix has not been accomplished yet.

The importance of this study is to introduce a new approach, which is to prepare masterbatch of polystyrene (PS)-BNNTs nanocomposites applying in-situ polymerization and to use their masterbatch in the melt mixing method. To the best of our knowledge, this approach is firstly used for the preparation of PS-BNNT composites.

The main objectives of this study are:

- to synthesize polystyrene via two different polymerization techniques and characterize them using FTIR, viscosity average molecular weight, GPC and MFI techniques,
- to synthesize BNNTs from the reaction of ammonia gas with a powder mixture of elemental boron and iron oxide, to purify them using acid treatment, and to characterize the purified BNNTs with the help of XRD, surface area measurement and SEM analysis,
- to prepare PS-BNNT composites through melt mixing, in-situ polymerization, and masterbatch with extrusion methods and to characterize them,
- to investigate the effect of BNNT concentration on mechanical and thermal properties of PS-BNNT composites prepared by masterbatch with extrusion method,
- to investigate the effect of composite preparation methods with the same BNNT loading on the mechanical and thermal behavior of composites.

CHAPTER 3

EXPERIMENTAL

3.1 Materials

3.1.1 Polystyrene

The polystyrene with a trade name of Styrolution PS 116 N/L was purchased from ULTRAPOLYMERS company. The pellet form of this material was used throughout the study. The properties of Styrolution PS 116 N/L which was given by the supplier are shown in Table 3.1 and chemical structure of polystyrene is given in Figure 3.1.

Table 3.1 Properties of polystyrene (Styrolution PS 116 N/L) [84]

Property	Standard	Value
Rheological		
Melt Volume Rate, (5kg/200 °C), cm ³ /10 min	ISO 1133	23
Thermal		
Vicat Softening Temperature, B/2 (120 °C/h, 50 N), °C	ASTMD 1525	85
Coefficient of Linear Thermal Expansion, 10-6/°C	ISO 11359	80
Heat Deflection Temperature A; (Annealed, 1.8 MPa), °C	ISO 75	75
Thermal Conductivity, W/(m.K)	DIN 52612-1	0.16
Mechanical		
Charpy Unnotched, 23 °C, kJ/m ²	ISO 179	9
Tensile Stress at Yield, 23 °C, MPa	ISO 527	40
Tensile Strain at Yield, 23 °C, %	ISO 527	1.5
Tensile Modulus, MPa	ISO 527	3100
Flexural Strength, MPa	ISO 178	70

Table 3.1 (Cont'd) Properties of polystyrene (Styrolution PS 116 N/L)

Property	Standard	Value
Mechanical		
Hardness, Ball Indentation, MPa	ISO-2039-1	150
Electrical		
Volume Resistivity, Ohm*m	IEC 60093	$> 1*10^{16}$
Surface Resistivity, Ohm	IEC 60093	$> 1*10^{13}$
Other Properties		
Density, kg/m ³	ISO 1183	1040

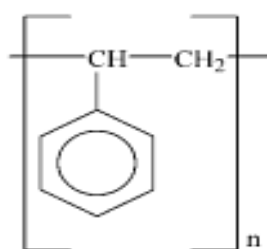


Figure 3.1 Chemical structure of polystyrene [85].

3.1.2 Styrene

Styrene, used as a monomer in polymerization was purchased from Sigma-Aldrich. Its chemical structure is shown in Figure 3.2 and some of properties are given in Table 3.2.

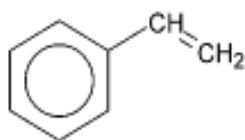


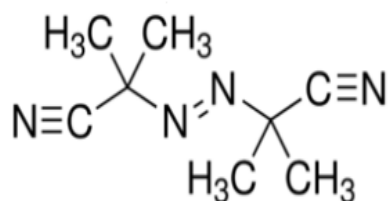
Figure 3.2 Chemical structure of styrene [85].

Table 3.2 Properties of styrene

Properties	Value
Molecular Weight (g/mol)	104.15
Boiling Point Temperature (°C)	145-146
Melting Point Temperature (°C)	-31
Autoignition Temperature (°F)	914
Density (g/mL at 25 °C)	0.906

3.1.3 Azobisisobutyronitrile

Azobisisobutyronitrile, abbreviated by AIBN was used as an initiator in the polymerization of styrene. It was purchased from Sigma-Aldrich. Its chemical structure and some of the important properties are given in Figure 3.3 and Table 3.3, respectively.

**Figure 3.3** Chemical structure of AIBN [86].**Table 3.3** Properties of AIBN

Chemical Formula	C ₈ H ₁₂ N ₄
Molecular Weight (g/mol)	164.21
Storage Temperature (°C)	2-8

3.2 Polymerization of Styrene

3.2.1 Experimental Procedure

3.2.1.1 Solution Polymerization

In general, polystyrene (PS) was synthesized by two different polymerization techniques. Firstly, solution polymerization was used to synthesize polystyrene. In this method, 500 mL three-necked balloon with condenser and thermometer were used for the synthesis. As a first step, 100 mL of toluene was gradually added into 0.25 gram of AIBN. This solution was mixed approximately 7 hrs at room temperature. Afterwards, 50 mL of styrene was added into this solution. Polymerization reaction time and temperature were 3 hrs and 95 °C, respectively. Then, 300 mL of ethanol was poured into polymer solution. The precipitated polymer was put in an oven at 90 °C for drying. Figure 3.4 is the schematic view of the procedure of solution polymerization technique.

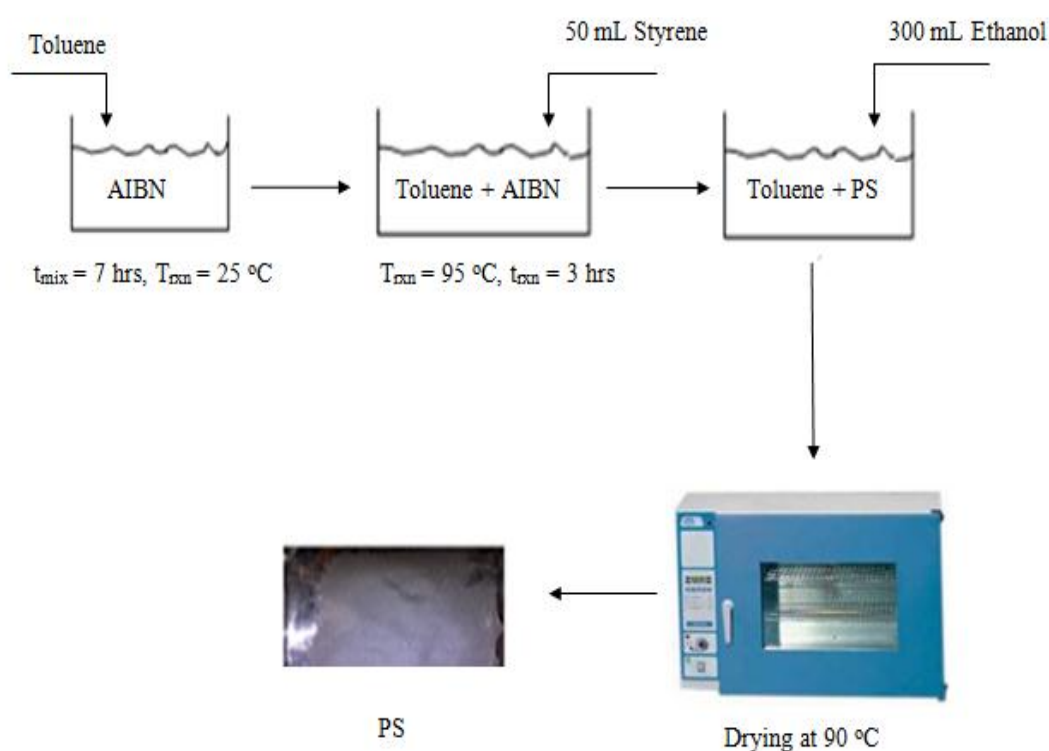


Figure 3.4 Schematic view of solution polymerization.

3.2.1.2 Bulk Polymerization

First, 100 mL of styrene was gradually added into 0.18 gram of AIBN. This solution was stirred 5 hrs in 500 mL three necked balloon. After that, polymerization was initiated by applying heat. The polymerization reaction time was 3 hrs and reaction temperature was 95 °C. At the end of the reaction, highly viscous polystyrene was obtained and it was poured onto aluminum mold and left for drying in an oven at 90 °C for 18 hrs. Dried PS was taken from aluminum mold and crushed into small pieces in mortar. Lastly, the small PS pieces were frozen inside liquid N₂ and then recrushed immediately in order to obtain powder form of PS. The experimental set-up used for PS synthesis is shown in Figure 3.5.

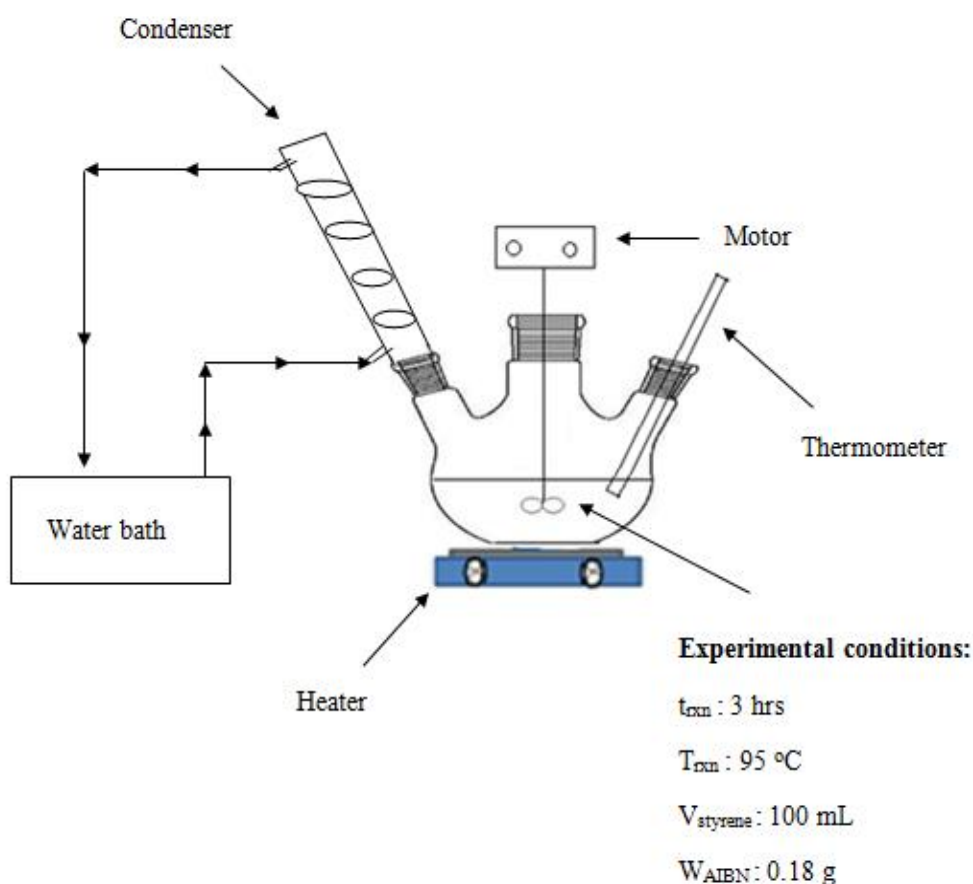


Figure 3.5 Schematic representation of bulk polymerization experimental set-up.

3.2.1.3 Polystyrene Synthesis Parameters

3.2.1.3.1 Optimization of Synthesis Parameters for Solution Polymerization

There were three main synthesis parameters for PS synthesis which are reaction temperature, reaction time, initiator concentration in the presence or absence of solvent.

Polymerization temperature and initiator concentration parameters were kept constant during the solution polymerization experiments. They were set to 95 °C and 0.03 mol/L, respectively. High molecular weight of PS was aimed in this synthesis. Therefore, reaction time was changed from 1.5 hrs to 9 hrs in order to investigate the effect of polymerization time on PS molecular weight in the presence of solvent. Polymerization medium was also changed depending on the presence or absence of solvent. Table 3.4 summarizes the polymerization time and medium which was tested to determine the best synthesis conditions for PS.

Table 3.4 Tested parameters in polystyrene synthesis for solution polymerization

Polymerization Run	t_{rxn} (hrs)	Polymerization Medium
1	1.5	with solvent
2	3	
3	6	
4	9	
5	3	without solvent

3.2.1.3.2 Optimization of Synthesis Parameters for Bulk Polymerization

By considering the tested parameters for solution polymerization and the aim of this study, polymerization reaction time and initiator concentration in bulk polymerization were changed in order to obtain high molecular weight PS which is close to commercial PS. Polymerization time between 1.5 and 6 hrs and initiator concentration from 0.03 to 0.01 mol/L were changed by keeping reaction

temperature at 95 °C. Table 3.5 shows the tested parameters to find the best synthesis condition for bulk polymerization.

Table 3.5 Tested parameters in polystyrene synthesis for bulk polymerization

Polymerization Run	t_{rxn} (hrs)	Initiator Concentration (mol/L)
1	1.5	0.03
2	3	
3	6	
4	3	0.03
5		0.02
6		0.01

3.3 Production of BNNTs

3.3.1 Experimental Set-Up

BNNTs production was performed by the reaction of ammonia gas with a mixture of elemental boron and iron oxide inside a horizontal tubular furnace. General view of the production of BNNT system is given in Figure 3.6.

Main part of BNNT production system is the Protherm PTF 16/50/450 horizontal tubular furnace. Type B thermocouple is used to measure temperature at the inner center of the furnace. Reaction chamber is a tubular form and made from alumina. Also, the inner diameter of chamber is 50 mm. High purity argon and ammonia were used and connected to the tubular reactor. Inlet flow rates of argon and ammonia were adjusted by rotameters. The inlet and outlet volumetric flow rates of both gases were checked using soap bubble meter. While the furnace was being purged by argon, 3-way valve was used to regulate the flow of ammonia with the help of bypass line [11].

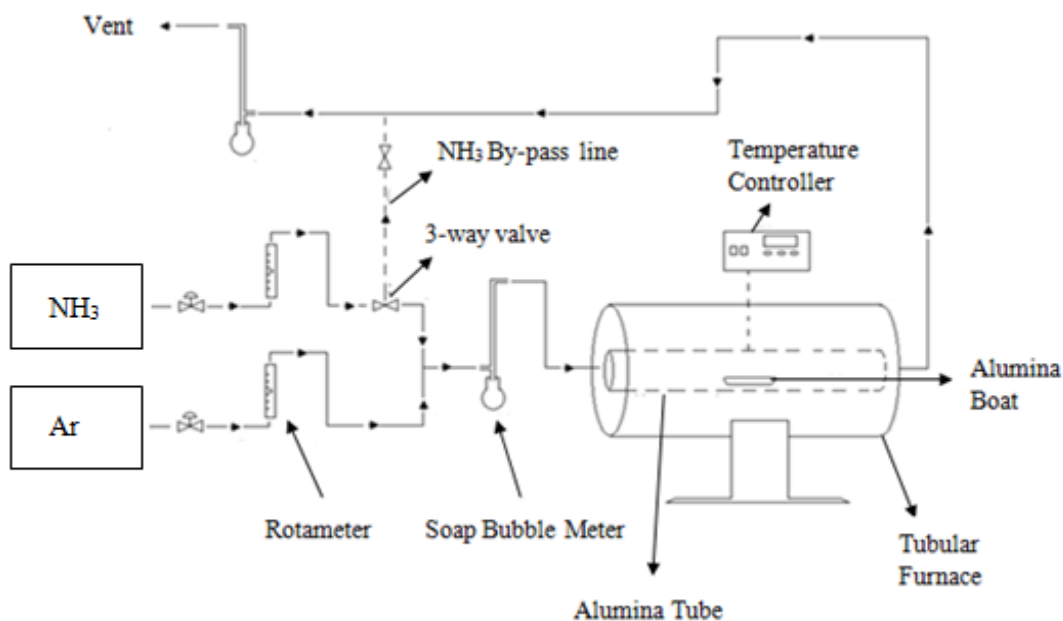


Figure 3.6 BNNT production system [11].

3.3.2 Experimental Procedure

Initially, 15/1 ratio of elemental boron to iron oxide mixture was prepared. The powder mixture was homogenized using agate mortar until the iron oxide disappears. Homogenized mixture was taken into alumina boat with dimensions of 120x30x15 mm. The alumina boat was centered into the tubular furnace. The furnace temperature was set 1300 °C using temperature controller. The regulators of argon and ammonia gas tubes were set at 2 bars.

While the temperature of tubular reactor was increasing with a heating rate of 8 °C/min up to 1300 °C, argon was also passed through the system at a flow rate of 125 cc/min for cleaning the system. When the temperature was reached 1300 °C, argon was shut off immediately and ammonia was fed to system with a flow rate of 125 cc/min. The reaction time was 2.15 hrs.

As the reaction period was completed, tubular reactor was cooled down with a cooling rate of 5 °C/min. After cooling, the product was taken from the system. Physical appearance, color and total weight of product were recorded.

Each batch of synthesized BNNTs had to be in powder form. Therefore, agate mortar was used for powdering the material.

3.3.3 Purification of BNNTs

BNNTs purification was necessary step for removing impurities in the synthesized product. The purification procedure given in Noyan's study [74] was modified. In the purification process, approximately 1 gram of synthesized BNNTs was used for purification. At the initial stage, BNNTs were dried at 40 °C for 3 hrs. After drying, 25 mL of pure water was added and the mixture was sonicated for 2 hrs at room temperature in order to get better dispersion. 25 mL of nitric acid was added to mixture in order to get rid of boron element from BNNTs.

This acid treatment procedure was repeated several times by adding same amount of pure water and nitric acid. In order to separate boron nitride nanotubes, the solution was filtrated by using filtration paper. To get rid of remaining iron content, BNNTs were taken from filtration paper by washed with pure water. 20 mL HCl and 10 mL HNO₃ was added into BNNTs. The mixture was boiled for 3 hrs in order to remove iron content. BNNTs were retrieved from mixture by filtration. Finally, BNNTs were dried for 3 hrs at 75 °C in an oven. This procedure was repeated several times in order to eliminate the boron and iron content from BNNTs. Figure 3.7 shows the whole procedure of BNNTs purification process.

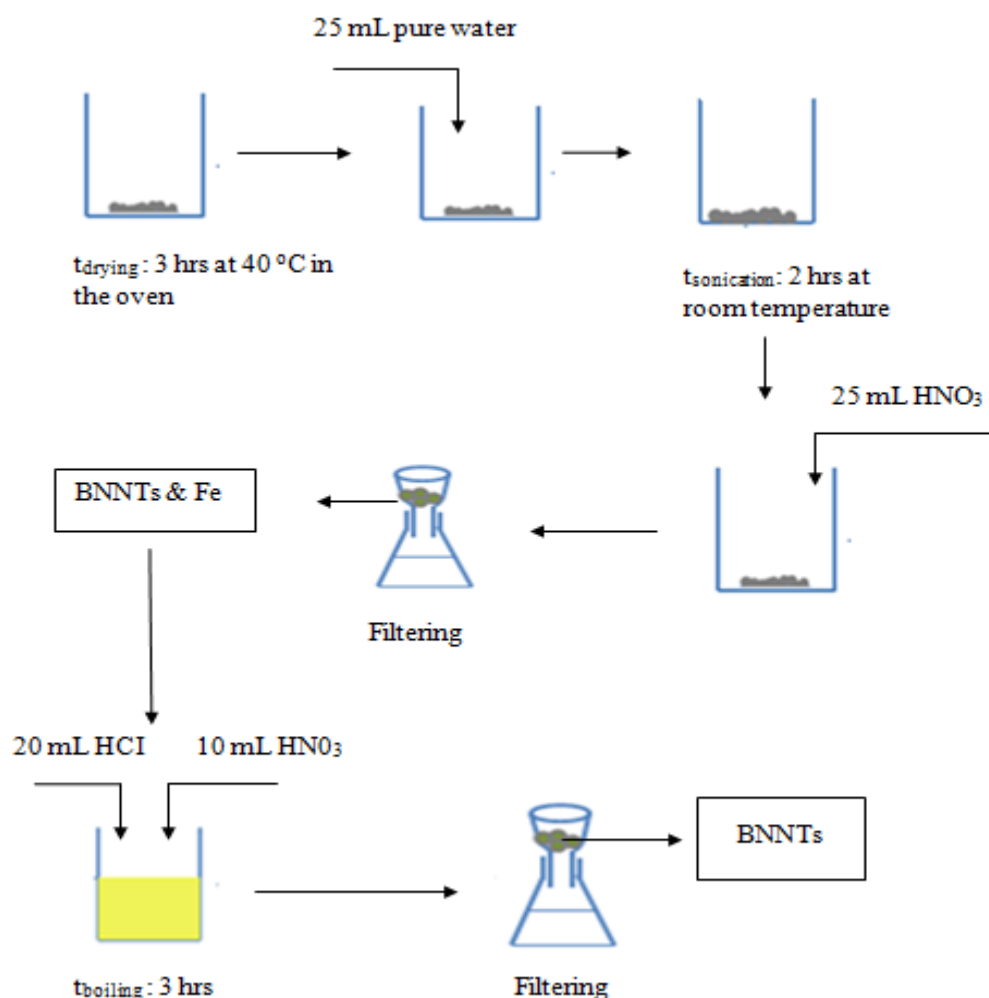


Figure 3.7 Purification of BNNTs.

3.4 Preparation of PS-BNNT Nanocomposites

Three different preparation methods which were melt blending, in-situ polymerization and masterbatch with extrusion were used in this study. The composites were first prepared by masterbatch with extrusion method at 0.5, 1.0 and 3.0 wt% BNNTs. Melt blending and in-situ polymerization methods were also applied separately in order to fabricate PS-BNNT composites at a selected composition.

3.4.1 Melt Blending Method

PS-BNNTs composites were prepared by melt compounding, in a co-rotating twin screw extruder. Thermoprism TSE 16 TC twin screw extruder (L/D = 24) was used in the fabrication of PS-BNNTs composites. Figure 3.8 shows the photograph of twin screw extruder. During the process, temperature profile and screw speed were kept constant. Temperature profile was set to 180-200-200-200-200 °C from main hopper to die and screw speed was specified as 120 rpm.

Prior to preparing nanocomposite, PS pellets were grinded to powder in order to obtain same form with BNNTs. PS and BNNTs were dried at 80 °C overnight and at 40 °C for 3 hrs, respectively. After drying, mixture of PS and BNNTs were fed from main feeder under specified temperature and screw speed conditions. The 0.5 wt% BNNTs extrudate was withdrawn from die and immersed immediately into a water bath in order to cool down. The nanocomposite was ground before using in injection molding machine.



Figure 3.8 Thermoprism TSE 16 TC twin screw extruder.

3.4.2 In-Situ Polymerization Method

In-situ polymerization method, purified BNNTs were dispersed into styrene monomer in order to synthesize nanocomposite by using bulk polymerization method. This process was initiated by adding 100 mL of styrene monomer into 0.18 gram of AIBN gradually. The mixture was stirred approximately 3 hrs. 0.25 gram of BNNTs was fed to styrene solution. In order to get better dispersion, the mixture was mixed 2 hrs at room temperature. Heat was given to the system in order to initiate the polymerization which took place at 95 °C and 3 hrs. The nanocomposite which was obtained at the end of polymerization was poured into aluminum molds and dried at 90 °C for 18 hrs. The nanocomposite was ground and prepared in powder form for the use in injection molding process.

3.4.3 Masterbatch with Extrusion Method

This technique was basically composed of two methods that are in-situ polymerization and melt blending. In initial stage, a concentrated mixture of PS-BNNT (masterbatch) was prepared. PS with high loading of BNNTs was synthesized using in-situ polymerization method. In the preparation of masterbatch, same procedure given for in-situ polymerization method was followed. At the end of polymerization, composite containing high amount of BNNTs was casted into aluminum molds and dried at 90 °C for 18 hrs. The concentrated composite was ground and prepared in powder form before extrusion. In the second part of masterbatch with extrusion method, a mixture of commercial PS and masterbatch in powder form was prepared in the extruder at desired compositions such as 0.5%, 1% and 3%. The mixture was fed from primary feeder of twin screw extruder by using same process condition reported in the melt blending method. The extrudate was taken from die and cooled down by using water bath. Finally, extrudate was ground into the pellet form to use in the injection molding process for characterization purpose.

All composites prepared by different methods in this study were given in Table 3.6. For simplicity, two different code names were given to the materials,

MPS + W

where M indicates the initials of preparation methods of nanocomposite. M represents the ME for the masterbatch with extrusion method, ISP is the initials of in-situ polymerization, and E denotes the extrusion method. By the way, cPS represents the commercial polystyrene used in extrusion process. W denotes weight percentage of BNNTs in the composites. BULK-sPS and SOL-sPS denote polystyrene synthesized via bulk and solution polymerization methods, respectively. The synthesis conditions of bulk polymerization are given in different format.

M-sPS-X-Y-Z

where X, Y, and Z denotes the reaction temperature ($^{\circ}\text{C}$), polymerization reaction time (hrs) and initiator (mol/L) concentration, respectively.

Table 3.6 Composition of all composites and their synthesis parameters

Synthesis & Processing Techniques	Composite Name	Polymer Synthesis Conditions (Type-Temperature-Time-Initiator Concentration)	Composition (wt%)	
			PS	BNNTs
Synthesis via Bulk Polymerization	BULK-sPS	BULK-sPS-95-3-0.01	100	-
Masterbatch with extrusion (ME)	ME-PS		100	-
	ME-PS + 0.5		99.5	0.5
	ME-PS + 1.0		99	1
	ME-PS + 3.0		97	3
In-Situ Polymerization (ISP)	ISP-PS + 0.5	99.5	0.5	
Extrusion (E)	E-cPS	-	100	-
	E-cPS + 0.5		99.5	0.5

3.5 Sample Preparation for Characterization

3.5.1 Injection Molding

DSM Xplore laboratory scale (10 cc) injection molding equipment was used for molding the specimens in order to use for characterization purpose. The photography of this equipment is shown in Figure 3.9. Two specimens which were tensile and impact samples were obtained in each operation of molding. Tensile and impact test specimens were in the dog bone shape and in the form of rectangular shape, respectively. Pressure cylinder unit with piston assembled helps to inject polymer melt inside the barrel into the steel mold.

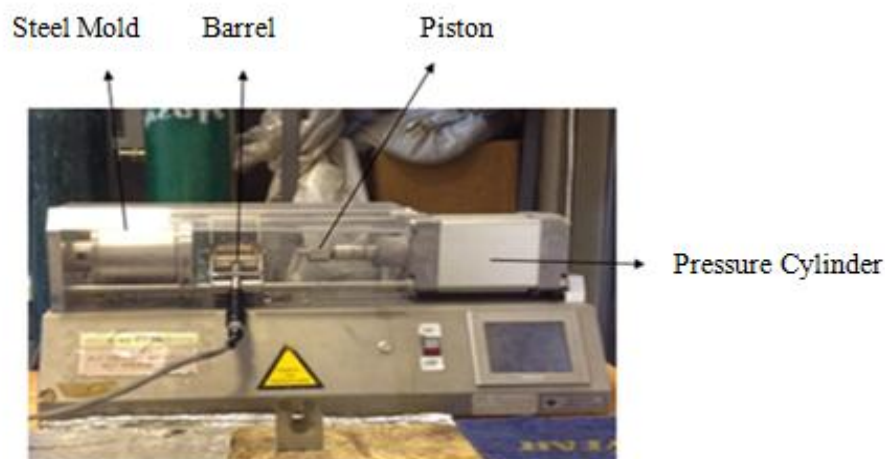


Figure 3.9 DSM Xplore injection molding.

Before molding the samples, both synthesized pure PS in powder form and polystyrene-BNNT composite pellets were dried overnight at 80 °C. The dried materials were put into barrel by using spoon and kept in the barrel in order to be melted for 3 mins. Molten polymer was injected into a steel mold with a pressure of 13 bars. During the molding process, melt and mold temperatures were 200 and 90 °C, respectively.

3.6 Characterization Studies

3.6.1. Characterization of Polymerization of Styrene

Determination of chemical structure of synthesized PS and its molecular weight was the main points of PS synthesis characterization studies. Chemical compositions of synthesized materials were analyzed by FTIR analyses. It was very helpful technique to prove whether the PS was synthesized or not. Also, it was given a chance about comparison of synthesized PS FTIR spectrum with commercial PS.

Molecular weight distribution of synthesized PS was mainly determined by viscosity average molecular weight and gel-permeation chromatography (GPC) technique. Melt flow index (MFI) was another option to obtain information molecular weight of PS. The molecular weight of synthesized PS was also compared with commercial PS using these molecular weight determination techniques.

3.6.1.1 Fourier Transform Infrared (FTIR) Spectroscopy

ATR-FTIR Spectroscopy analysis was carried out to analyze the chemical composition of synthesized PS and the nanocomposites. IR- Prestige-21 Shimadzu instrument was used for understanding the chemical structure of materials. Synthesized PS and their nanocomposites were detected between wavenumbers from 650 cm^{-1} to 4000 cm^{-1} .

3.6.1.2 Measurement of Molecular Weight

3.6.1.2.1 Viscosity Average Molecular Weight (M_v)

Viscosity average molecular weight analysis was aimed to measure viscosity of dilute polymer solutions. Dilute synthesized PS solutions were prepared from 1 g/dl to 0.2 g/dl. Flow times of the solutions were measured at $30\text{ }^\circ\text{C}$ using a Ubbelohde viscometer. Inherent and reduced viscosities were plotted relative to concentration of solutions to find intrinsic viscosity. The viscosity average molecular weight of synthesized PS was calculated using intrinsic viscosity in Mark-Houwink equation [20].

3.6.1.2.2 Gel Permeation Chromatography (GPC)

GPC was one of the most common methods to determine the molecular weight distribution of polymers. GPC analyses were performed using Agilent Technologies 1200 series. ELSD (Evaporative Light Scattering Detector) and ZORBAX PSM 300-S column (6.2x250 mm with $5\text{ }\mu$ size of particles) were used in these analyses. Measurable molecular weight was ranging from 3000-300.000 in the column.

Tetrahydrofuran (THF) was used to dissolve polymer samples in order to prepare for analyses. During the experiment, the temperature of the column was held constant at room temperature and the flow rate of the eluent (THF) was 0.6 mL/min . The calibration curve was determined using PS standards with different molecular weights (M_p : 3950, 10210, 29510, 72450, 205000, 467000).

3.6.1.3 Melt Flow Index (MFI) Measurement

Melt flow index (MFI) measurement was carried out according to the procedure identified in ASTM D1238-79 using an Omega Melt Flow Indexer. The experiment was carried out at a temperature of 200 °C using 5 kg polymer load. The weight of polymer melt which passes through the die in 10 seconds was obtained. At least five measurements of each sample were taken to get more accurate result. The MFI value was reported in grams/10 min.

3.6.2 Characterization of Purified BNNTs

Crystalline structure, morphology, and physical properties of purified BNNTs were characterized using XRD, BET and SEM methods. XRD was the technique to obtain information about crystalline phase which exists in BNNTs. Surface area measurement was used to determine physical properties of synthesized BNNTs like surface area, total pore volume and average pore size distribution. SEM method was used to obtain information about surface morphology of purified BNNTs.

3.6.2.1 X- Ray Diffraction (XRD)

Rigaku X-Ray diffractometer was used to determine crystalline phases in the BNNT. CuK_α radiation source was used. Bragg angle range was from 20° to 90° with a scanning rate of 1°/min. Voltage and current was held at 40 kV and 40 mA, respectively.

3.6.2.2 Surface Area Measurement

Multi-point BET surface analysis of purified BNNTs was performed using a Micromeritics TriStar II. The material was dried at 110 °C overnight and degassed for 45 minutes. The main reason for degassing was to remove moisture and other possible adsorbed gases in the pores of the material.

Nitrogen adsorption/desorption isotherms of the BNNT were obtained at a relative pressure range of 5×10^{-2} to 0.99 at liquid nitrogen temperature.

3.6.2.3 Scanning Electron Microscopy (SEM)

Quanta 400 F Field Emission Scanning Electron Microscope was used to monitor the surface morphology of purified BNNTs. Before examining the surface of the BNNTs, the sample was coated with gold-palladium alloy to become electrically conductive.

3.6.3 Characterization of PS-BNNT Composites

3.6.3.1 Morphological Analysis

3.6.3.1.1 Scanning Electron Microscopy (SEM)

Powder form of synthesized PS and impact fracture surfaces of PS/BNNT composites were examined using a Quanta 400 F Field Emission Scanning Electron Microscope in order to monitor surface morphology. It was necessary to examine the dispersion of BNNTs in the polymer matrix and failure mechanisms of the materials. The surface of synthesized materials and the nanocomposites were coated with gold-palladium alloy to get an electrically conductive surface.

3.6.3.2 Mechanical Analysis

Tensile and impact tests were performed to observe the effect of BNNT loading on mechanical properties of the composites.

3.6.3.2.1 Tensile Test

Shimadzu AG-IS 100 kN testing machine was used for tensile test. Stress-strain curves were obtained for each PS-BNNT composite based on the standards of ISO-527. Tensile test specimen and their dimensions are given in Figure 3.10 and Table 3.7, respectively.

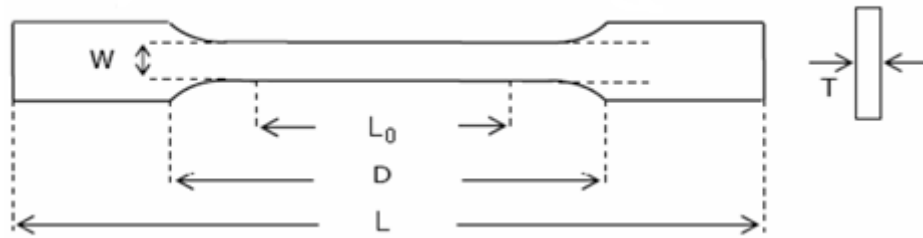


Figure 3.10 Tensile Test Specimen.

Table 3.7 Dimensions of the tensile test specimen

Dimension	Value (mm)
L- Overall Length	72
D- Distance between grips	40
Lo- Gauge length	30
W- Width of narrow portion	4
Thickness	2

The crosshead speed (rate of strain) was set to 3 mm/min for all composites. A small gap was formed in injection molded tensile test specimen while removing the specimens from steel mold. Therefore, one side of specimen was coated with play dough. Distance between the clamped points of tensile specimens was adjusted to 30 mm. The test was carried out at 23 °C and conducted until the specimen fails. Tensile strength, Young's modulus and elongation at break values were calculated as the average of at least five specimens with standard deviations.

3.6.3.2.2 Impact Test

Ceast Resil Impactor was used to perform the un-notched charpy impact test. Dimensions of samples are 80x10x4 mm according to ISO 179. Photograph of device is given in Figure 3.11. Each composition was tested at 23 °C and values of all composite results were calculated by taking at least the average of five measurements.



Figure 3.11 Ceast Resil Impactor.

3.6.3.3 Thermal Analysis

Differential scanning calorimetry (DSC) and thermal gravimetric analysis (TGA) characterization techniques were used in order to determine the effect of BNNT addition on thermal properties of the glass transition and thermal stability on the composites, respectively.

3.6.3.3.1 Differential Scanning Calorimetry (DSC)

A Shimadzu DSC-60 differential scanning calorimeter was used in order to observe the glass transition temperature (T_g) of polystyrene and PS based composites. The sample was heated from 20 °C to 250 °C with a heating rate of 10 °C/min, and then cooled to room temperature, and heated to 250 °C again. The experiment was performed under nitrogen atmosphere. The samples were cut from tensile test specimen.

3.6.3.3.2 Thermal Gravimetric Analysis (TGA)

In this study, a Shimadzu DTG-60/60H was used to see thermal stability behavior of PS and PS-BNNT composites. The samples were heated from 20 °C to 700 °C with a constant heating rate of 10 °C/min, under nitrogen atmosphere with a flow rate of 70 ml/min. TGA specimens were also cut from the tensile test specimen.

CHAPTER 4

RESULTS AND DISCUSSION

This section of the thesis is considered under three main parts. In the first part, PS synthesis using solution and bulk polymerization techniques is taken into account together with its characterization in terms of FTIR, viscosity average molecular weight (M_v), GPC, and MFI analyses. The synthesized PS is also compared with commercial PS to see whether or not they possess the same structure and properties. The second part is related to the synthesis of BNNTs from the reaction of ammonia gas with the powder mixture of elemental boron and iron oxide, and its purification. This part also concentrates on the characterization of purified BNNTs by XRD, surface area measurement and SEM analyses. In the last part, preparation of masterbatch which is a concentrated mixture of PS-BNNTs obtained through polymerization of styrene monomer containing high amount of BNNTs is studied. Mixing of masterbatch with commercial PS is mainly focused to obtain PS-BNNT composites at desired compositions mentioned in Table 3.6. They are also characterized with respect to their morphology, mechanical, and thermal properties. Composite preparation techniques in terms of masterbatch with extrusion, in-situ polymerization and extrusion are also taken into account at a selected BNNT loading. These three preparation methods are compared in terms of the properties mentioned above.

4.1 Polystyrene Synthesis and Characterization

4.1.1 Effect of Synthesis Parameters in Solution Polymerization Technique on Molecular Weight of PS

As it is mentioned before, first solution polymerization method was used to synthesize PS (SOL-sPS). In order to determine the best conditions for PS synthesis, solution polymerization experiments were conducted at different polymerization reaction times (1.5 to 9 hrs) in the presence or absence of solvent. During these experiments, polymerization temperature and initiator concentration were kept constant at 95 °C and 0.03 mol/L, respectively. Synthesis of high molecular weight PS is the main concern of this study. High molecular weight PS which is close to the molecular weight of commercial PS is also needed.

Table 4.1 gives the viscosity average molecular weight of synthesized PS with respect to the reaction time in the presence or absence of solvent. Calculations of intrinsic viscosities of synthesized polymers and the values obtained through these calculations are given in Appendix A. It is noted that measurement of viscosity average molecular weight is directly related with intrinsic viscosity $[\eta]$ of polymer solution. Molecular weight of the polymer in solution, the polymer-solvent system and the temperature are the main parameters affecting the intrinsic viscosity [21]. It is the easiest and rapid technique to get information about the molecular weight of synthesized polymer [53]. Therefore, it is selected as a primary method to determine molecular weight of synthesized polymers via solution polymerization technique.

As can be seen in Table 4.1, viscosity average molecular weight of synthesized polystyrene in the presence of solvent is extremely low at each reaction time. The main reason is that solvent lowers the viscosity of medium. In other words, increase in viscosity during polymerization is affected negatively due to the use of solvent [53]. Furthermore, solvent decreases the polymerization rate and average chain length of polymer. Chain transfer occurs during polymerization, and solvent acts as a chain transfer agent leading to obtain shorter chains [21]. Therefore, extent of branching and molecular weight distribution (MWD) of synthesized polymers are restricted because of using solvent in the polymerization.

Table 4.1 Viscosity average molecular weight of SOL-sPS with respect to polymerization reaction time at a polymerization reaction temperature of 95 °C and initiator concentration of 0.03 mol/L.

Polymerization Run	t_{rxn} (hrs)	M_v (*10⁻³)	Polymerization Medium
1	1.5	51.6	with solvent
2	3	64.0	
3	6	33.1	
4	9	41.8	
5	3	239.7	without solvent

It can also be seen from Table 4.1 that, the molecular weight of PS at a polymerization reaction time of 3 hrs in the presence of solvent is higher than the others. Therefore, this criterion is selected as the best parameter for the solution polymerization. The best synthesis conditions among tested parameters for PS production using solution polymerization technique are summarized in Table 4.2.

Table 4.2 The best synthesis conditions for PS production via solution polymerization.

Polymerization Type	Polymerization Reaction Temperature (°C)	Polymerization Reaction Time (hrs)	Initiator Concentration (mol/L)
Solution Polymerization	95	3	0.03

Because of the low molecular weight of synthesized PS, polystyrene synthesis was performed in the absence of solvent at the optimum synthesis conditions of solution polymerization technique.

It is observed that the molecular weight of PS synthesized at a polymerization reaction time of 3 hrs is almost six times higher than that of solution polymerization. Therefore, the effect of synthesis parameters in bulk polymerization on molecular weight of PS is studied subsequently in order to obtain higher molecular weight of synthesized PS which is close to commercial PS (cPS).

4.1.2 Effect of Synthesis Parameters in Bulk Polymerization Technique on Molecular Weight of PS

By taking into account the tested parameters in solution polymerization and the aim of this study, polymerization time and initiator concentration in bulk polymerization were changed in order to obtain high molecular weight PS which is close to commercial one.

4.1.2.1 Effect of Polymerization Reaction Time on Molecular Weight of PS

Polymerization reaction time was changed from 1.5 hrs to 6 hrs in order to observe the effect of reaction time on the molecular weight of PS in bulk polymerization. During the experiments, polymerization reaction temperature and initiator concentration were kept constant at 95 °C and 0.03 mol/L, respectively. Synthesized PS using bulk polymerization technique (BULK-sPS) and commercial PS (cPS) are compared in terms of viscosity average molecular weight (M_v) and MFI values given in Table 4.3. The molecular weight of BULK-sPS was compared with that of cPS. Calculation of intrinsic viscosity values of both BULK-sPS and cPS and their plots which are related to inherent and reduced viscosity as a function of concentration are given in Appendix B.

As seen from Table 4.3, when the polymerization reaction time is changed from 1.5 to 3 hrs, the viscosity average molecular weight of BULK-sPS increases from 146200 to 173200. After 3 hrs, a slight decrease is observed for viscosity average molecular weight. It can be explained that free radical polymerization is highly exothermic reaction. The heat dissipation occurs especially for this type of polymerization. Therefore during polymerization, the viscosity of medium increases rapidly. The viscosity and exothermic effects limit the termination rate of free radical

polymerization. This means that the rate of termination becomes lower than the propagation rate [20]. For this reason, the molecular weight of BULK-sPS either slightly decreases or remains constant at certain polymerization time. Hence, a 3 hr polymerization reaction time in bulk polymerization is decided to be used in PS synthesis.

Table 4.3 Viscosity average molecular weight and MFI test results of both cPS and BULK-sPS synthesized using an initiator concentration of 0.03 mol/L at a reaction temperature of 95 °C and at different reaction times.

Polymerization Run	t_{rxn} (hrs)	M_v (*10⁻³)	MFI (g/10 min)
1	1.5	146.2	47.2
2	3	173.2	39.3
3	6	161.9	-
cPS	-	169.8	19.7

Although the viscosity average molecular weight of BULK-sPS synthesized at this 3 hr polymerization reaction time is much closer to that of cPS, the exact value of molecular weight cannot be finalized using this measurement technique [53]. Another measurement technique is essential to make assessment for the effect of polymerization reaction time on the molecular weight of PS synthesized through bulk polymerization. Therefore, Melt Flow Index (MFI) test was carried out to gather more information about the viscosity and molecular weight of polymer. MFI value is inversely proportional to viscosity or molecular weight of polymer. This means that MFI value decreases with increasing molecular weight of polymer [57]. The last column of Table 4.3 represents the MFI results of both cPS and BULK-sPS synthesized at different reaction times. Nevertheless the MFI value for BULK-sPS at a polymerization reaction time of 6 hrs was not available because the measurement could not be performed due to very low amount of PS obtained in the polymerization reaction. As can be seen from Table 4.3, the MFI values of BULK-sPS are much higher than that of cPS. This shows that the molecular weight of BULK-sPS is much lower than the cPS. The MFI test results help to make qualitative comparison for the

results of viscosity average molecular weight. Among these reaction times, 3 hr reaction time is selected as the best reaction time due to the fact that the viscosity average molecular weight of BULK-sPS is close to that of cPS. Even if the viscosity average molecular weight value of BULK-sPS is very close to cPS, it is not easy to make exact conclusions on the molecular weight of BULK-sPS. Therefore, the synthesis parameter was changed to observe the effect of initiator concentration on the molecular weight of PS.

4.1.2.2 Effect of Initiator Concentration on Molecular Weight of PS

After determination of polymerization time as 3 hrs, this initiator concentration was varied in the range of 0.01 and 0.03 mol/L in the polymerization medium. Polymerization reaction time of 3 hrs and polymerization reaction temperature of 95 °C were kept constant throughout these experiments. As it is mentioned before, the molecular weight of BULK-sPS was aimed to be same as the molecular weight of cPS. Therefore, three different techniques which are viscosity average molecular weight, MFI, and GPC measurements were used to make a more accurate comparison between molecular weights of the BULK-sPS and cPS.

Table 4.4 shows the viscosity average molecular weight and MFI results of BULK-sPS synthesized using different initiator concentrations at constant polymerization reaction time and temperature. Calculation of viscosity average molecular weight for BULK-sPS synthesized using different initiator concentrations and the related plots used in the calculation are also given in Appendix B.

It is observed from Table 4.4 that the viscosity average molecular weight of BULK-sPS reaches the desired molecular weight at an initiator concentration of 0.01 mol/L. The viscosity average molecular weights of BULK-sPS are approximately in the same order of magnitude with cPS. The same behavior is also observed in optimizing the reaction time. It is notable that the MFI results of BULK-sPS decrease with a decrease in initiator concentration.

Table 4.4 Viscosity average molecular weight and MFI test results of both cPS and BULK-sPS synthesized at different initiator concentrations at constant reaction temperature of 95 °C and time of 3 hrs.

Polymerization Run	Initiator Concentration (mol/L)	M_v (*10⁻³)	MFI (g/10 min)
1	0.03	171.3	39.2
2	0.02	171.7	31.7
3	0.01	220.1	20.3
cPS	-	169.8	19.7

The lower MFI value indicates the higher molecular weight of polymer. Based on this approach, the MFI value of BULK-sPS obtained at 0.01 mol/L initiator concentration is very close to that of cPS. It can be said that the rate of initiation step in free radical polymerization is directly related with initiator concentration and initiator efficiency [55]. Therefore, initiator concentration itself is the main parameter of the rate of initiation step [20]. If the initiator concentration is decreased, the rate of polymerization becomes slower and the number of free-radicals becomes less. This situation leads to increase in molecular weight of the polymer [87].

After studying the effect of initiator concentration on molecular weight of PS using viscosity average molecular weight and MFI analyses, the additional method is needed to make a more accurate comparison between molecular weights of synthesized and commercial PS. Therefore, Gel Permeation Chromatography (GPC) method was used to determine both number average and weight average molecular weights of BULK-sPS.

Table 4.5 represents molecular weights of both BULK-sPS samples and cPS via GPC. Molecular weight distribution curves of both BULK-sPS and cPS are given in Appendix C. It is observed that polydispersity index of all BULK-sPS are larger than that of cPS. The main reason is that the synthesized PS via bulk polymerization exhibits broad molecular weight distribution which indicates that the molecular

weight of chains varies in a wide range [88,53]. When the change of molecular weight of BULK-sPS with respect to initiator concentration is taken into account, the number average and weight average molecular weights of BULK-sPS increase with a decrease in initiator concentration. The results of viscosity average molecular weight and MFI of BULK-sPS with respect to initiator concentration are ensured with GPC results. Hence, it can be said that the number and weight average molecular weights of BULK-sPS at 0.01 mol/L concentration are in the same order of magnitude with the cPS and the closest values to those of cPS, respectively.

Table 4.5 GPC results of both cPS and BULK-sPS synthesized at different initiator concentrations and at constant polymerization reaction temperature of 95 °C and time of 3 hrs.

Polymerization Run	Initiator Concentration (mol/L)	M_n (*10⁻³)	M_w (*10⁻³)	PDI (M_w/M_n)
1	0.03	50.8	169.8	3.34
2	0.02	70.8	265.4	3.74
3	0.01	99.5	273.8	2.75
cPS	-	143.2	278.0	1.94

The best synthesis conditions for PS production with the desired molecular weight via bulk polymerization are shown in Table 4.6.

Table 4.6 The best synthesis conditions for PS production via bulk polymerization.

Polymerization Type	Polymerization Reaction Temperature (°C)	Polymerization Reaction Time (hrs)	Initiator Concentration (mol/L)
Bulk Polymerization	95	3	0.01

4.1.3 Characterization of Synthesized PS

4.1.3.1 Fourier Transform Infrared (FTIR) Analysis

Polystyrene synthesized using two polymerization techniques based on the best synthesis conditions given in Tables 4.2 and 4.6 was characterized. FTIR analysis is a reasonable way to determine the chemical structure of the synthesized materials. Figure 4.1 gives FTIR spectra of synthesized PS and commercial PS (cPS). FTIR spectra of all synthesized PS samples that are used in parameter optimization for different polymerization techniques are given in Appendix D. FTIR spectrum of styrene monomer is also included in Appendix D.

The peaks which are observed at wavenumbers of 1492 cm^{-1} and 1600 cm^{-1} are related with benzene ring modes [52]. These two peaks signify the presence of benzene ring which is attached to the carbon atom in the chemical structure of polystyrene. The peaks observed at wavenumbers of 2846 cm^{-1} and 2920 cm^{-1} are associated with CH_2 symmetric and asymmetric stretching, respectively. The peak observed at 906 cm^{-1} also belongs to aromatic C-H stretching [89]. Furthermore, one of the major peaks detected at a wavenumber of 1450 cm^{-1} signifies the CH_3 asymmetric bend. The peak observed at 3024 cm^{-1} indicates the aromatic C-H stretching [52]. The main difference between the molecular structure of styrene and polystyrene is the double bond between carbon atoms in the styrene structure which appears at the wavenumber of 1627 cm^{-1} .

As this specified peak of styrene is not detected for both synthesized and cPS in Figure 4.1, it can be said that polystyrene synthesis is completed through these synthesis conditions. For the other synthesized PS samples, same spectra are observed (Figures D.1-D.4 in Appendix D).

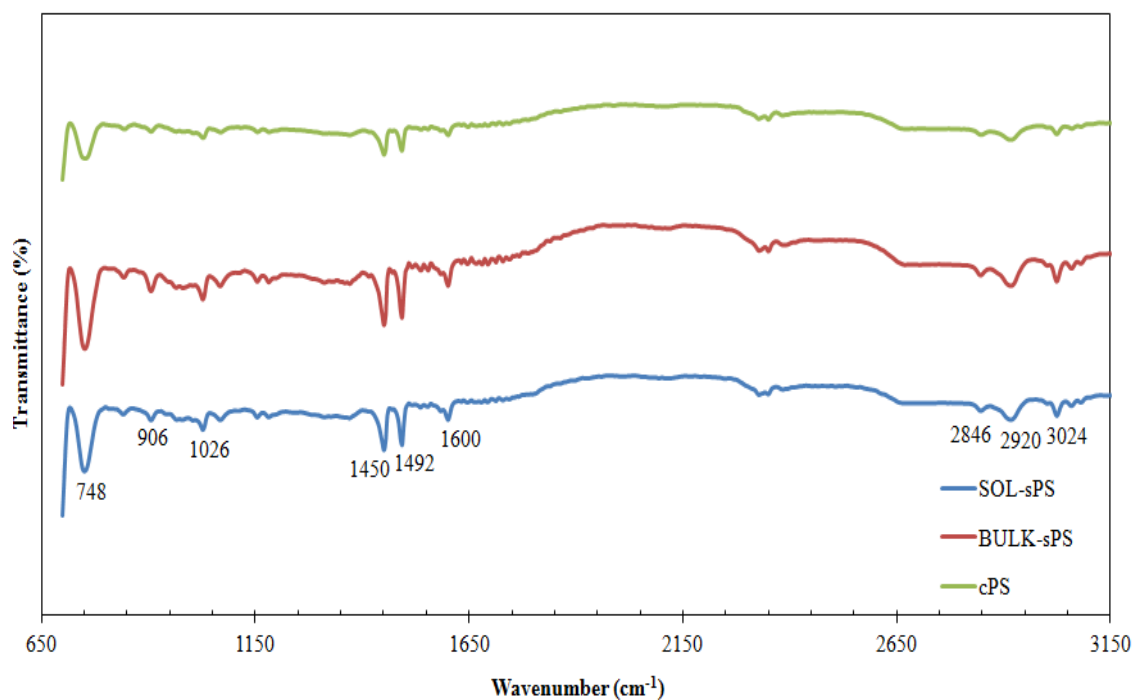


Figure 4.1 FTIR spectra of polystyrene synthesized at the optimum conditions using solution and bulk polymerization methods.

4.1.3.2 X-Ray Diffraction (XRD) Analysis

XRD analysis of the synthesized PS was carried out between 2θ values of 5° and 40° . Figure 4.2 shows XRD pattern of synthesized PS based on the best synthesis conditions which are given in Tables 4.2 (SOL-sPS) and 4.6 (BULK-sPS). XRD pattern of commercial PS (cPS) is also shown in Figure 4.2 to compare its pattern with the synthesized PS samples. XRD patterns of the other synthesized PS are also given in Appendix D.

It can be seen from Figure 4.2 that, XRD patterns of both PS synthesized from different polymerization techniques and commercial PS are similar to each other. The broad and unique peak which is observed at 2θ angle of 20.5° shows the

amorphous structure of polystyrene [90]. Same XRD patterns are observed for the other synthesized PS samples (Figures D.6-D.9 in Appendix D).

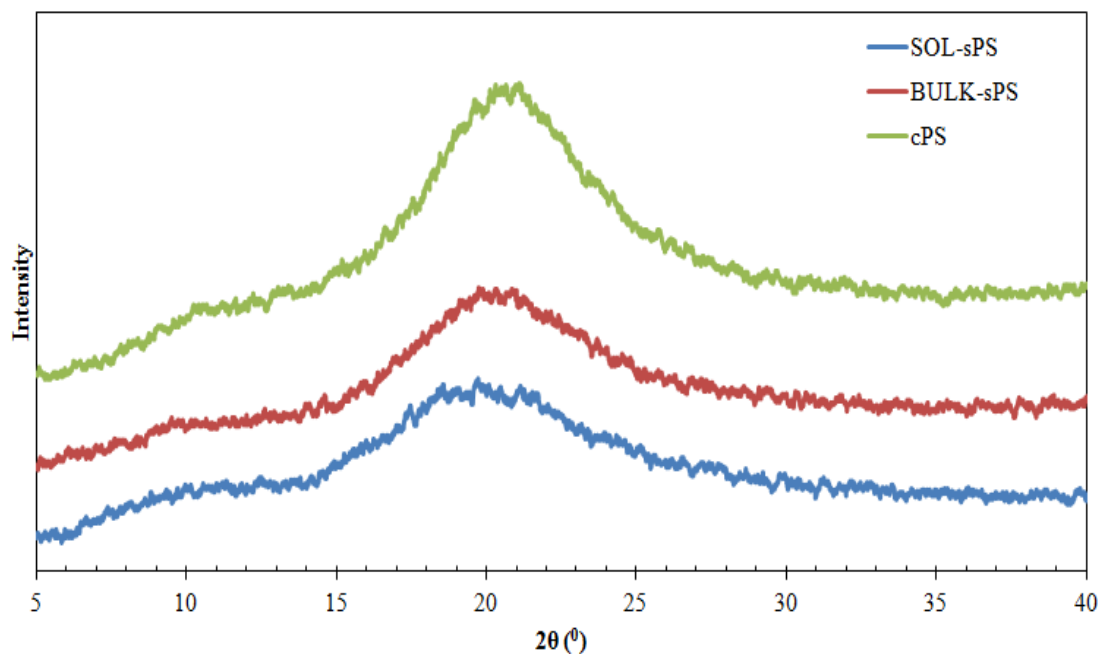


Figure 4.2 XRD patterns of polystyrene synthesized at optimum conditions using solution and bulk polymerization methods.

4.2 Synthesis, Purification and Characterization of BNNTs

In the previous studies, Özmen et al. [44] synthesized BNNTs by the reaction of ammonia gas with a powder mixture of boron and iron oxide at a reaction temperature of 1300 °C and a B/Fe₂O₃ weight ratio of 15/1. Then, Demir improved the synthesis condition for BNNT production by changing initial powder mixture amount to 0.8 g and inlet ammonia flow rate to 125 cm³/min at constant reaction temperature and time [11]. In the present study, the optimum synthesis conditions obtained from these studies were used in the synthesis of BNNTs (Table 4.7).

Table 4.7 Synthesis conditions for BNNT synthesis [11,44].

Production Parameter	Initial Weight (g)	B/Fe₂O₃ weight ratio	Reaction Temperature (°C)	Reaction Time (hrs)	Ammonia Inlet flow rate (cm³/min)
Value	0.8	15	1300	2.15	125

The color of synthesized BNNT is white-gray and in one batch amount of as-synthesized material is in the range of 1.2 and 1.4 g. The produced amounts and visual appearance of BNNTs are affected by the concentration of ammonia gas inside the furnace and the diffusion of ammonia into the powder mixture of reactants [11]. Therefore, the ammonia inlet flow rate should be kept constant throughout the experiment in order to obtain approximate amount of BNNTs. The grayish appearance of BNNTs signified the existence of unreacted boron and iron oxide.

To remove these impurities, which are unreacted boron and iron oxide, from the synthesized product, the as-synthesized was purified. Based on the purification procedure, amount of purified BNNT is approximately half of the as-synthesized material amount.

4.2.1 X-Ray Diffraction (XRD) Analysis

In this study, the reproducibility and also purification of synthesized BNNTs are important concerns for the further usage of BNNTs in the composite preparation. Same properties are expected from each batch of purified BNNTs. A typical XRD pattern of purified BNNTs is shown in Figure 4.3.

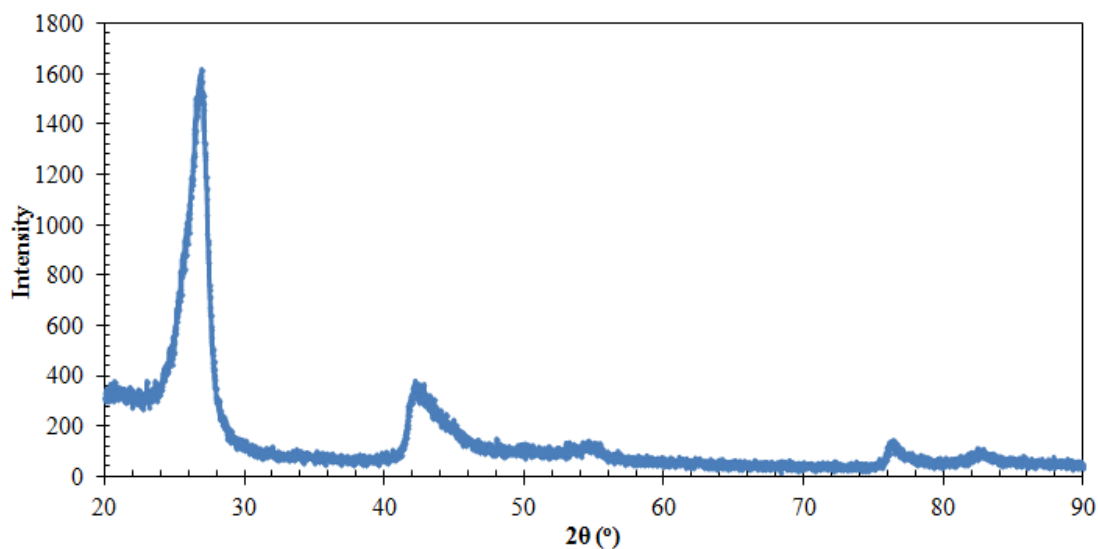


Figure 4.3 XRD pattern of the purified BNNTs.

Peaks observed at 2θ values of 26.5° , 42.1° , 53.9° , 76.2° , 82.4° indicate hexagonal boron nitride. The main characteristic peak of iron oxide (Fe_2O_3) is shown at 2θ angles of 33.1° . In Figure 4.3, the characteristic peak of iron oxide is not seen in the purified BNNTs. Therefore, the crystalline structure contains mainly hexagonal boron nitride. Same XRD patterns were observed for purified BNNT samples synthesized at different batches.

4.2.2 Surface Area Measurement

Figure 4.4 shows the nitrogen adsorption/desorption isotherms of the purified BNNTs. Full dots represent the adsorption of nitrogen molecules by BNNTs sample. Empty dots show the desorption of nitrogen molecules from the purified sample.

Based on the classification of BDDT (Brauner, Deming, Deming, Teller), the isotherm of purified BNNTs correspond to Type II isotherm which occurs only if the material is porous or nonporous powders in which their pore diameters are larger than those of micropores [91].

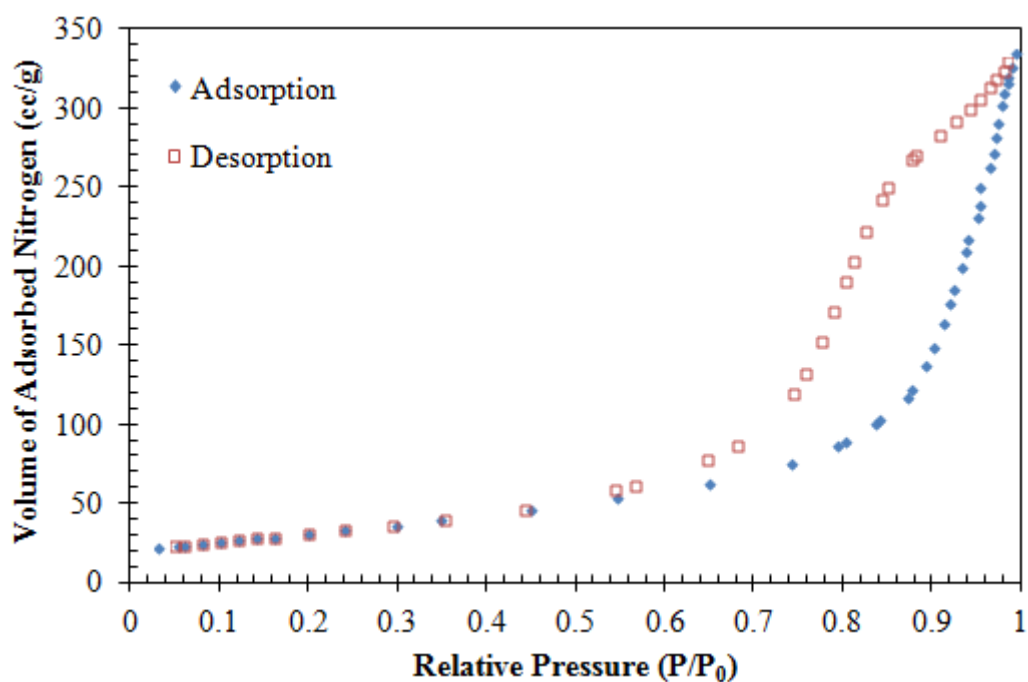


Figure 4.4 Adsorption/desorption isotherms of purified BNNTs.

A hysteresis is seen at a relative pressure of 0.44 for the purified nanotubes. Based on the De Boer hysteresis classification, the hysteresis of purified BNNTs can be matched with both Type A and Type B. Type A hysteresis shows the formation of cylindrical pore channels in the material. Type B hysteresis shows the existence of slit shaped pores or the space between parallel plates [92].

Type A hysteresis is explained by the existence of the hollow cylindrical shape in nanotubes. Type B hysteresis is probably related to voids which are formed between multiwall nanotubes.

Multi-point BET surface area of purified BNNT is found to be 114.1 m²/g. On the other hand, the surface area of the as-synthesized BNNTs without purification is 16.8 m²/g [11]. As the synthesized BNNTs are purified, the surface area of material increases tremendously. Total pore volume of purified BNNTs is found as 0.51 cm³/g.

The pore size distribution of purified BNNTs given in Figure 4.5 is relatively broad. This means that, the main peak is observed at 98 Å indicates the average mesopore diameter. On the other hand, small peaks detected at 78 Å and around 120 Å shows non-uniform nanotube diameter.

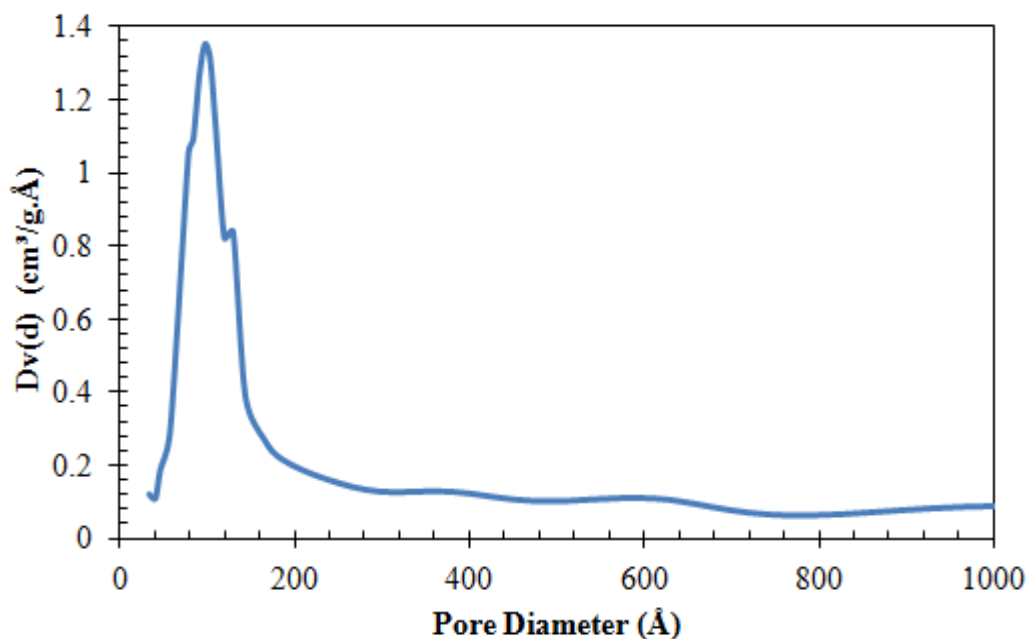


Figure 4.5 Desorption pore size distribution of purified BNNTs.

4.2.3 Scanning Electron Microscopy (SEM) Analysis

SEM analysis was performed to understand the surface morphology of purified BNNTs. The SEM images of purified BNNTs are given in Figure 4.6. As it is seen from Figure 4.6, the purified BNNTs are agglomerated because of the entanglements of nanotubes during the growth stage [44]. The tendency to agglomeration can be explained by two different aspects; (i) low bending stiffness, (ii) high aspect ratio of the nanotubes [93].

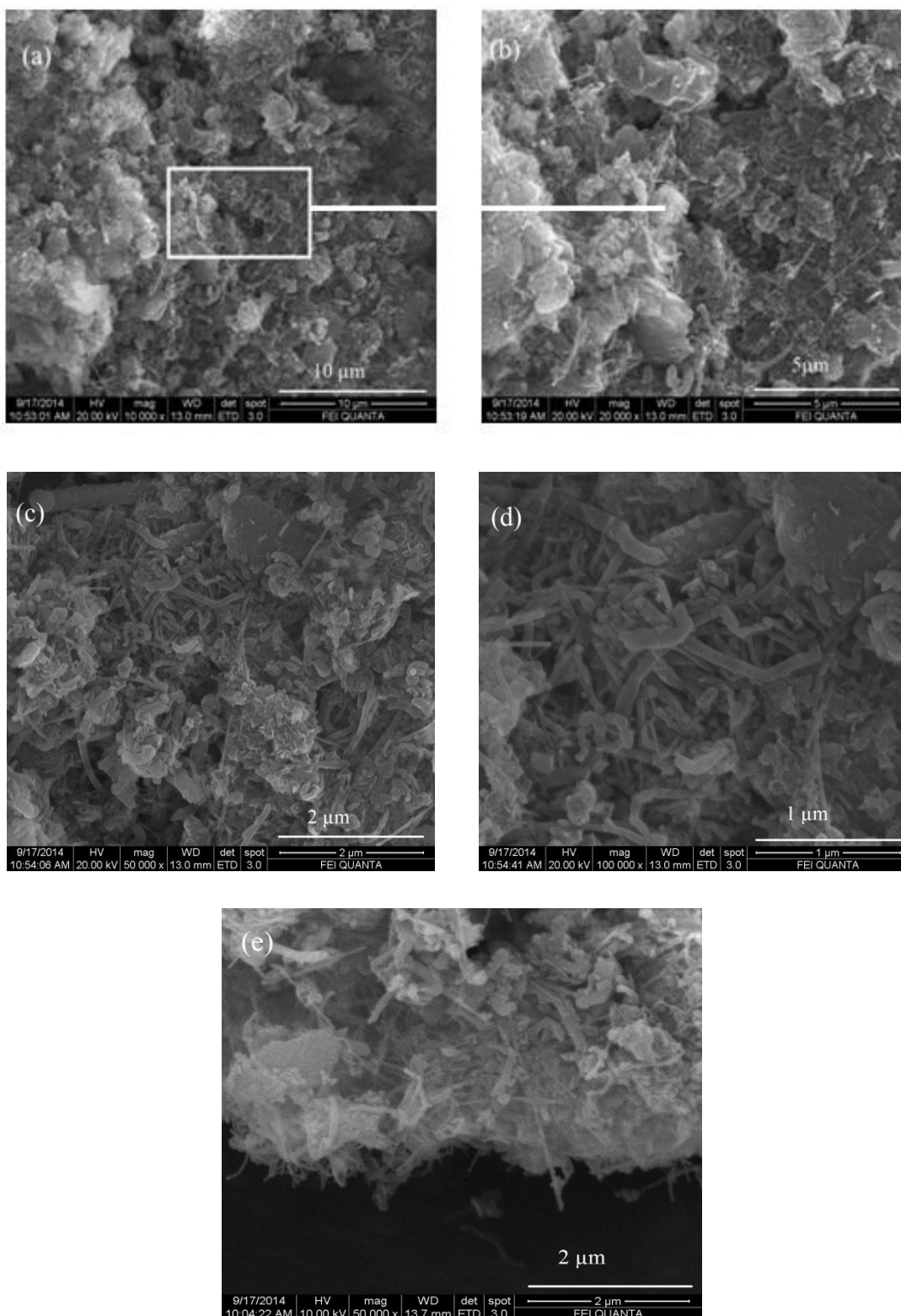


Figure 4.6 SEM images of the purified BNNTs (a) 10,000x magnification, (b) 20,000x magnification, (c) 50,000x magnification, (d) 100,000x magnification, and (e) another view of the sample at 50,000x magnification.

4.3 Preparation and Characterization of PS-BNNTs Composites

Three different preparation methods which are masterbatch with extrusion, melt blending and in-situ polymerization were used to obtain the nanocomposites. First, masterbatch with extrusion method was applied in order to prepare PS-BNNT composites at 0.5, 1 and 3 wt% of purified BNNTs. Morphology, mechanical and thermal properties of these composites were investigated. Also, the effects of composite preparation methods on morphology and physical properties of PS-BNNT composites were studied through the comparison of these techniques at 0.5 wt% BNNT loading.

Scanning electron microscopy (SEM), tensile and impact tests, differential scanning calorimetry (DSC) and thermal gravimetric analyses (TGA) were used in order to characterize the PS-BNNT composites. As mentioned before, compositions of all the composites prepared by different preparation methods are given in Table 3.6.

4.3.1 Scanning Electron Microscopy (SEM) Analysis

Scanning Electron Microscopy is usually preferred in order to observe the dispersion of the nanotubes throughout the polymer matrix. Impact fractured surface of neat PS and the prepared composites were used to observe the surface morphology of the samples.

SEM photographs of neat PS (BULK-sPS) synthesized under the best synthesis conditions and commercial polystyrene (cPS) at magnifications of x1000 and x10000 are shown in Figures 4.7 and 4.8, respectively.

As seen in Figures 4.7 and 4.8, both synthesized and commercial polystyrene have similar sharp propagation lines because of their brittle nature. Zigzagged or tortuous lines do not exhibit in such polymers. Crack propagation may be enhanced due to the homogeneous structure of neat PS. Also, this situation causes fracture of PS with a small amount of energy [94].

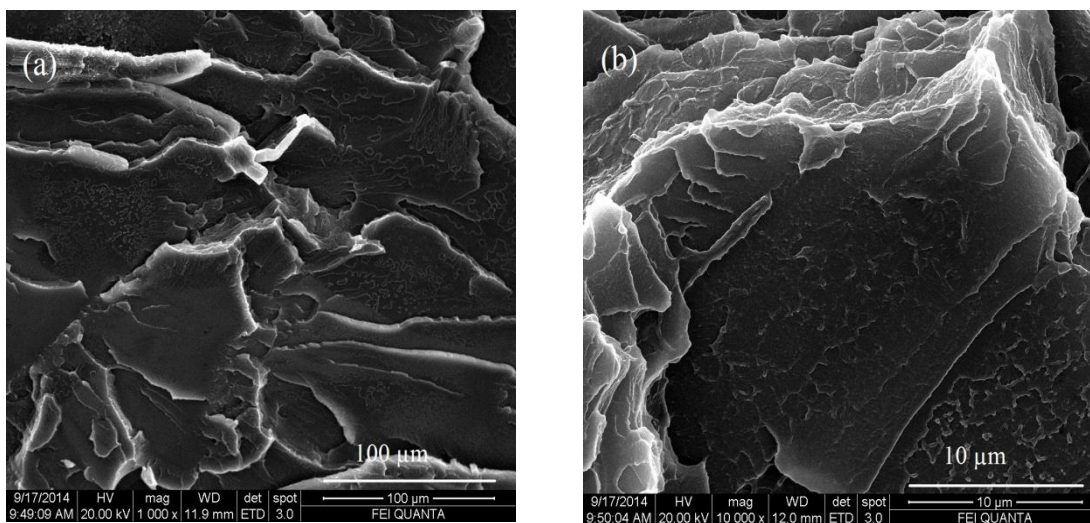


Figure 4.7 SEM images of the BULK-SPS under the best synthesis conditions (a) 1,000x magnification, and (b) 10,000x magnification.

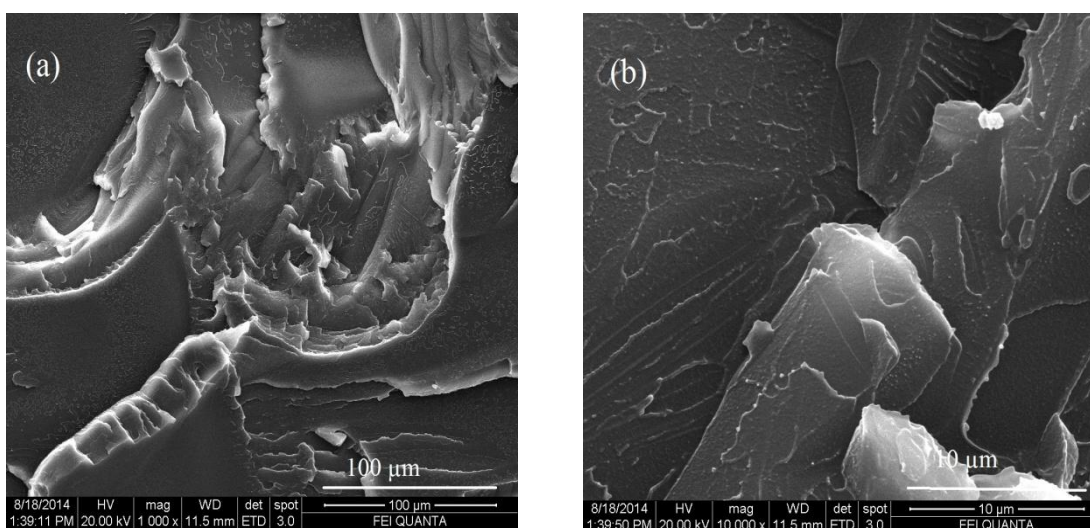


Figure 4.8 SEM images of the cPS (a) 1,000x magnification, and (b) 10,000x magnification.

The SEM images of neat PS and PS-BNNT composites prepared by masterbatch with extrusion method at 0.5, 1 and 3 wt.% BNNT loadings are given in Figures 4.9-4.12. Figure 4.9 shows the impact fractured surface of neat PS which is the combination of the synthesized and commercial PS. Similar sharp propagation lines observed from Figures 4.7 (a) and 4.8 (a) are also seen in Figure 4.9 due to the brittle nature of PS.

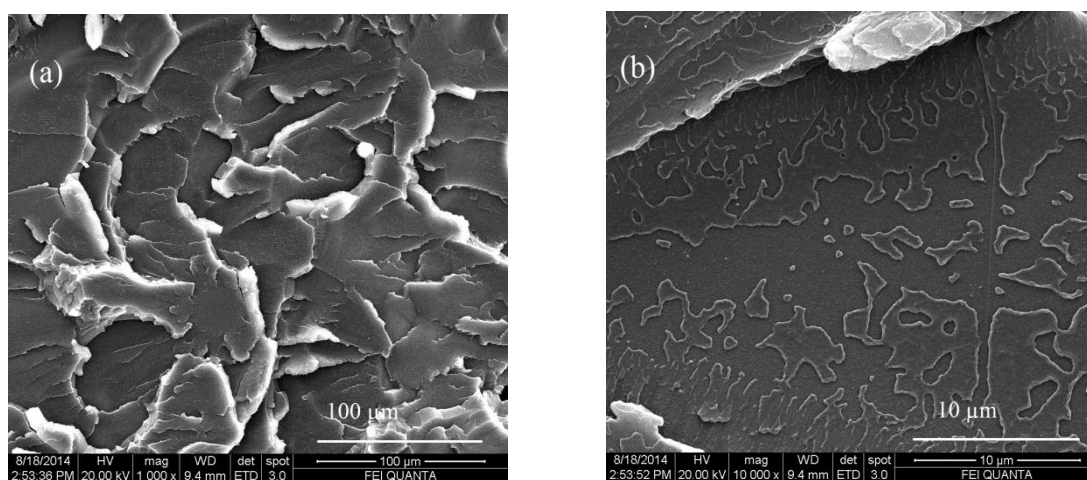


Figure 4.9 SEM images of neat PS prepared by masterbatch with extrusion method (a) 1,000x magnification, and (b) 10,000x magnification.

Although higher magnifications are used to observe the nanotubes in the polymer matrix, it is usually difficult to detect these nanotubes at 0.5 wt% BNNT loading. As seen in Figure 4.10, the bright dots are attributed to BNNTs inside the polymer matrix. BNNTs at 1.0 wt% and 3.0 wt% are seen in Figures 4.11 and 4.12, respectively. It can be said that, the nanotubes at 0.5 wt% loading are dispersed more homogeneously in the polymer matrix when compared with those of 1 and 3 wt% loadings. In other words, when the fractions of BNNTs are increased in the polymer matrix, the possibility of agglomeration increases remarkably because of the interactions among the nanotubes [13]. As it is seen in Figure 4.6 given before, purified BNNTs have high tendency for agglomeration.

Therefore, a large aggregate of BNNTs in the polymer matrix is observed in Figure 4.12 (a) at lower magnification.

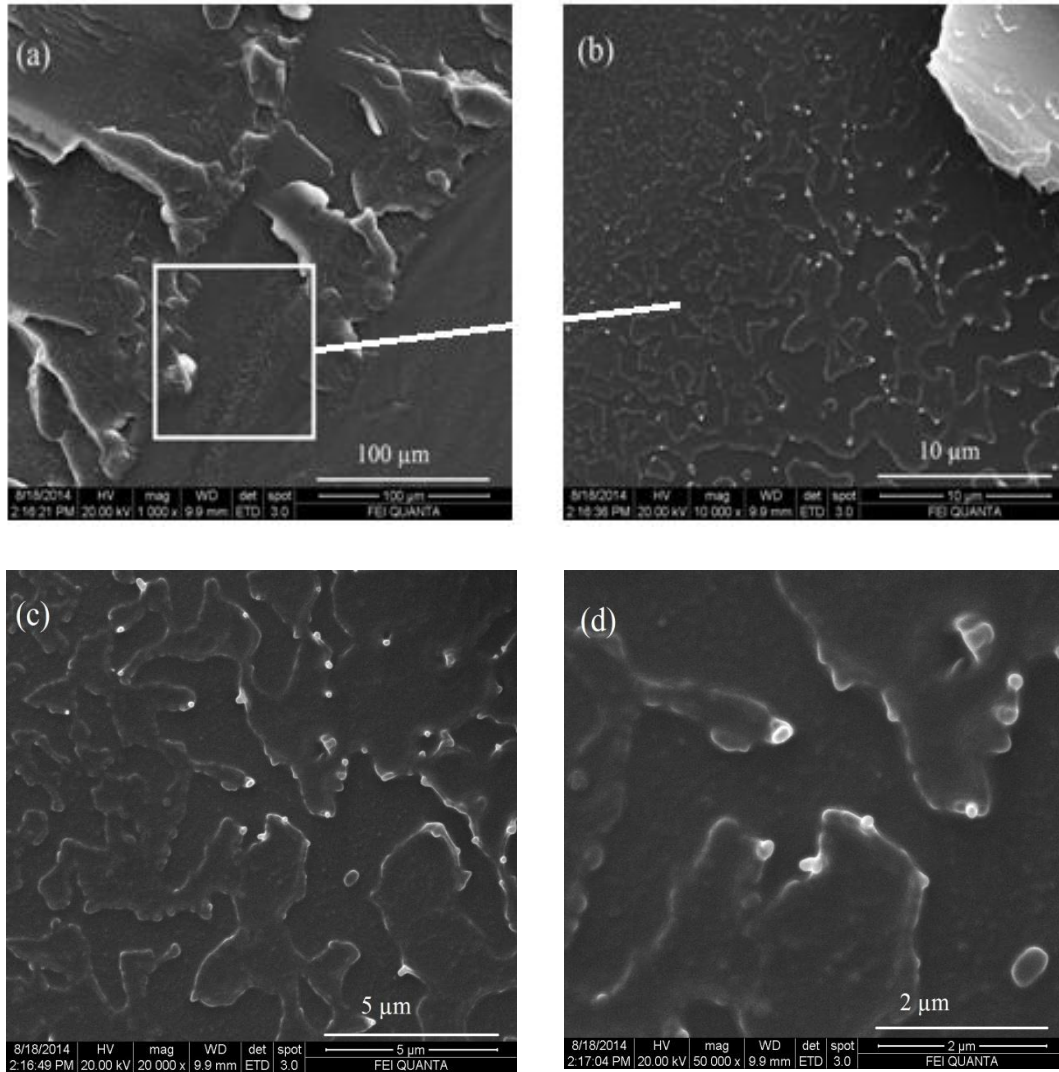


Figure 4.10 SEM images of PS-BNNT composites prepared by masterbatch with extrusion method at 0.5 wt% BNNTs (a) 1,000x magnification, (b) 10,000x magnification, (c) 20,000x magnification, and (d) 50,000x magnification.

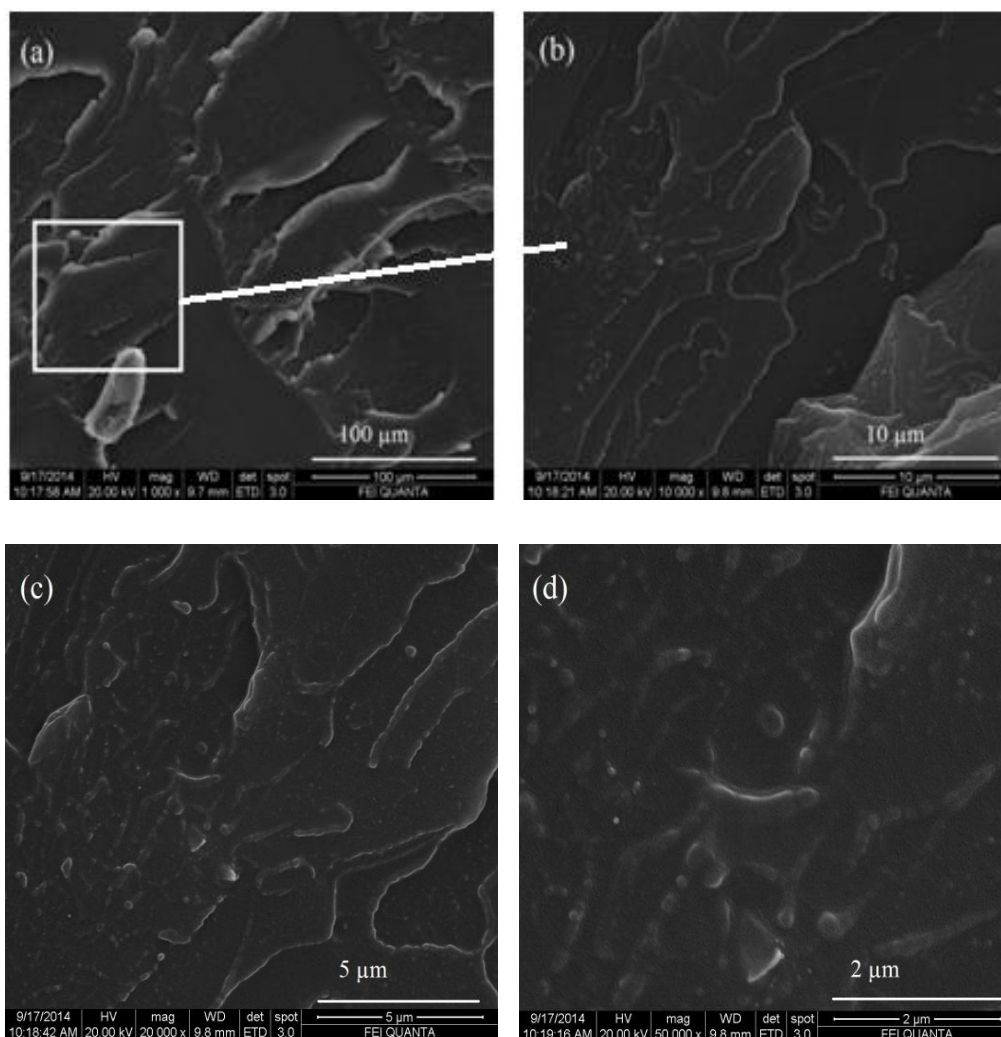


Figure 4.11 SEM images of PS-BNNT composites prepared by masterbatch with extrusion method at 1.0 wt% BNNTs (a) 1,000x magnification, (b) 10,000x magnification, (c) 20,000x magnification, and (d) 50,000x magnification.

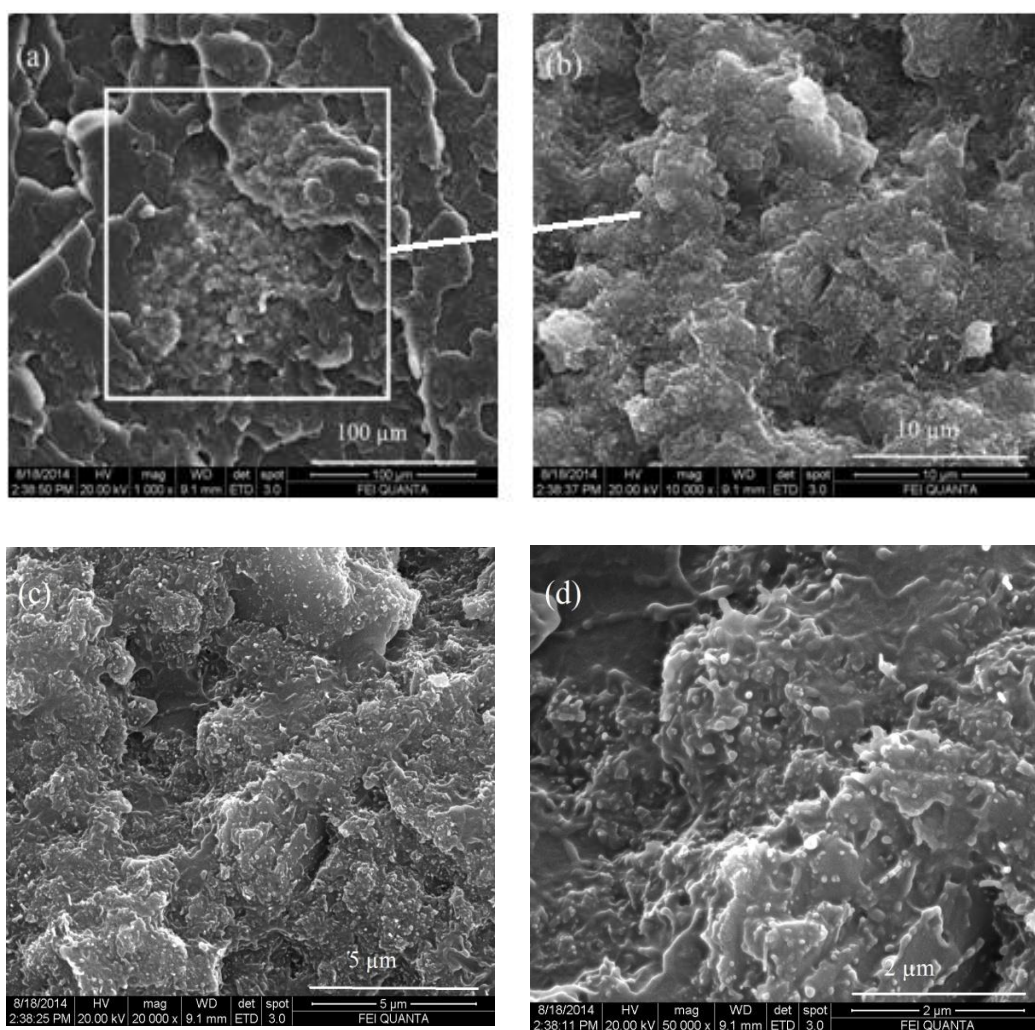


Figure 4.12 SEM images of PS-BNNT composites prepared by masterbatch with extrusion method at 3.0 wt% BNNTs (a) 1,000x magnification, (b) 10,000x magnification, (c) 20,000x magnification, and (d) 50,000x magnification.

In order to compare the effect of preparation method on the morphology of PS-BNNT composites, SEM images of the composites containing 0.5 wt% BNNTs prepared by in-situ polymerization and extrusion method are shown in Figures 4.13 and 4.14, respectively. Based on the mechanical test results which will be discussed later, the composite with 0.5 wt% BNNTs prepared by masterbatch with extrusion method is selected as the reference composite in order to make this comparison mentioned above.

Figures 4.13 and 4.14 show that the inclusion of BNNTs into the polymer matrix using two different preparation methods results in the imperfect dispersion in the matrix although low concentration of BNNTs is used. As seen from Figure 4.10, interfacial adhesion between the polymer matrix and nanotubes for the composite prepared by masterbatch with extrusion method yields better dispersion of the nanotubes in the matrix.

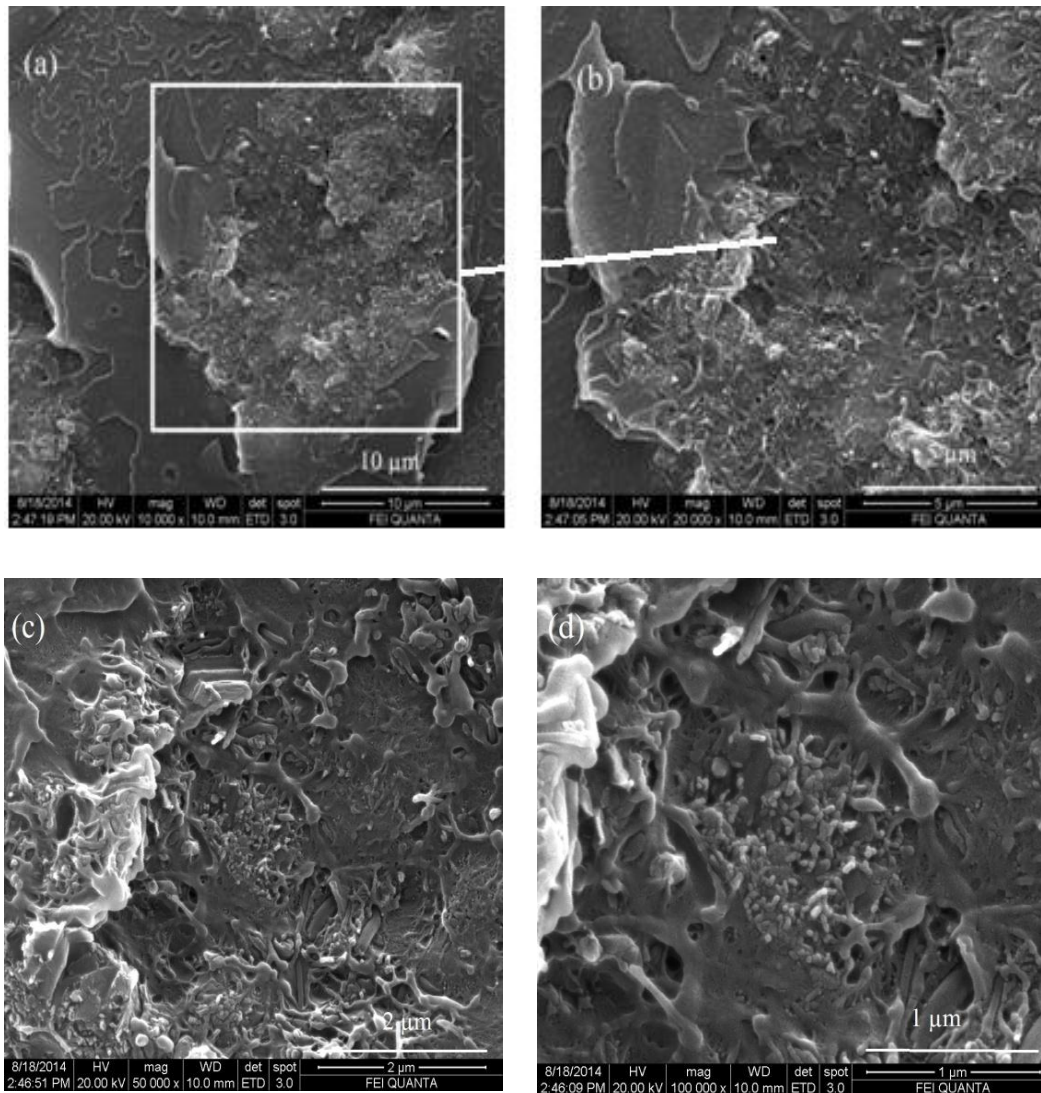


Figure 4.13 SEM images of PS-BNNT composites prepared by in-situ polymerization method at 0.5 wt% BNNT (a) 10,000x magnification, (b) 20,000x magnification, (c) 50,000x magnification, and (d) 100,000x magnification.

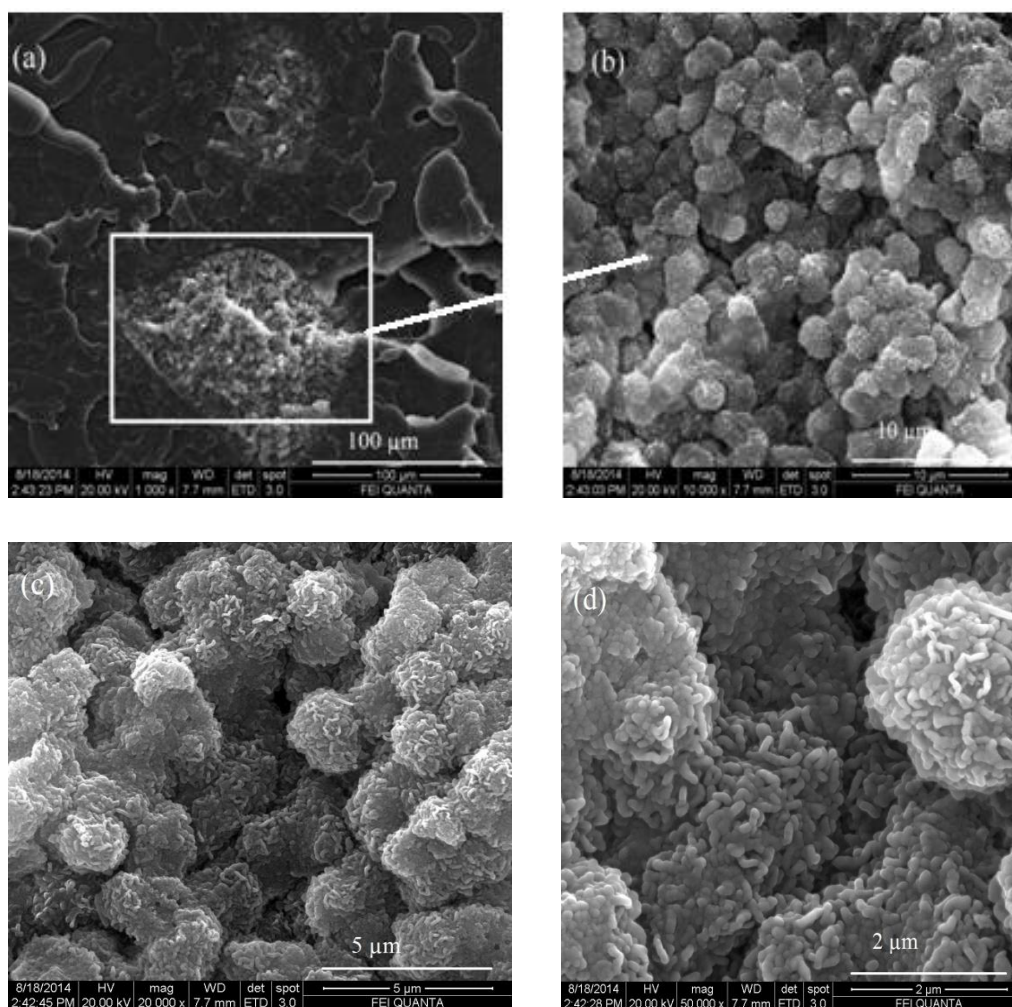


Figure 4.14 SEM images of PS-BNNT composites prepared by extrusion method at 0.5 wt% BNNT (a) 1,000x magnification, (b) 10,000x magnification, (c) 20,000x magnification, and (d) 50,000x magnification.

4.3.2 Mechanical Analysis

In order to investigate the mechanical properties of the composites and neat PS, tensile and impact tests were applied to the materials. Tensile and impact test results of all the composites and neat PS are given in Appendix E.

4.3.2.1 Tensile Test

Tensile test was carried out to obtain stress-strain behavior of the composites. Then, mechanical properties such as tensile strength, Young's modulus and elongation at break values were obtained from these stress-strain curves of the composites. Representative stress-strain curves of neat PS and all the composites which are tabulated in Table 3.6 are shown in Appendix F.

Tensile properties of commercial PS (cPS), synthesized PS (BULK-sPS) and extruded PS (E-cPS) are given in Table 4.8. Also, graphical representations of tensile strength, Young's modulus and elongation at break of all neat polystyrene's are shown in Figures 4.15-4.17, respectively.

As seen in Table 4.8 and Figure 4.17, elongation at break values are low for all the PS samples. Although PS is a preferable material due to its easy processing and transparency, the nature of PS is brittle and hard [32]. Its brittle nature leads to a low elongation at break value. For this reason, PS is fractured easily with a small deformation. As shown in Figure 4.15, the tensile strength value of BULK-sPS is relatively lower than cPS. Even if there is an agreement between the molecular weight of BULK-sPS with cPS in terms of the same order of magnitude, BULK-sPS has a broad molecular weight distribution compared to cPS. This means that, BULK-sPS has a relative amount of lower molecular weight chains than cPS. The existence of lower molecular weight chains results in the lower tensile strength values [35]. In Figure 4.16, the Young's moduli of BULK-sPS and E-cPS are relatively high with respect to cPS due to the restriction in chain mobility.

Table 4.8 Tensile properties of cPS, BULK-sPS, and E-cPS.

Property \ Sample	cPS	BULK-sPS	E-cPS
Tensile Strength (MPa)	45.6	22.7	30.7
Young's Modulus (MPa)	1319	1944.8	1806
Elongation at break (%)	5.3	2.0	3.8

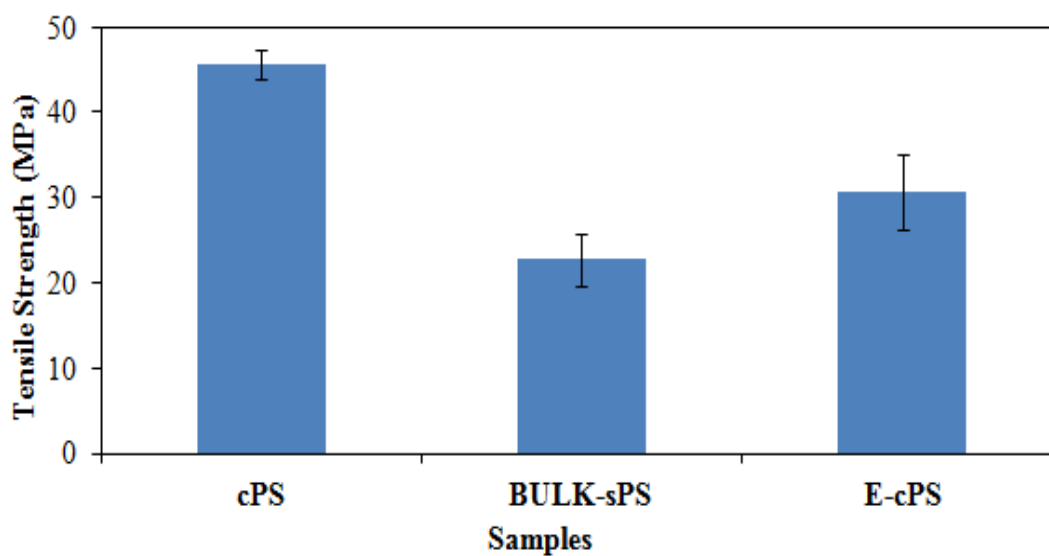


Figure 4.15 Tensile strengths of PS samples. (cPS: commercial PS, BULK-sPS: synthesized via bulk polymerization, E-cPS: extruded commercial PS).

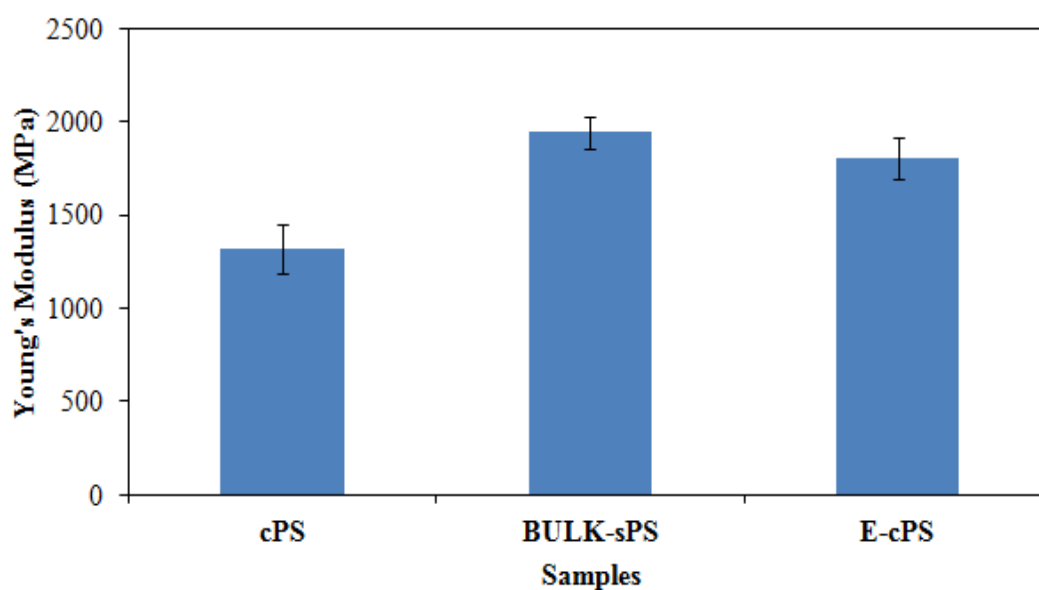


Figure 4.16 Young's moduli of PS samples. (cPS: commercial PS, BULK-sPS: synthesized via bulk polymerization, E-cPS: extruded commercial PS).

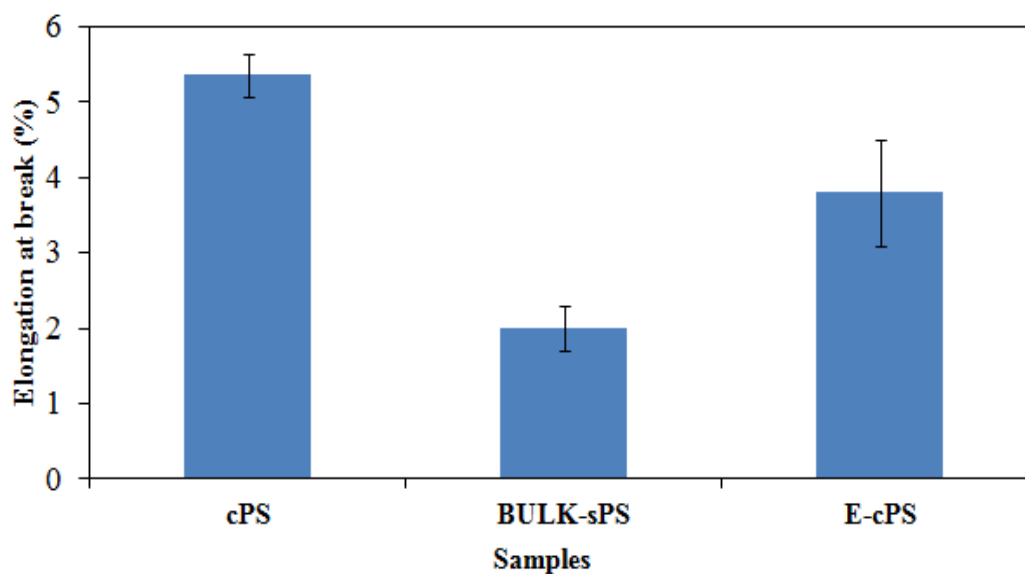


Figure 4.17 Elongation at break of PS samples. (cPS: commercial PS, BULK-sPS: synthesized via bulk polymerization, E-cPS: extruded commercial PS).

Tensile strength, Young's modulus and elongation at break (%) of neat PS and PS-BNNT composites prepared by masterbatch with extrusion method are presented in Figures 4.18-4.20, respectively.

Tensile properties of BULK-sPS, E-cPS and ME-PS are included in Figures 4.18 through 4.20 for comparison purposes. Standard deviations of the measurements in tensile properties are also shown in the figures.

As seen in Figure 4.18, PS-BNNT composite with 0.5 wt% BNNTs (ME-PS+ 0.5) exhibits higher tensile strength value than BULK-sPS, E-cPS and also neat PS prepared by masterbatch with extrusion method (ME-PS). This is not surprising since BNNT addition increases tensile strength of neat PS. When concentration of BNNT is increased, the tensile strength decreases because of the poor dispersion of BNNTs in the polymer matrix. At 0.5 wt% BNNT loading, load transfer from the nanotubes to the matrix is much better when compared to that of the composites containing 1.0 and 3.0 wt% BNNTs. Use of unmodified nanotubes in the polymer matrix results in agglomeration inside the polymer matrix because of weak van der Waals forces among the nanotubes. SEM images of purified BNNTs shown in Figure 4.6 support this consequence. The uniformity of filler size is also important for better interfacial strength between the polymer and nanotubes [95]. As a result, agglomeration of the nanotubes may act as stress concentrated points in the polymer matrix affecting the tensile strength negatively.

As it is seen in Figures 4.15-4.17, the mechanical properties of BULK-sPS are generally affected from non-uniform molecular weight distribution obtained through the synthesis. Also, it is known that masterbatch with extrusion method contains use of synthesized PS (masterbatch) and commercial PS together which should improve the adhesion in the polymer matrix. Therefore, tensile strength of ME-PS is higher than the other forms of PS, namely BULK-sPS and E-cPS. When BNNTs are added to ME-PS, the adhesion between the nanotubes and the polymer matrix is enhanced owing to the use of masterbatch in the preparation of the composite. This is not very effective at higher BNNT loadings because agglomeration of the nanotubes become dominant over the adhesion.

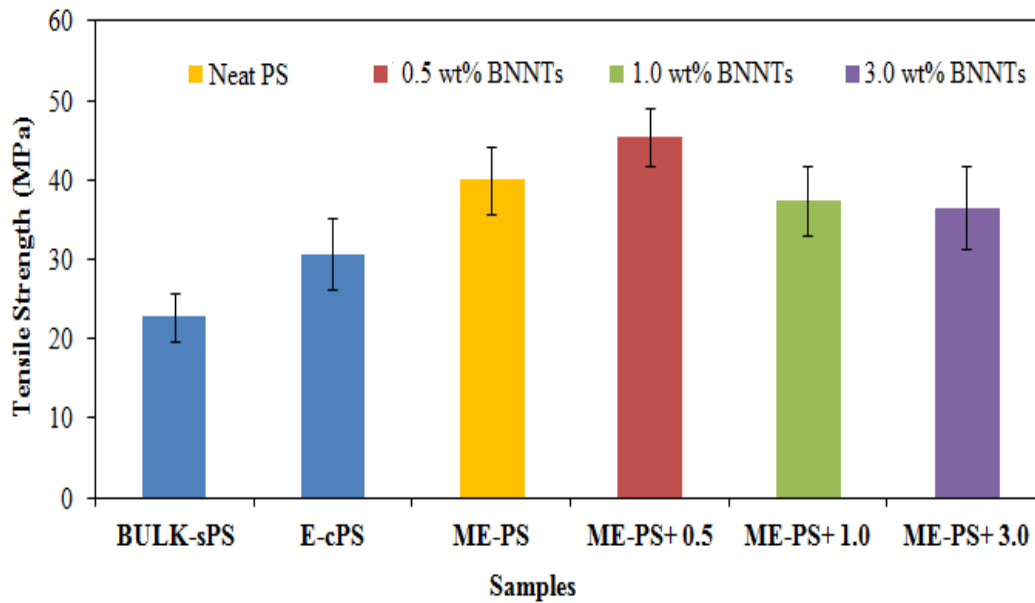


Figure 4.18 Tensile strengths of neat PS and PS-BNNT composites containing 0.5, 1 and 3 wt% BNNTs. (BULK-sPS: synthesis via bulk polymerization, E-cPS: Extrusion, ME-PS: Masterbatch with extrusion).

Figure 4.19 represents the Young's modulus values of neat PS samples and PS-BNNTs composites prepared by masterbatch with extrusion method. The Young's modulus of neat PS samples which are BULK-sPS, E-cPS and ME-PS decrease significantly with the addition of 0.5 wt% BNNTs (ME-PS+0.5). When the BNNT addition is increased from 0.5 wt% to 1 wt%, the Young's modulus of ME-PS+1.0 increases to the value of E-cPS and with further increase to 3wt% BNNT, the modulus starts to decrease. On the other side, the improvement in mechanical properties of neat polymer in terms of modulus is not clear as in the trend of tensile strength. In other words, the expected result is that the Young's modulus of all different forms of neat PS samples would increase dramatically at 0.5 wt% BNNTs composite by considering tensile strength behavior. However, the relationship between tensile strength and Young's modulus is a complex phenomenon and they are highly affected by the alignment of nanotubes, dispersion of nanotubes and types of nanotubes. The poor alignment of the nanotubes along the loading direction may affect the Young's modulus negatively [96].

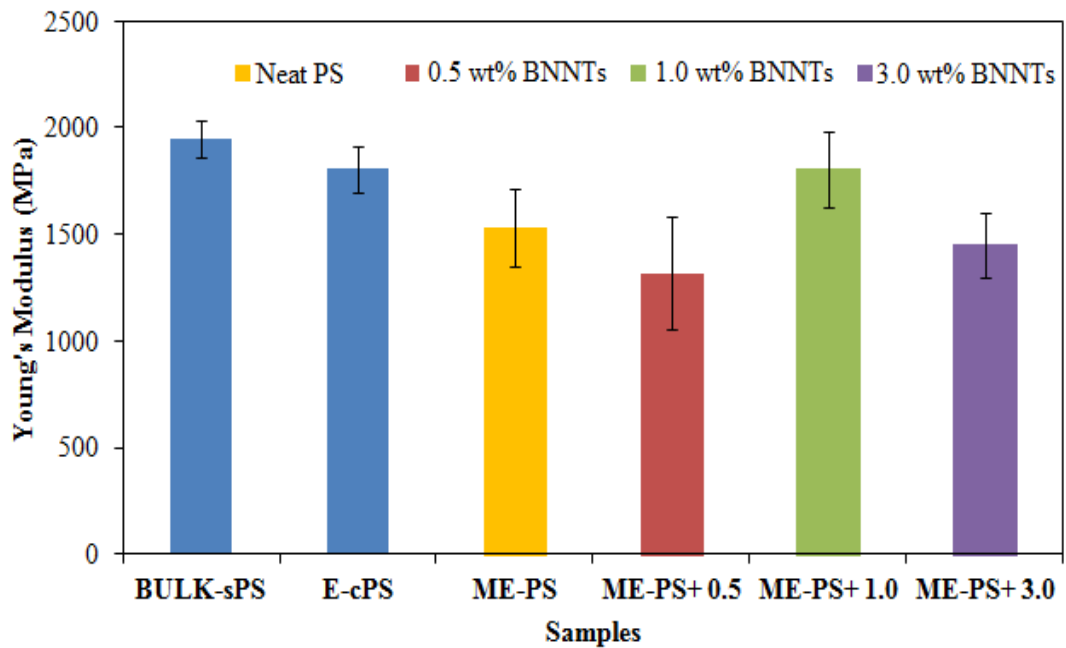


Figure 4.19 Young's moduli of PS and PS-BNNT composites containing 0.5, 1 and 3 wt% BNNTs. (BULK-sPS: synthesis via bulk polymerization, E-cPS: Extrusion, ME-PS: Masterbatch with extrusion).

Elongation at break values of neat PS and PS-BNNTs composites are represented in Figure 4.20. Percent elongation values of PS-BNNTs composites are shown to be inversely related with the addition of BNNTs. In other words, the highest elongation at break value is determined at 0.5 wt% BNNTs (ME-PS +0.5), then the value starts to decrease with the addition of higher amounts of BNNTs (1 and 3 wt% BNNTs). At these higher loadings, the test specimen fracture earlier than the others. Normally, when rigid fillers like BNNTs are added to a polymer matrix, the elongation at break starts to decrease with increasing fraction of nanotubes. Surprisingly, if the good adhesion is obtained between polymer matrix and nano-reinforcement, and if the fracture path proceeds through particle to particle path rather than a perfectly smooth fracture, the elongation at break value with respect to neat polymer may be enhanced [62]. However, the lower elongation at break value when obtained at 1 and 3 wt% BNNT loadings are probably due to the agglomeration of the nanotubes inside the polymer matrix affecting the elongation at break values negatively.

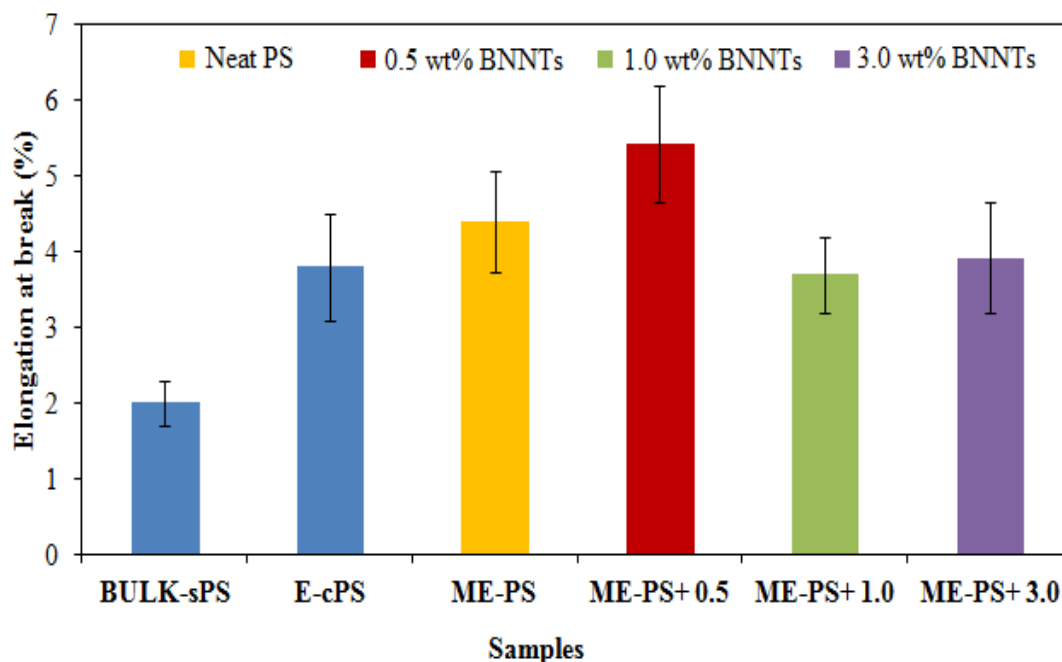


Figure 4.20 Elongation at break of PS and PS-BNNT composites containing 0.5, 1 and 3 wt% BNNTs. (BULK-sPS: synthesis via bulk polymerization, E-cPS: Extrusion, ME-PS: Masterbatch with extrusion).

After completing the comparison of mechanical analysis of PS-BNNT composites and neat PS, the effect of three preparation methods on mechanical behavior of the composites containing 0.5 wt% BNNTs is investigated. Besides masterbatch with extrusion method, in-situ polymerization and extrusion method are also taken into account as mentioned before. The addition of BNNTs into the polymer matrix has to be at the same weight fraction in order to make a comparison about mechanical properties of the composites. According to tensile strength result which is depicted in Figure 4.18, the 0.5 wt.% BNNTs loading is determined to be used for the subsequent preparations of the composites because a remarkable improvement is observed at this concentration with respect to neat polystyrene samples.

Tensile strength, Young's modulus and elongation at break (%) of PS-BNNT composites prepared by masterbatch with extrusion method (ME-PS+0.5), in-situ polymerization (ISP-PS+0.5) and extrusion (E-cPS+0.5) are given in Figures 4.21-4.23, respectively.

Figure 4.21 shows tensile strength of PS-BNNT composites prepared by three different methods at 0.5 wt% BNNTs. The highest tensile strength value is observed for ME-PS+0.5 when compared to ISP-PS+0.5 and E-cPS+0.5. Tensile strengths of PS-BNNT composite prepared through in-situ polymerization and extrusion methods, are nearly the same. Without performing any surface modification on the nanotubes, the extrusion method itself is not enough to disperse the nanotubes in the polymer matrix if the interfacial interactions between polymer and filler are low [79]. Also, the agglomeration of BNNTs in the polymer matrix is proved through SEM images (Figure 4.14) for PS-BNNT composites prepared by extrusion method. Therefore, the tensile strength value of the composite obtained from melt blending method is relatively low due to agglomeration of the nanotubes inside the polymer matrix. The preparation of PS-BNNT composites via in-situ polymerization method is based on the synthesis of PS by adding appropriate amount of BNNTs during the synthesis. The molecular weight of composite is a crucial parameter in order to evaluate the mechanical property of the composite. As it is mentioned before, the molecular weight distribution of synthesis polystyrene (BULK-sPS) is relatively broad with respect to commercial PS (cPS). The existence of lower molecular weight of chains in the composite affect the mechanical properties. Hence, tensile strength of the composite prepared via in-situ polymerization (ISP-PS+0.5) is lower than the masterbatch with extrusion methods (ME-PS+0.5). In other words, the masterbatch with extrusion method consists of polymerization of styrene with a high amount of BNNT loading followed by extrusion. Even if the molecular weight of the composite lowers in the synthesis part, the mixing of concentrated masterbatch with cPS via extrusion method compensates the reduction of molecular weight due to narrow molecular weight distribution of cPS. Hence, the tensile strength of ME-PS+0.5 is relatively higher than the samples from the other methods.

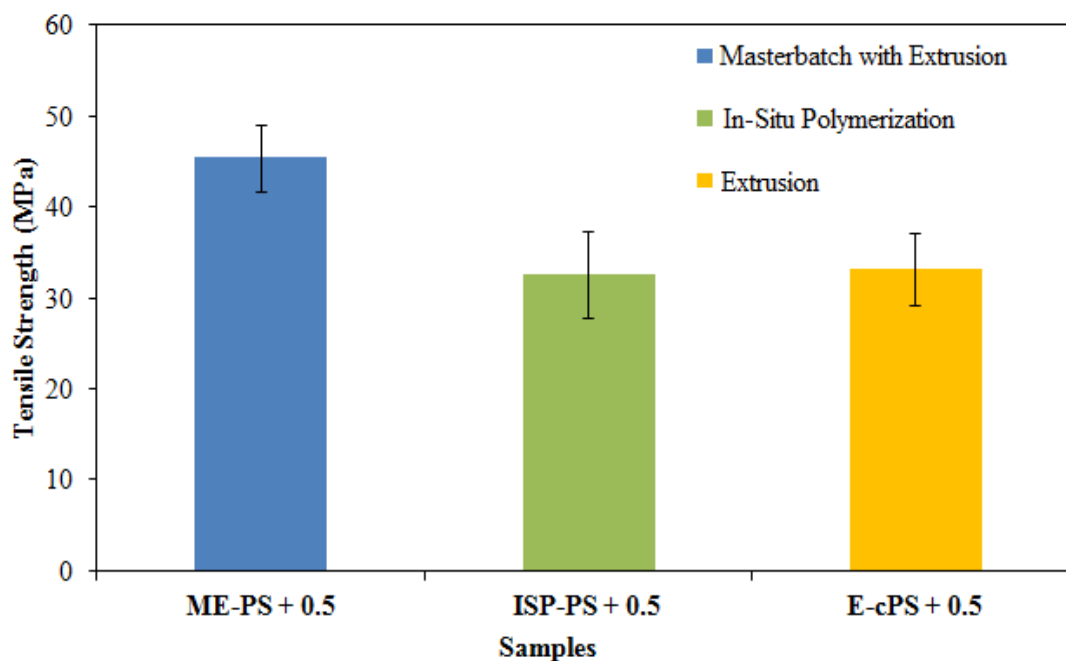


Figure 4.21 Tensile strengths of PS-BNNT composites prepared by three different methods at 0.5 wt% BNNTs loading. (ME-PS+0.5: composite prepared by masterbatch with extrusion method, ISP-PS+0.5: composite prepared by in-situ polymerization, E-cPS+0.5: composite prepared by extrusion).

Young's moduli of PS-BNNT composites prepared by three different methods at 0.5 wt% BNNTs are shown in Figure 4.22. Composite prepared by both in-situ polymerization (ISP-PS+0.5) and extrusion method (E-cPS+0.5) have relatively higher elastic modulus than the composite obtained from the masterbatch with extrusion method (ME-PS+0.5). In masterbatch method, a highly concentrated composite was first synthesized and mixed with cPS in the extrusion in order to obtain 0.5 wt% BNNTs fraction in the composite. On the other hand, the composites from both in-situ polymerization and extrusion method were prepared in a single stage. More preparation steps in masterbatch with extrusion method when compared to the other methods may cause more degradation and eventually lower tensile modulus value of ME-PS+0.5.

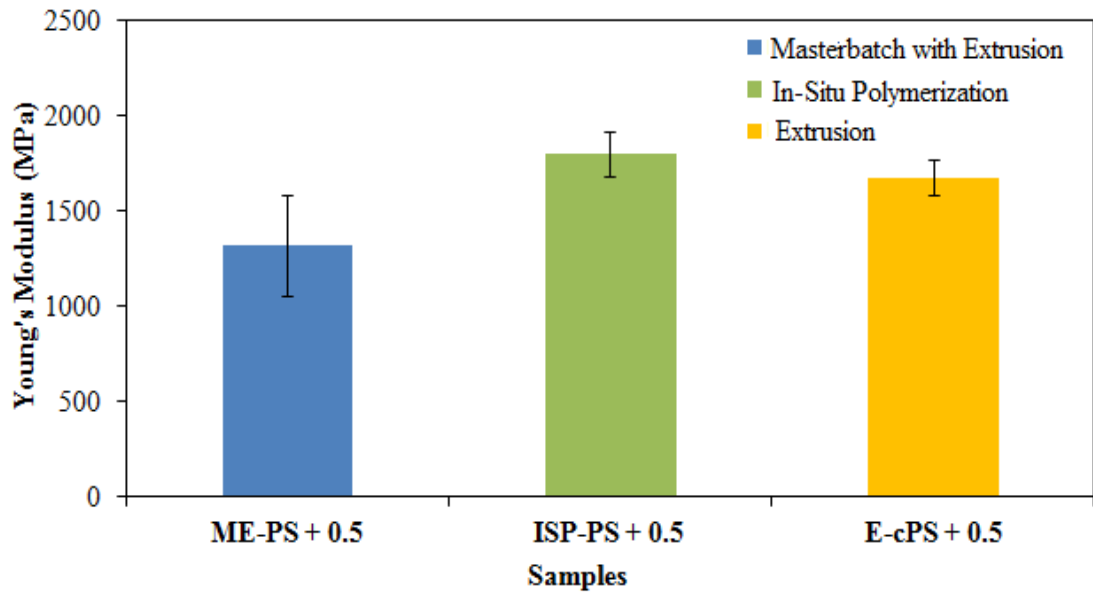


Figure 4.22 Young's moduli of PS-BNNT composites prepared by three different methods at 0.5 wt% BNNTs loading. (ME-PS+0.5: composite prepared by masterbatch with extrusion method, ISP-PS+0.5: composite prepared by in-situ polymerization, E-cPS+0.5: composite prepared by extrusion).

Elongation at break values of PS-BNNT composites prepared by masterbatch with extrusion (ME-PS+0.5), in-situ polymerization (ISP-PS+0.5) and extrusion method (E-cPS+0.5) are given in Figure 4.23. Percent elongation of PS-BNNT composites prepared by masterbatch with extrusion method (ME-PS+0.5) is higher than those obtained from the extrusion method (E-cPS+0.5) and in-situ polymerization (ISP-PS+0.5). During the preparation of the composite via masterbatch with extrusion, BNNTs are dispersed relatively better than the ones in the other methods, and this may cause an increase in the percent elongation.

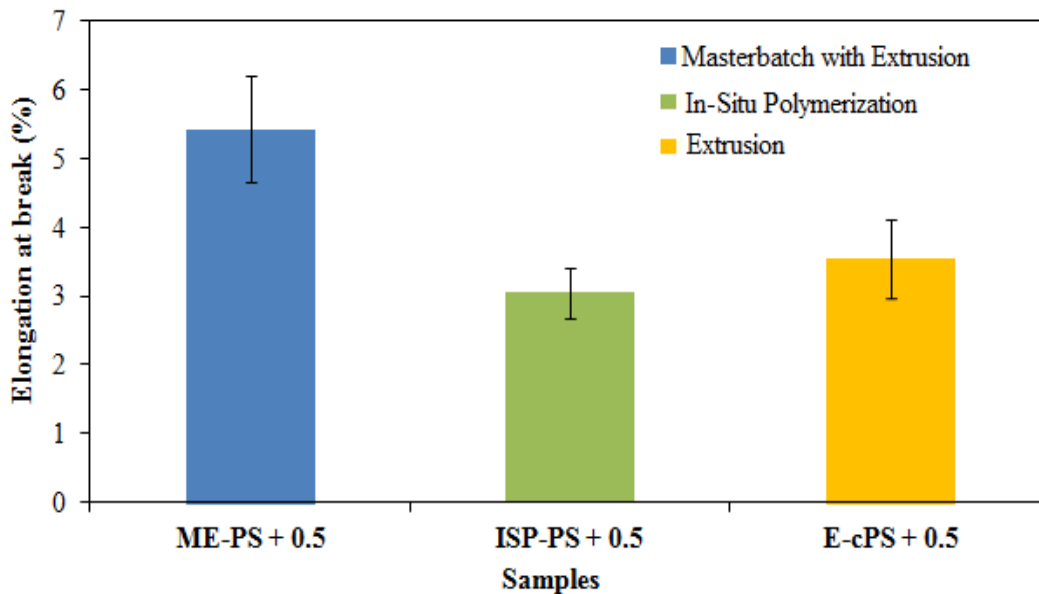


Figure 4.23 Elongation at break of PS-BNNT composites prepared by three different methods at 0.5 wt% BNNTs loading. (ME-PS+0.5: composite prepared by masterbatch with extrusion method, ISP-PS+0.5: composite prepared by in-situ polymerization, E-cPS+0.5: composite prepared by extrusion).

4.3.2.2 Impact Test

Unnotched Charpy impact test method was used to obtain information about toughness of the material. Impact results of all the composites and neat PS are given in Appendix E.

In Figure 4.24, impact strengths of commercial PS (cPS), synthesized PS (BULK-sPS) and extruded PS (E-cPS) are shown, respectively. Impact values of all different types of polystyrene samples are relatively low due to the brittle nature of polystyrene [35].

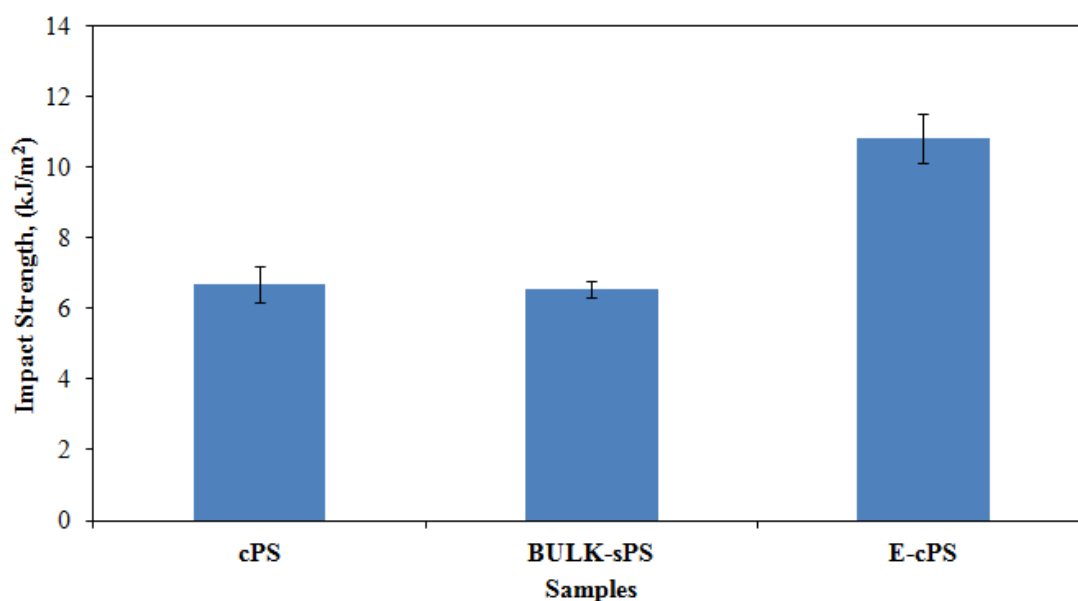


Figure 4.24 Impact strengths of PS samples. (cPS: commercial PS, BULK-sPS: Synthesis via bulk polymerization, E-cPS: extruded commercial PS).

Impact strengths of neat PS and PS-BNNT composites prepared by masterbatch with extrusion method are given in Figure 4.25. The highest impact strength value is obtained at 0.5 wt% BNNTs (ME-PS+0.5). When the loadings of BNNTs are increased in the polymer matrix, the impact strengths of the composites decrease due to the extensive agglomeration of the nanotubes in the polymer matrix [62]. When the nano-particles form agglomerates or they prefer each other, stress concentrated regions can form, and this situation leads to a significant loss in impact energy of the specimen [97].

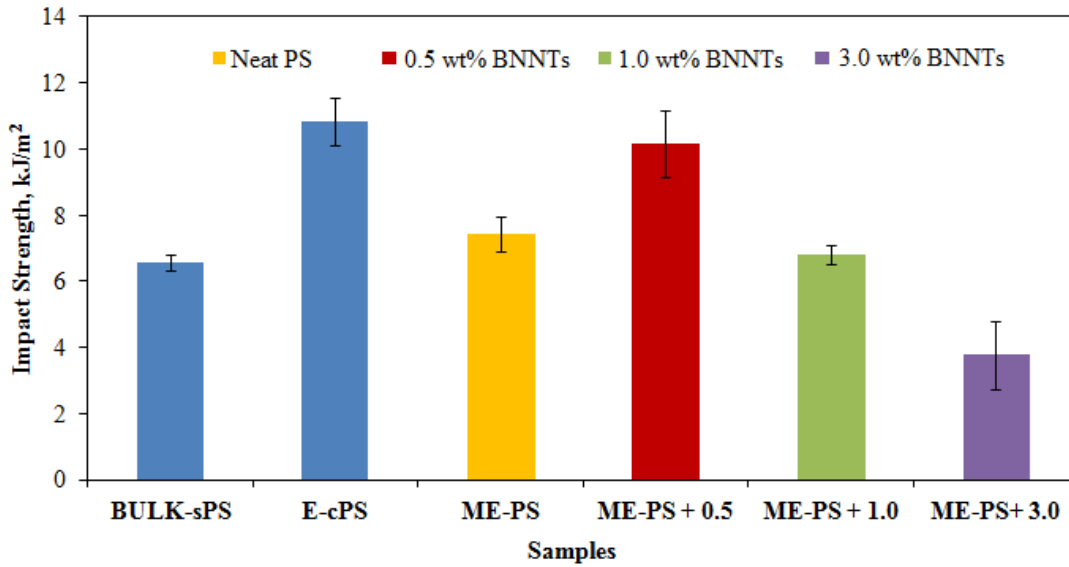


Figure 4.25 Impact strengths of PS-BNNT composites prepared by masterbatch with extrusion method. (BULK-sPS: synthesis via bulk polymerization, E-cPS: Extrusion, ME-PS: Masterbatch with extrusion).

Impact strength values of PS-BNNT composites prepared by masterbatch with extrusion, in-situ polymerization and melt blending method are shown in Figure 4.26. The impact strength value of composite prepared by masterbatch with extrusion (ME-PS+0.5) is significantly higher than the composites prepared by in-situ polymerization (ISP-PS+0.5) and extrusion (E-cPS+0.5). Use of both masterbatch and extrusion together provides better dispersion of the nanotubes in PS which results in improvement in the impact strength. On the other hand, as seen in the SEM images of the composites prepared by in-situ polymerization (Figure 4.13) and extrusion (Figure 4.14) methods at 0.5 wt% BNNTs, BNNTs exist in the form of agglomerates in the polymer matrix. The agglomeration of BNNTs lowers the impact strength of the composites by forming stress concentrated regions even if the composites are prepared at 0.5 wt% BNNTs.

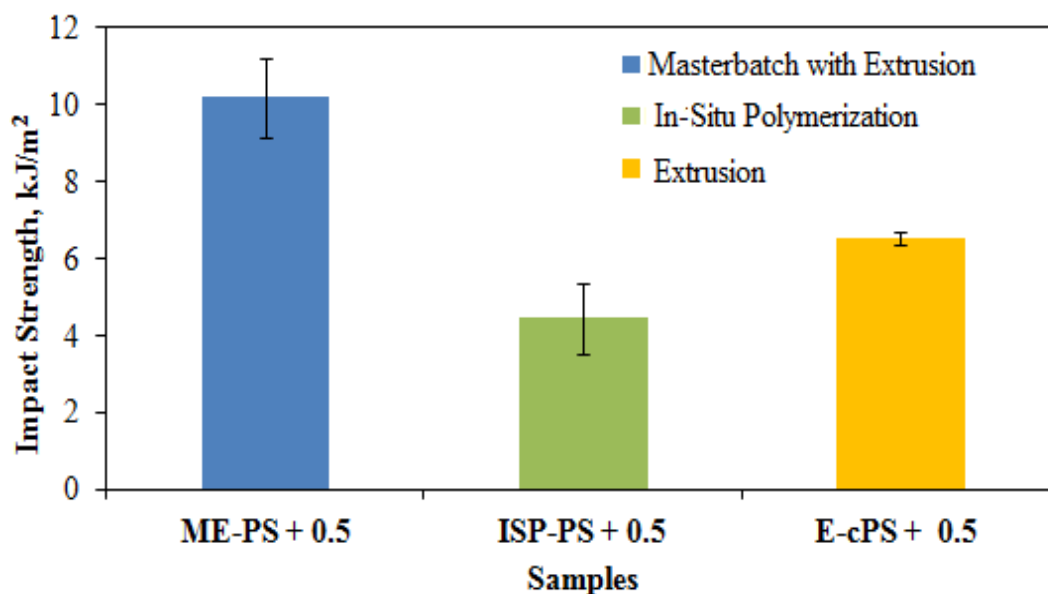


Figure 4.26 Impact strengths of PS-BNNT composites prepared by three different methods at 0.5 wt% BNNTs loading. (ME-PS+0.5: composite prepared by masterbatch with extrusion method, ISP-PS+0.5: composite prepared by in-situ polymerization, E-cPS+0.5: composite prepared by extrusion).

4.3.3 Thermal Analysis

In order to investigate thermal properties of the composites and neat resin, Differential Scanning Calorimetry (DSC) and Thermal Gravimetric analysis (TGA) techniques were used to determine the glass transition temperature values and thermal stability behavior of the samples, respectively.

4.3.3.1 Differential Scanning Calorimetry (DSC)

Glass transition temperatures (T_g) of neat polystyrene and PS-BNNT composites were determined from DSC curves. Representative DSC plots of all the samples specified in Table 3.6 are given in Appendix G. The average glass transition temperatures which are determined from the 2nd runs of the analyses are tabulated in Table 4.9.

The glass transition temperatures of PS-BNNT composites and neat PS (ME-PS) prepared by masterbatch with extrusion method at 0.5 (ME-PS+0.5), 1 (ME-PS+1.0) and 3 wt% (ME-PS+3.0) BNNTs decrease remarkably as compared to synthesized polystyrene (BULK-sPS) prepared through the best synthesis conditions. In other words, glass transition temperatures are not affected with increasing addition of BNNTs. The chain length is one of the important factors to affect the glass transition temperature. Shorter chain length contributes to chain mobility and decrease the glass transition [21]. The synthesis of polystyrene via bulk polymerization method has a broad molecular weight distribution containing lower molecular weight chains as well. Surprisingly, the glass transition temperature of the composite prepared by in-situ polymerization method (ISP-PS+0.5) is close to the glass transition of synthesized PS (BULK-sPS). This result is unexpected regarding the results of the composites prepared by masterbatch with extrusion and extrusion method. This may be due to the single step preparation of the samples through in-situ polymerization method. In other words, when considering the other techniques, more thermal degradation occurs in the process of masterbatch with extrusion and melt mixing method as compared to the in-situ polymerization method. Therefore, less degradation possibility in the polymer matrix does not lead to decrease in the glass transition temperature of the polymer (BULK-sPS and ISP-PS+0.5).

The glass transition temperature of the composite prepared by extrusion method (E-cPS+0.5) also decreases with respect to synthesized PS (BULK-sPS). The lower extent of polymer-filler interaction causes increase in the mobility of chains and therefore decreases the glass transition temperature of the nanocomposites [98].

Table 4.9 DSC results of pure PS and the PS-BNNT composites.

Sample	Glass Transition Temperature
	2 nd Run (°C)
cPS	86.8
BULK-sPS	102.3
E-cPS	87.8
ME-PS	90.6
ME-PS + 0.5	90.1
ME-PS + 1.0	90.0
ME-PS + 3.0	88.6
ISP-PS + 0.5	99.7
E-cPS + 0.5	86.9

4.3.3.2 Thermal Gravimetric Analysis (TGA)

Thermal degradation behaviors of polystyrene and PS-BNNT composites were determined using TGA.

Figure 4.27 represents the TGA plots of all types of neat polystyrene which are commercial PS (cPS), synthesized PS (BULK-sPS), extruded PS (E-cPS) and the neat PS (ME-PS) prepared by masterbatch with extrusion method, respectively. In Figure 4.27, the weight loss of the PS samples are observed in the temperature range of 266- 438 °C due to chain degradation of PS. On the other hand, weight loss of BULK-sPS sample starts from temperature of 240 °C and ends at 422 °C. The absence of potential additives that are available in commercial PS may be the possible reason for this earlier degradation.

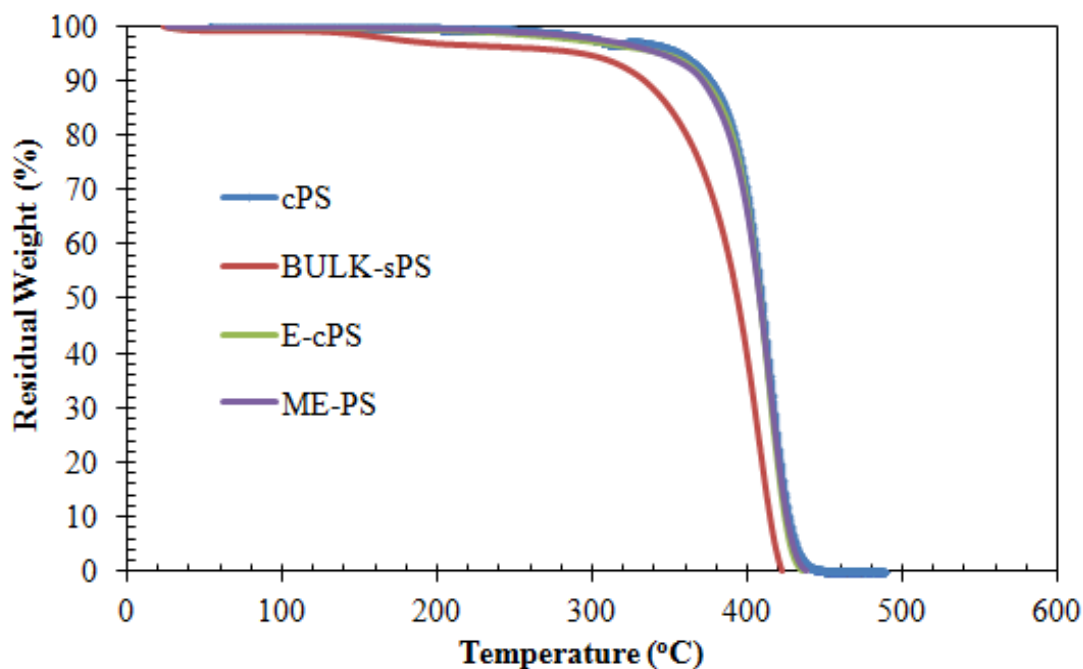


Figure 4.27 TGA plots of PS samples. (cPS: commercial PS, BULK-sPS: Synthesis via bulk polymerization, E-cPS: extruded commercial PS, ME-PS: neat PS prepared through masterbatch with extrusion method).

Figure 4.28 shows the TGA plots of neat PS and PS-BNNT composites prepared by masterbatch with extrusion method at 0.5 (ME-PS+0.5), 1.0 (ME-PS+1.0) and 3.0 (ME-PS+3.0) wt% BNNTs. The weight losses of all the composites are observed in the temperature range of 270-432 °C. It can be said that no significant improvement in thermal stability is obtained with the addition of BNNTs. Although BNNTs have high thermal and chemical stability [8], thermal stability of the composites are not shifted to much higher temperatures with the BNNT addition when compared to neat PS.

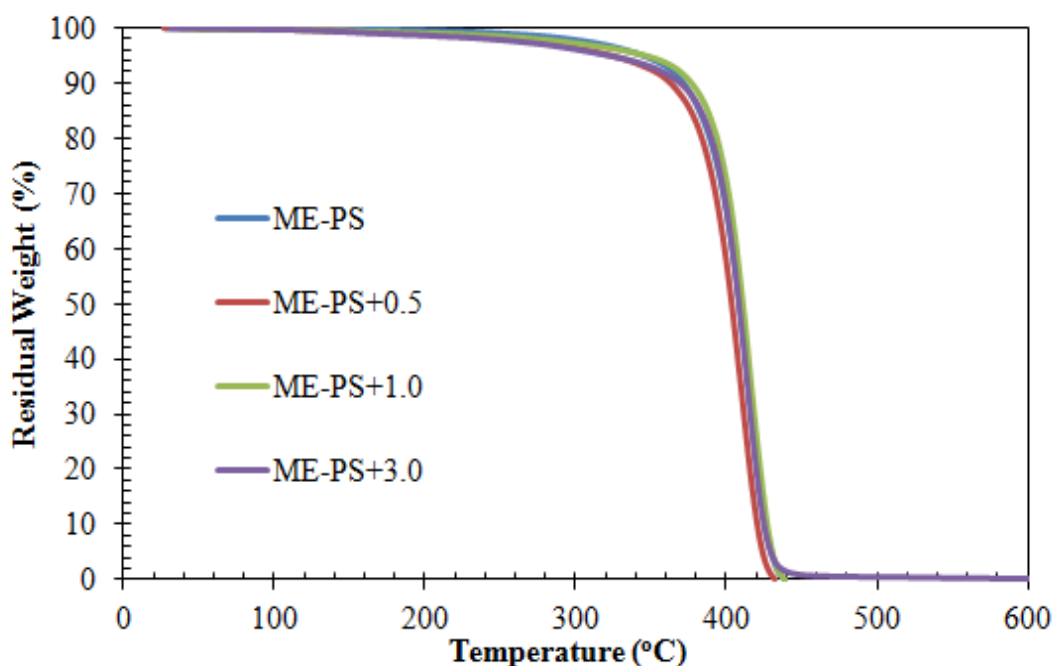


Figure 4.28 TGA plots of the composites prepared by masterbatch with extrusion method at different BNNTs loading. (ME-PS: composite prepared by masterbatch with extrusion method).

Figure 4.29 represents the TGA plots of PS-BNNT composites prepared by masterbatch with extrusion method (ME-PS+0.5), in-situ polymerization (ISP-PS+0.5) and extrusion (E-cPS+0.5) methods. Thermal stability of ISP-PS+0.5 composite is shifted to higher temperature when compared with ME-PS+0.5 and E-cPS+0.5 composites. The melt mixing process is the common preparation stage for both masterbatch with extrusion and also for extrusion method apart from the in-situ polymerization method containing only the synthesis process. During the extrusion process, more thermal degradation can occur under high temperature in the barrel (180 °C) when compared with the synthesis method. Therefore, it is reasonable that the composite prepared by in-situ polymerization method should show a higher thermal stability than those of masterbatch with extrusion and extrusion method, respectively in which polymer is subjected to the high process temperature of the extrusion process.

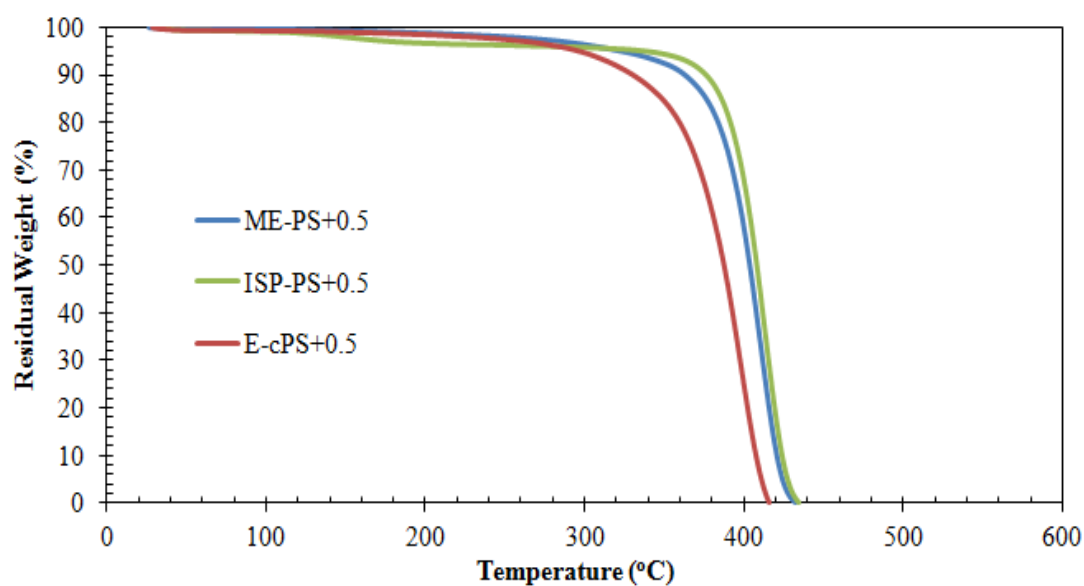


Figure 4.29 TGA plots of the composites prepared by three different methods at 0.5 wt% BNNTs. (ME-PS+0.5: composite prepared by masterbatch with extrusion method, ISP-PS+0.5: composite prepared by in-situ polymerization, E-cPS+0.5: composite prepared by extrusion).

CHAPTER 5

CONCLUSIONS

This study was mainly evaluated under three main parts: synthesis and characterization of polystyrene obtained using polymerization techniques of solution (SOL-sPS) and bulk polymerization (BULK-sPS); synthesis, purification and characterization of BNNTs, and also preparation and characterization of PS-BNNT composites prepared through melt mixing, in-situ polymerization and masterbatch with extrusion method. The following conclusions can be drawn from the thesis:

- Polystyrene was successfully synthesized via solution and bulk polymerization techniques.
- The best synthesis conditions for the polymerization of BULK-sPS were determined as 3 hrs reaction time, 0.01 mol/L initiator concentration and 95 °C reaction temperature.
- Viscosity average molecular weight, number and weight average molecular weights and polydispersity index of synthesized PS prepared through bulk polymerization under the best conditions were determined as 220100, 99500, 273800, and 2.75, respectively.
- MFI value of BULK-sPS was reported as 20.3 g/10min.
- FTIR and molecular weight results and MFI value of BULK-sPS were in agreement with those of cPS.
- BNNTs were successfully synthesized by the reaction of ammonia gas with a powder mixture of boron and iron oxide and purified by the acid treatment to get rid of reaction impurities.
- The structure of hexagonal boron nitride was proved through the XRD patterns of purified BNNTs.

- Surface area of the purified BNNTs was 114.1 m²/g and the purified BNNTs had broad pore-size distribution.
- SEM analysis of BNNTs revealed agglomerations of the nanotubes.
- SEM analyses of PS-BNNT composites prepared by masterbatch with extrusion method indicated that the homogeneous dispersion of the nanotubes in the polymer matrix was observed at 0.5 wt% BNNTs loading.
- Tensile test results showed that tensile strengths of the composites prepared by masterbatch with extrusion method decreased with the addition of BNNTs.
- Impact strengths of the composites prepared by masterbatch with extrusion method also decreased with increasing BNNT loading.
- The highest tensile strength, elongation at break and impact strength results were obtained for the PS-BNNT composite prepared by masterbatch with extrusion method at 0.5 wt% BNNTs. The homogeneous dispersion of nanotubes into the polymer matrix was also detected at this composite.
- DSC plots showed that the glass transition temperatures of PS synthesized through bulk polymerization and the composite prepared via in-situ polymerization had the highest values among the other samples.
- Glass transition temperatures of the composites prepared by masterbatch with extrusion method were remained constant with the addition of BNNTs.
- Thermal stability of the composites prepared by masterbatch with extrusion method was remained unchanged when compared to that of neat polymer prepared by the combination of masterbatch and extrusion methods.
- Thermal stability of PS-BNNT composites prepared by in-situ polymerization method was shifted to higher temperatures in comparison with PS-BNNT composites prepared by both masterbatch with extrusion and extrusion method.
- The masterbatch with extrusion method was observed to be the best one in the composite preparation techniques of this study.

REFERENCES

- [1] Mazumdar, S.K., "Composites Manufacturing Materials, Product, Process Engineering", CRC press, USA, 2002.
- [2] Jordan, J., Jacob, K.I., Tannenbaum, R., Sharaf, M.A., and Jasiuk, I., "Experimental Trends in Polymer Nanocomposites—a Review", *Material Science and Engineering A*, vol. 393, pp. 1–11, 2005.
- [3] Gacitua, W.E., Ballerini, A.A., and Zhang J. , "Polymer Nanocomposites : Synthetic and Natural Fillers", *Maderas Ciencia y tecnologia*, vol. 7, no. 3, pp. 159–178, 2005.
- [4] Kawasumi, M., "The Discovery of Polymer-Clay Hybrids", *Journal of Polymer Science Part A Polymer Chemistry*, vol. 42, no. 4, pp. 819–824, 2004.
- [5] Iijima, S., "Helical microtubules of graphitic carbon", *Nature*, vol.354, pp.56-58, 1991.
- [6] Andrews, R., and Weisenberger, M., "Carbon Nanotube Polymer Composites", *Current Opinion in Solid State and Material Science*, vol. 8, no. 1, pp. 31–37, 2004.
- [7] Chopra, N.G., Luyken, R.J., Cherrey, K., Crespi, V.H., Cohen, M.L., Louie, S.G., and Zettl, A., "Boron Nitride Nanotubes", *Science*, vol. 269, no.5226, pp. 966–67, 1995.
- [8] Chen, Y., Zou, J., Campbell, S. J., and Le Caer, G., "Boron Nitride Nanotubes: Pronounced Resistance to Oxidation", *Applied Physics Letters*, vol. 84, no.13, p. 2430-2432, 2004.

- [9] Zhi, C.Y., "Boron Nitride Nanotube/Polystyrene Composites", *JSM NanotechnolNanomed*, vol. 1, no.1, pp. 1–2, 2013.
- [10] Zhi, C., Bando, Y., Tang, C., Honda, S., Kuwahara, H., and Golberg, D., "Boron Nitride Nanotubes/Polystyrene composites", *Material Research Society*, vol. 21, no. 11, pp. 2794–2800, 2006.
- [11] Demir, C., "Production of Boron Nitride Nanotubes and Their Uses in Polymer Composites", 2010, Chemical Engineering MS Thesis, Middle East Technical University, Ankara, Turkey.
- [12] Zhi, C.Y., Bando, Y., Wang, W.L., Tang, C.C., Kuwahara, H., and Golberg, D., "Mechanical and Thermal Properties of Polymethyl Methacrylate-BN Nanotube Composites", *Journal of Nanomaterials*, vol. 2008, pp. 1–5, 2008.
- [13] Li, L., Chen, Y., and Stachurski, Z.H., "Boron Nitride Nanotube Reinforced Polyurethane Composites", *Progress in Natural Science: Materials International*, vol. 23, no. 2, pp. 170–173, 2013.
- [14] Zhi, C., Bando, Y., Tang, C., Honda, S., Sato, K., Kuwahara, H., and Golberg D., "Characteristics of Boron nitride Nanotube-Polyaniline Composites", *Angewandte Chemie Int. Ed.*, vol. 44, no. 48, pp. 7929–7932, 2005.
- [15] Berthelot, J.M., "Composite Materials: Mechanical Behavior and Structural Analysis", Springer-Verlag, USA, 1999.
- [16] Kaw, K., "Mechanics of Composite Materials", CRC Press, New York, 1997.
- [17] Jones, R.M., "Mechanics of Composite Materials", Taylor & Francis, Philadelphia, 1999.
- [18] Evans, A., Marchi, S.C., and Mortensen, A. "Metal Matrix Composites in Industry: An Introduction and a Survey", Kluwer Academic Publisher, Massachusetts, 2003.

- [19] Raether, F., "Ceramic Matrix Composites – an Alternative for Challenging Construction Tasks", *Ceramic applications*, vol. 1, pp. 45–49, 2013.
- [20] Fried, J.R., "Polymer Science & Technology", Prentice Hall, New Jersey, 2003.
- [21] Rosen, S.L., "Fundamental Principles of Polymeric Materials", John Wiley & Sons, New York, 1993.
- [22] Kopeliovich, D., "Classification of Composites",
http://www.substech.com/dokuwiki/doku.php?id=polymer_matrix_composites_introduction
 Last visited on: October 2014.
- [23] Paul, D.R., and Robeson, L.M., "Polymer Nanotechnology: Nanocomposites, Polymer", vol. 49, no. 15, pp. 3187–3204, 2008.
- [24] Gupta, R.K., Kennel, E., and Kim, K.J., "Polymer Nanocomposites Handbook", CRC Press Taylor & Francis Group, New York, 2010.
- [25] Davim, J.P., and Charitidis, C.A., "Nanocomposites: Materials, Manufacturing and Engineering", De Gruyter, Berlin, 2013.
- [26] Mani, G., Fan, Q., Ugbohue, S.C., and Yang, Y., "Morphological Studies of Polypropylene -Nanoclay Composites", *Journal of Applied Polymer Science*, vol. 97, no. 1, pp. 218–226, 2005.
- [27] Alexandre, M., and Dubois, P., "Polymer-Layered Silicate Nanocomposites : Preparation, Properties and Uses of a New Class of Materials", *Materials Science and Engineering*, vol. 28, pp. 1–63, 2000 .
- [28] Bhattacharya, S.N., Gupta, R.K., and Kamal, M.R., "Polymer Nanocomposites: Theory and Practice", Carl Hanser Publishers, Munich, 2008.

- [29] Beyou, E., Akbar, S., Chaumont, P., and Cassagnau, P., "Polymer Nanocomposites Containing Functionalised Multiwalled Carbon NanoTubes: a Particular Attention to Polyolefin Based Materials", Intech, id: 10.5772/50710, pp. 78-115, 2013.
- [30] Maul, J., "Ullmann's Encyclopedia of Industry Chemistry : Polystyrene and Styrene Copolymers", Wiley-VCH Verlag, Weinheim, 2007.
- [31] Peacock, A., and Calhoun, A., "Polymer Chemistry Properties and Applications", Hanser Publishers, Munich, 2006.
- [32] Ebewele, R.O., "Polymer Science and Technology", CRC Press LLC, USA, 2000.
- [33] Seymour, R.B., and Carraher, C.E."Structure-Property Relationships in Polymers", Plenum Press, New York, 1984.
- [34] Salamone, J.C., "Polymeric Materials Encyclopedia", CRC Press, vol.9, pp.6806-6813, New York, 1996.
- [35] Carraher, C.E.Jr., "Seymour/Carraher's Polymer Chemistry", 7th edition, CRC Press Taylor & Francis Group, USA, 2008.
- [36] Golberg, D., Bando, Y., Tang, C.C.,and Zhi, C.Y., "Boron Nitride Nanotubes", Advanced Materials, vol. 19, no. 18, pp. 2413–2432, 2007.
- [37] Terrones, M., Romo-Herrera, J.M., Cruz-Silva, E., López-Urías, F., Muñoz-Sandoval, E., Velázquez-Salazar, J.J., Terrones, H., Bando, Y.,and Golberg, D., "Pure and Doped Boron Nitride Nanotubes", Materials Today, vol. 10, no. 5, pp. 30–38, 2007.
- [38] Chopra, N.G. and Zettl, A., "Measurement of the Elastic Modulus of a Multi-Wall Boron Nitride Nanotube", Solid State Communications, vol. 105, no.5, pp. 297-300,1998.

- [39] Golberg, D., Bando, Y., Tang, C.C., and Zhi, C.Y., "Functional Boron Nitride Nanotubes", <http://www.cityu.edu.hk/ieeeeinec/abstract/golberg.pdf>, Last visited on : October 2014.
- [40] Ishigami, M., Aloni, S. and Zettl, A., "Properties of Boron Nitride Nanotubes", Scanning Tunneling Microscopy / Spectroscopy and Related Techniques: 12th international conference edited by Koenraad P.M., Kemerink M., pp. 94–99, 2003.
- [41] Wang, J., Lee, C.H., Bando, Y., Golberg, D., and Yap, Y.K., "Multiwalled Boron Nitride Nanotubes: Growth, Properties, and Applications", B-C-N Nanotubes and Related Nanostructures, pp. 23–45, 2009.
- [42] Zhi, C.Y., Bando, Y., Tang, C.C., Huang, Q., and Golberg, D., "Boron Nitride Nanotubes: Functionalization and Composites", Journals of Materials Chemistry, vol. 18, no. 33, p. 3900, 2008.
- [43] Gogotsi Y. "Nanotubes and Nanofibers", CRC Press Taylor & Francis Group, Pennsylvania, 2006.
- [44] Özmen, D., Sezgi, N.A., and Balçı, S., "Synthesis of Boron Nitride Nanotubes from Ammonia and a Powder Mixture of Boron and Iron Oxide", Chemical Engineering Journal, vol. 219, pp. 28–36, 2013.
- [45] Lourie, O.R., Jones, C.R., Bartlett, B.M., Gibbons, P.C., Ruoff, R.S., and Buhro, W.E., "CVD Growth of Boron Nitride Nanotubes", vol.12, no.7, pp. 1808–1810, 2000.
- [46] Chen, Y., Gerald, J.F., Williams, J.S., and Bulcock, S., "Synthesis of Boron Nitride Nanotubes at Low Temperatures Using Reactive Ball Milling", Chemical Physics Letters, vol.299, pp. 260–264, 1999.
- [47] Dike, A.S., "Nanocomposites Based on Blends of Polystyrene", 2011, Polymer Science and Technology PhD Thesis, Middle East Technical University, Ankara, Turkey.

- [48] Crawford, R.J., "Plastic Engineering", Butterworth-Heinemann, Oxford, 1998.
- [49] Wang, Y., "Compounding in Co-Rotating Twin-Screw Extruders", Rapra Technology Limited, United Kingdom, 2000.
- [50] Middleman, S., "Fundamentals of Polymer Processing", McGraw-Hill, USA, 1977.
- [51] Muccio, E.A., "Plastics Processing Technology", ASM International, USA, 1994.
- [52] Smith, B., "Infrared Spectral Interpretation : A Systematic Approach", CRC Press LLC, Florida, 1999.
- [53] Bag, S.D., "Principles of Polymers :An Advanced Book", Nova Science Publishers, New York, 2013.
- [54] http://www.ias.ac.in/initiat/sci_ed/resources/chemistry/Viscosity.pdf
Last visited on: October 2014.
- [55] Billmeyer, F.W., "Textbook of Polymer Science", John Wiley & Sons, New York, 1971.
- [56] Rodriguez, F., Cohen, C., Ober, C. and Archer, L.A., "Principles of Polymer Systems", Taylor & Francis Group, USA, 2003.
- [57] Progelhof, R.C., and Throne, J.L., "Polymer Engineering Principles : Properties, Processes, Tests for Design", Hanser/Gardner Publications, Cincinnati, 1993.
- [58] Işık, I., "Impact Modified Polyamide-Organoclay Nanocomposites", 2007, Chemical Engineering PhD Thesis, Middle East Technical University, Ankara, Turkey.
- [59] Callister, D.W., "Materials Science and Engineering: An Introduction", John Wiley & Sons, Inc., USA, 2007.

- [60] Jens, A.N., and McMorrow, D., "Elements of Modern X-ray Physics", John Wiley & Sons, United Kingdom, 2011.
- [61] <http://www.aboutcivil.org/tension-test-tensile-strength-test.html>
Last visited on: October 2014.
- [62] Nielsen, L.E., and Landel, R.F., "Mechanical Properties of Polymers and Composites", Marcel Dekker, New York, 1994.
- [63] Yeniova, C., "Impact Modified Polystyrene Based Nanocomposites", 2009, Chemical Engineering MS Thesis, Middle East Technical University, Ankara, Turkey.
- [64] Gabbott, P., "Principles and Applications of Thermal Analysis", Blackwell Publishing, United Kingdom, 2008.
- [65] Altares, T., Wyman, D. P., and Allen, V. R., "Synthesis of Low Molecular Weight Polystyrene by Anionic Techniques and Intrinsic Viscosity-Molecular Weight Relations Over a Broad Range in Molecular Weight", 145th Meeting American Chemical Society, vol. 2, pp. 4533–4544, 1964.
- [66] McIntyre, D., Fetters, L. J., and Slagowski, E., "Polymers: Synthesis and Characterization of Extremely High-Molecular-Weight Polystyrene", Science, New Series, vol. 176, no. 4038, pp. 1041–1043, 1972.
- [67] Choi, K. Y., Liang, W. R., and Lei, G. D., "Kinetics of Bulk Styrene Polymerization Catalyzed by Symmetrical Bifunctional Initiators", Journal of Applied Polymer Science, vol. 35, no. 6, pp. 1547–1562, 1988.
- [68] Patra, B.N. and Bhattacharjee, M., "Synthesis of High Molecular Weight Polystyrene and Poly(Methyl Methacrylate) with Low Polydispersity by [Cp₂ZrCl₂] Catalyzed Aqueous Polymerization", Journal of Polymer Science Part A: Polymer Chemistry, vol. 43, no. 17, pp. 3797–3803, 2005.

- [69] Tang, C.C., De Chapelle, M.L., Li, P., Liu, Y.M., Dang, H.Y., and Fan, S.S., "Catalytic Growth of Nanotube and Nanobamboo Structures of Boron Nitride", *Chemical Physics Letters*, vol. 342, pp. 492–496, 2001.
- [70] Tang, C., Bando, Y., Sato, T., and Kurashima, K., "A Novel Precursor for Synthesis of Pure Boron Nitride Nanotubes", *Chem. Commun.*, id: 10.1039/b202177c, pp. 1290–1291, 2002.
- [71] Tang, C., Bando, Y., and Golberg D., "Multi-walled BN nanotubes synthesized by carbon-free method", *Journal of Solid State Chemistry*, vol. 177, no. 8, pp. 2670–2674, 2004.
- [72] Zhi, C., Bando, Y., Tan, C., and Golberg, D., "Effective precursor for high yield synthesis of pure BN nanotubes", *Solid State Communications*, vol. 135, no. 1–2, pp. 67–70, 2005.
- [73] Lee, C.H., Wang, J., Kayatsha, V.K., Huang, J.Y., and Yap, Y.K., "Effective Growth of Boron Nitride Nanotubes by Thermal Chemical Vapor Deposition", *Nanotechnology*, vol. 19, no. 45, pp. 1–5, 2008.
- [74] Noyan, S., "Production of Boron Nitride Nanotubes from the Reaction of NH_3 with Boron and Iron Powder Mixture", 2012, *Chemical Engineering MS Thesis*, Middle East Technical University, Ankara, Turkey.
- [75] Tong, X., Liu, C., Cheng, H., Zhao, H., Yang, F., and Zhang, X., "Surface Modification of Single-Walled Carbon Nanotubes with Polyethylene via In Situ Ziegler–Natta Polymerization", *Journal of Applied Polymer Science*, vol. 92, pp. 3697–3700, 2004.
- [76] Park, J.U., Cho, S., Cho, K.S., Ahn, K.H., Lee, S.J., and Lee, S.J., "Effective In-Situ Preparation and Characteristics of Polystyrene-Grafted Carbon Nanotube Composites", *Korea-Austrian Rheology Journal*, vol. 17, no. 2, pp. 41–45, 2005.

- [77] Mhetre, S.K., Patra, P.K., Kim, Y.K., and Warner, S.B., "In-Situ Polymerized Nylon 6 / MwnT Nanocomposite Fibers", *RJTA*, vol. 11, no. 3, pp. 35–41, 2007.
- [78] Lahelin, M., Annala, M., Nykänen, A., Ruokolainen, J., and Seppälä, J., "In situ polymerized nanocomposites: Polystyrene/CNT and Poly(methyl methacrylate)/CNT composites", *Composite Science and Technology*, vol. 71, no. 6, pp. 900–907, 2011.
- [79] Annala, M., Lahelin, M., and Seppälä, J., "Utilization of poly (methyl methacrylate) – Carbon nanotube and Polystyrene – Carbon Nanotube In Situ Polymerized Composites as Masterbatches for Melt Mixing", *express Polymer Letters*, vol. 6, no. 10, pp. 814–825, 2012.
- [80] Harrison, C., Weaver, S., Bertelsen, C., Burgett, E., Hertel, N., and Grulke, E., "Polyethylene/Boron Nitride Composites for Space Radiation Shielding", *Journal of Applied Polymer Science*, vol. 109, no. 4, pp. 2529–2538, 2008.
- [81] Ravichandran, J., Manoj, A.G., Liu, J., Manna, I. and Carroll, D.L., "A Novel Polymer Nanotube Composite for Photovoltaic Packaging Applications", *Nanotechnology*, vol. 19, no. 8, pp. 1-5, 2008.
- [82] Zhi, C., Bando, Y., Terao, T., Tang, C., Kuwahara, H., and Golberg, D., "Towards Thermoconductive, Electrically Insulating Polymeric Composites with Boron Nitride Nanotubes as Fillers", *Advanced Functional Materials*, vol. 19, no. 12, pp. 1857–1862, 2009.
- [83] Terao, T., Bando, Y., Mitome, M., Zhi, C., Tang, C., and Golberg, D., "Thermal Conductivity Improvement of Polymer Films by Catechin-Modified Boron Nitride Nanotubes", *J. Phys. Chem. C*, vol. 113, no. 31, pp. 13605–13609, 2009.

- [84] Styrolution PS 116 N/L,
<http://ultrapolymers.com/products/detail-7586/>
Last Visited on: September, 2014.
- [85] McKeen, L.W., "The Effect of Temperature and Other Factors on Plastics and Elastomers", 2nd edition, Plastic Design Library, USA, 2008.
- [86] 2,2'-Azobis (2-methylpropionitrile)
<http://www.sigmaaldrich.com/catalog/product/aldrich/441090>
Last Visited on: December, 2014.
- [87] Braun, D., Cherdron, H., Rehahn, M., Ritter, H., and Voit, B., "Polymer Synthesis: Theory and Practice, Fundamentals, Methods, Experiments", 4th edition, Springer-Verlag, Berlin, 2005.
- [88] Mitchell, B.S., "An Introduction to Materials Engineering and Science", Wiley-Interscience, New Jersey, 2004.
- [89] Büyükyavaş, A., "Synthesis and Characterization of Monoacetylferrocene and Sulfonated Polystyrene", 2004, Department of Chemistry Ms.Thesis, Middle East Technical University, Ankara, Turkey.
- [90] Kim, J., Kim, K., Park, S., Jeong, K. and Lee, M., "Preparation and Characterizations of C₆₀ / Polystyrene Composite Particle Containing Pristine C₆₀ Clusters", Bull. Korean Chem. Soc., vol. 33, no. 9, pp. 2966–2970, 2012.
- [91] Lowell, S., Shields, J.E., Thomas, M.A., and Thommes, M., "Characterization of Porous Solids and Powders: Surface Area, Pore Size and Density", 4th edition, Springer, Netherlands, 2006.
- [92] Thomas, J.M., and Thomas, W.J., "Principles and Practice of Heterogeneous Catalysis", VCH Publishers, New York, 1996.

- [93] Shi, D.L., Feng, X.Q., Huang, Y.Y., Hwang, K.C., and Gao, H., "The Effect of Nanotube Waviness and Agglomeration on the Elastic Property of Carbon Nanotube-Reinforced Composites", *Journal of Engineering Materials and Technology*, vol. 126, no. 3, pp. 250-257, 2004.
- [94] Yilmazer, U. and Ozden, G., "Polystyrene–Organoclay Nanocomposites Prepared by Melt Intercalation, In Situ, and Masterbatch Methods", *Polymer Composites*, vol. 27, no. 3, pp. 249–255, 2006.
- [95] Moniruzzaman, M. and Winey, K.I., "Polymer Nanocomposites Containing Carbon Nanotubes", *Macromolecules*, vol. 39, pp. 5194-5205, 2006.
- [96] Wang, W., Ciselli, P., Kuznetsov, E., Peijs, T., and Barber, A.H., "Effective Reinforcement in Carbon Nanotube-Polymer Composites", *Philosophical Transaction Royal Society A.*, vol. 366, no. 1870, pp. 1613–1626, 2008.
- [97] Wetzel, B., Hauptert, F., Friedrich, K., Zhang, M.Q., and Rong, M.Z., "Impact and Wear Resistance of Polymer Nanocomposites at Lower Filler Content", *Polymer Engineering and Science*, vol. 42, no. 9, pp. 1919–1927, 2002.
- [98] Pham, J.Q., Mitchell, C.A., Bahr, J.L., Tour, J.M., Krishnamoorti, R., and Green, P.F., "Glass Transition of Polymer/Single-Walled Carbon Nanotube Composite Films", *Journal of Polymer Science: Part B: Polymer Physics*, vol. 41, no. 24, pp. 3339–3345, 2003.
- [99] Mark, J. E., "Polymer Data Handbook", Oxford University Press, UK, 1999.

APPENDIX A

CALCULATION OF VISCOSITY AVERAGE MOLECULAR WEIGHT OF POLYMER SYNTHESIZED USING SOLUTION POLYMERIZATION TECHNIQUE

In the viscosity average molecular weight measurement experiments, flow times of synthesized PS (SOL-sPS) dissolved in toluene were recorded as a function of concentration. Flow time values are tabulated in Tables A.1-A.5.

Table A.1 Flow times of SOL-sPS synthesized at 1.5 hrs polymerization reaction time in the presence of solvent.

Concentration (g/dl) Measurements	Time(s)					
	0	1	0.8	0.6	0.4	0.2
1	214	258	249	240	231	222
2	211	261	247	239	230	225
3	214	257	249	239	230	225
4	214	258	249	239	230	226
5	214	257	249	240	230	227
<i>Average</i>	<i>213.4</i>	<i>258.2</i>	<i>248.6</i>	<i>239.4</i>	<i>230.2</i>	<i>225</i>

Table A.2 Flow times of SOL-sPS synthesized at 3 hrs polymerization reaction time in the presence of solvent.

Concentration (g/dl) Measurements	Time(s)					
	0	1	0.8	0.6	0.4	0.2
1	214	259	251	244	234	225
2	211	259	251	243	231	227
3	214	260	251	242	232	227
4	214	259	250	242	230	227
5	214	261	251	242	231	227
<i>Average</i>	<i>213.4</i>	<i>259.6</i>	<i>250.8</i>	<i>242.6</i>	<i>231.6</i>	<i>226.6</i>

Table A.3 Flow times of SOL-sPS synthesized at 6 hrs polymerization reaction time in the presence of solvent.

Concentration (g/dl) Measurements	Time(s)					
	0	1	0.8	0.6	0.4	0.2
1	214	264	251	240	231	222
2	211	264	249	240	231	223
3	214	260	250	238	229	221
4	214	259	252	240	229	222
5	214	261	252	246	229	223
<i>Average</i>	<i>213.4</i>	<i>261.4</i>	<i>250.8</i>	<i>240.8</i>	<i>229.8</i>	<i>222.2</i>

Table A.4 Flow times of SOL-sPS synthesized at 9 hrs polymerization reaction time in the presence of solvent.

Concentration (g/dl) Measurements	Time(s)					
	0	1	0.8	0.6	0.4	0.2
1	214	270	259	246	233	223
2	211	269	256	245	234	225
3	214	269	254	244	232	224
4	214	270	255	244	233	224
5	214	269	256	245	232	223
<i>Average</i>	<i>213.4</i>	<i>269.4</i>	<i>256</i>	<i>244.8</i>	<i>232.8</i>	<i>223.8</i>

Table A.5 Flow times of PS synthesized at 3 hrs polymerization reaction time in the absence of solvent.

Concentration (g/dl) Measurements	Time(s)					
	0	1	0.8	0.6	0.4	0.2
1	214	389	361	320	284	249
2	211	389	362	322	283	249
3	214	389	363	321	284	249
4	214	390	362	322	283	249
5	214	391	362	321	284	247
<i>Average</i>	<i>213.4</i>	<i>389.6</i>	<i>362</i>	<i>321.2</i>	<i>283.6</i>	<i>248.6</i>

Initially, relative (η_r) and specific (η_{sp}) viscosities are calculated from equations A.1 & A.2 using the average flow time values of polymer solutions.

$$\eta_r = \frac{t_{\text{conc.}}}{t_{\text{solvent}}} \quad (\text{A.1})$$

$$\eta_{sp} = 1 - \eta_r \quad (\text{A.2})$$

Then, reduced (η_{red}) and inherent (η_{inh}) viscosities are calculated using equations A3 & A4.

$$\eta_{red} = \frac{\eta_{sp}}{c} \quad (\text{A.3})$$

$$\eta_{inh} = \frac{\ln \eta_r}{c} \quad (\text{A.4})$$

Calculated viscosities of PS solutions are given in Tables A.6- A.10.

Table A.6 Calculated viscosities of SOL-sPS synthesized at 1.5 hrs polymerization reaction time in the presence of solvent.

Concentration (g/dl)	1	0.8	0.6	0.4	0.2
Viscosities					
η_r	1.209	1.164	1.121	1.078	1.054
η_{sp}	0.209	0.164	0.121	0.078	0.054
η_{red} (dl/g)	0.210	0.204	0.199	-	0.265
η_{inh} (dl/g)	0.190	0.189	0.188	-	0.258

* Average time values given in Table A.1 are used.

Table A.7 Calculated viscosities of SOL-sPS synthesized at 3 hrs polymerization reaction time in the presence of solvent.

Concentration (g/dl)	1	0.8	0.6	0.4	0.2
Viscosities					
η_r	1.216	1.175	1.136	1.085	1.061
η_{sp}	0.216	0.175	0.136	0.085	0.061
η_{red} (dl/g)	0.216	0.217	0.224	-	0.301
η_{inh} (dl/g)	0.195	0.200	0.210	-	0.292

* Average time values given in Table A.2 are used.

Table A.8 Calculated viscosities of SOL-sPS synthesized at 6 hrs polymerization reaction time in the presence of solvent.

Concentration (g/dl)	1	0.8	0.6	0.4	0.2
Viscosities					
η_r	1.224	1.175	1.128	1.076	1.041
η_{sp}	0.224	0.175	0.128	0.076	0.041
η_{red} (dl/g)	0.225	0.217	0.210	-	0.200
η_{inh} (dl/g)	0.202	0.200	0.198	-	0.196

* Average time values given in Table A.3 are used.

Table A.9 Calculated viscosities of SOL-sPS synthesized at 9 hrs polymerization reaction time in the presence of solvent.

Concentration (g/dl) Viscosities	1	0.8	0.6	0.4	0.2
η_r	1.262	1.199	1.147	1.090	1.048
η_{sp}	0.262	0.199	0.147	0.090	0.048
η_{red} (dl/g)	0.262	0.247	0.241	-	0.237
η_{inh} (dl/g)	0.232	0.225	0.225	-	0.232

* Average time values given in Table A.4 are used.

Table A.10 Calculated viscosities of PS synthesized at 3 hrs polymerization reaction time in the absence of solvent.

Concentration (g/dl)	1	0.8	0.6	0.4	0.2
Viscosities					
η_r	1.825	1.696	1.505	1.328	1.164
η_{sp}	0.825	0.696	0.505	0.328	0.164
η_{red} (dl/g)	0.825	-	0.828	0.815	0.804
η_{inh} (dl/g)	0.601	-	0.670	0.705	0.745

* Average time values given in Table A.5 are used.

After the calculation of viscosity values, reduced and inherent viscosities of polymer solutions as a function of concentration are plotted in Figures A.1-A.5.

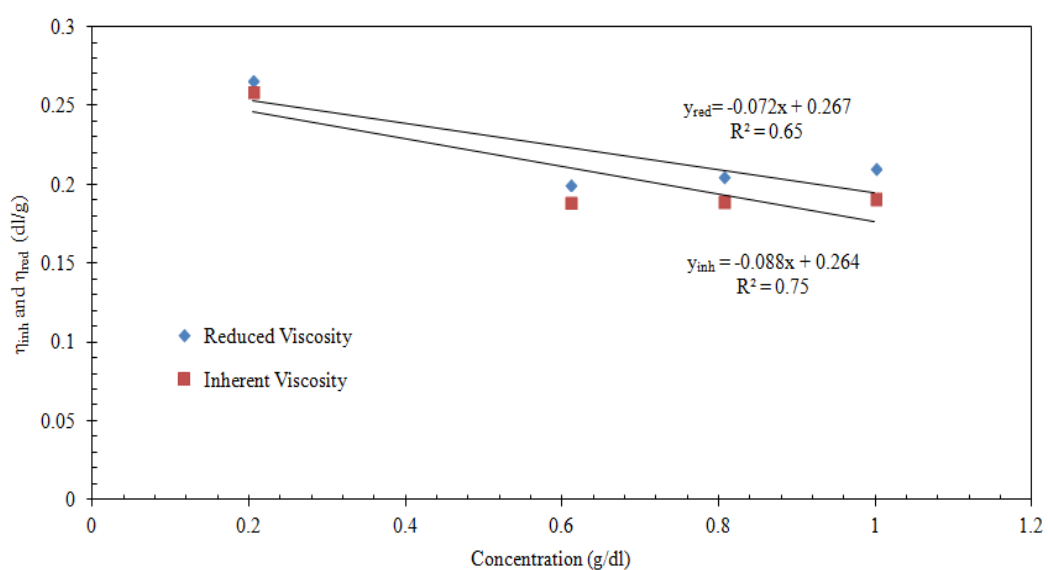


Figure A.1 Variation of reduced and inherent viscosities of SOL-sPS synthesized at 1.5 hrs polymerization reaction time in the presence of solvent with respect to concentration.

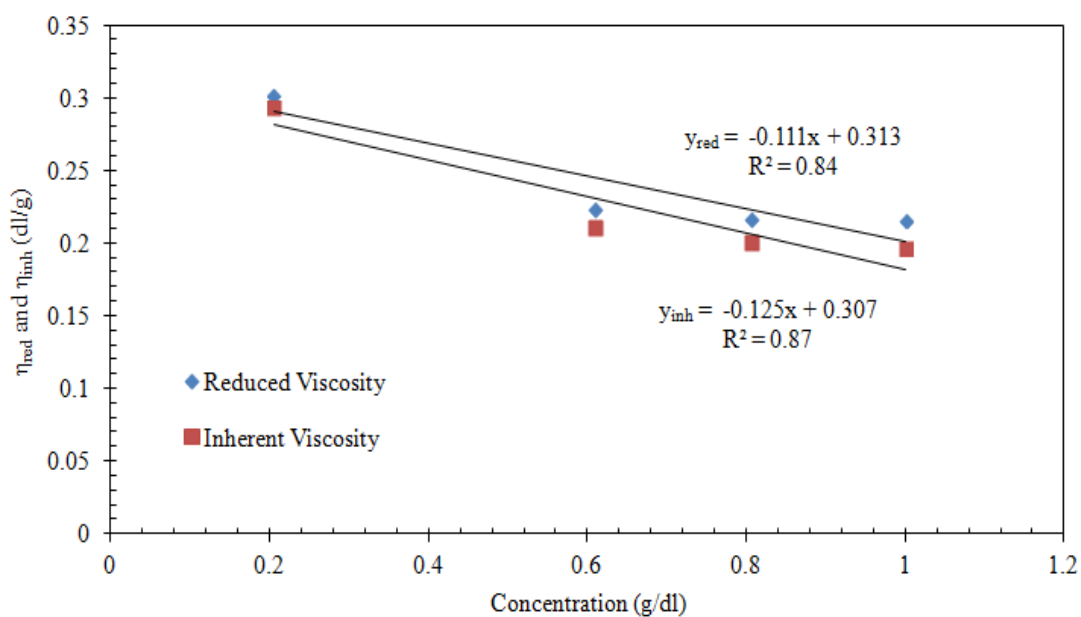


Figure A.2 Variation of reduced and inherent viscosities of SOL-sPS synthesized at 3 hrs polymerization reaction time in the presence of solvent with respect to concentration.

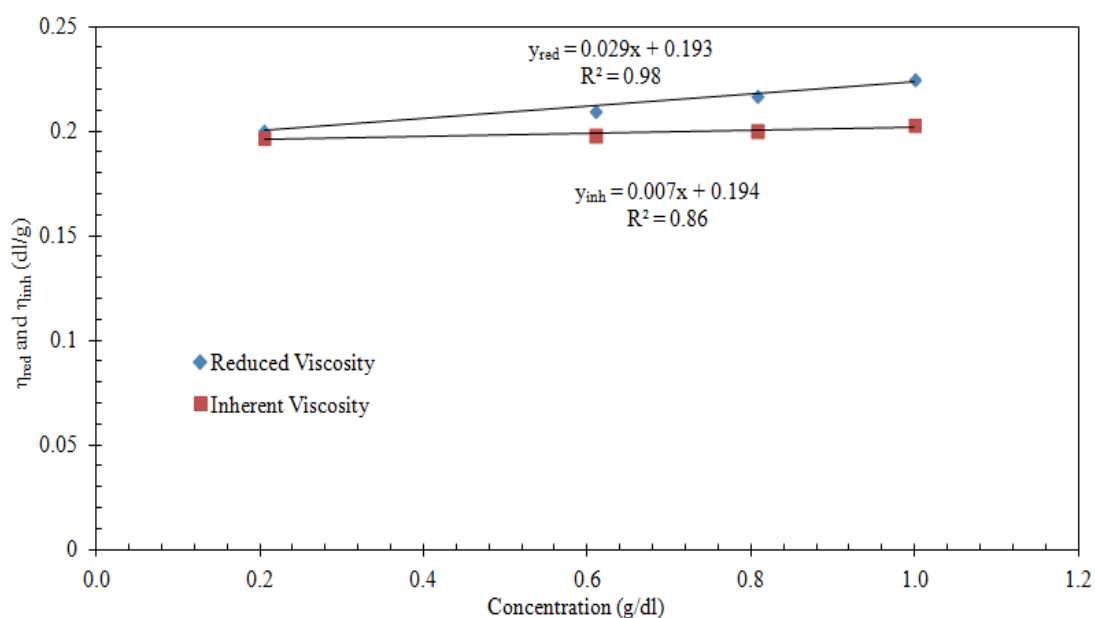


Figure A.3 Variation of reduced and inherent viscosities of SOL-sPS synthesized at 6 hrs polymerization reaction time in the presence of solvent with respect to concentration.

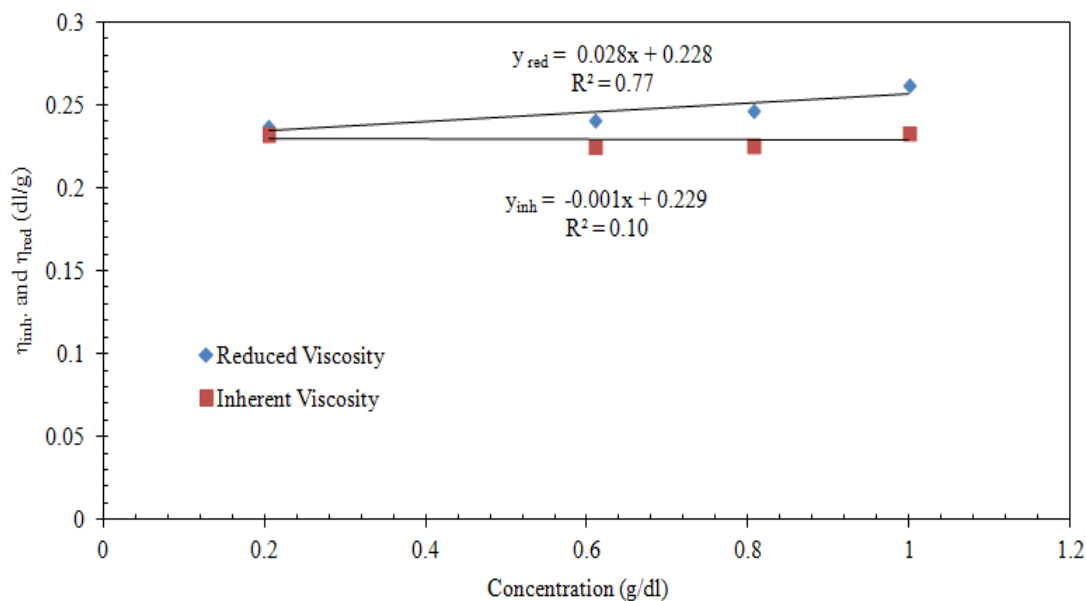


Figure A.4 Variation of reduced and inherent viscosities of SOL-sPS synthesized at 9 hrs polymerization reaction time in the presence of solvent with respect to concentration.

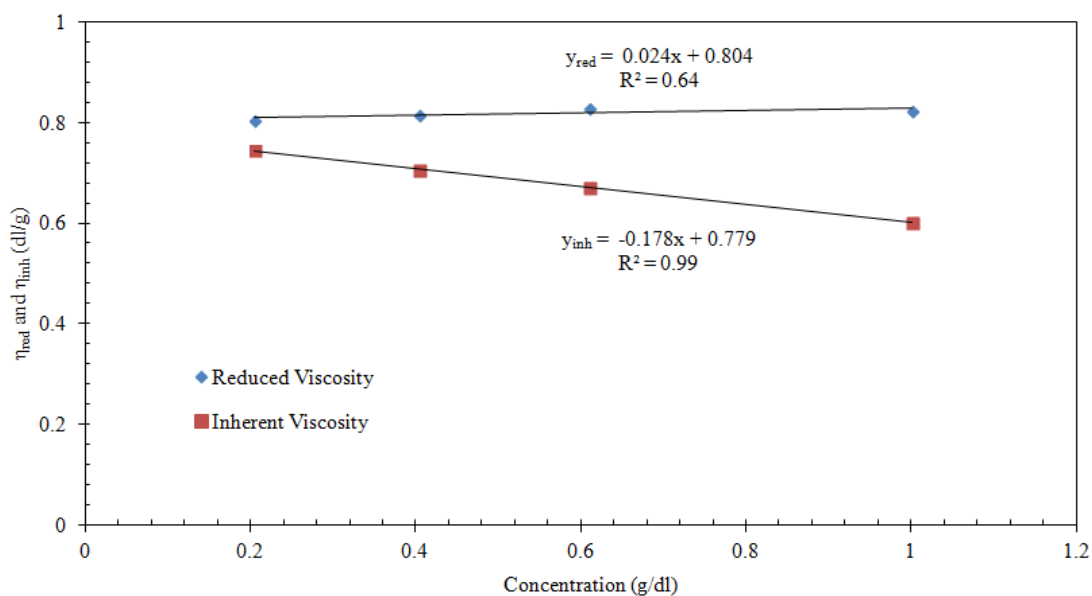


Figure A.5 Variation of PS synthesized at 3 hrs polymerization reaction time in the absence of solvent with respect to concentration.

Linear relations drawn for both η_{red} and η_{inh} were extrapolated to zero concentration in order to find intrinsic viscosity. Viscosity average molecular weight of synthesized PS were determined using Mark-Houwink-Sakurada equation (given in section 2.8.2.1). K and a values of Mark-Houwink-Sakurada equation were taken as 120000 and 0.71, respectively for polystyrene-toluene system at 30 °C [99].

APPENDIX B

CALCULATION OF VISCOSITY AVERAGE MOLECULAR WEIGHT OF POLYMER SYNTHESIZED USING BULK POLYMERIZATION TECHNIQUES

Flow time values of synthesized PS (BULK-sPS) dissolved in toluene with respect to concentration, and commercial PS (cPS) are tabulated in Tables B.1–B.4.

Table B.1 Flow times of BULK-sPS synthesized at a polymerization reaction time of 1.5 hrs.

Concentration (g/dl) Measurements	Time(s)				
	0	1	0.8	0.4	0.2
1	214	348	321	263	239
2	214	351	320	263	239
3	213	349	321	264	238
4	213	352	320	263	238
5	213	352	318	262	238
<i>Average</i>	<i>213.4</i>	<i>350.4</i>	<i>320</i>	<i>263</i>	<i>238.4</i>

Table B.2 Flow times of BULK-sPS synthesized at a polymerization reaction time of 3 hrs.

Concentration (g/dl) Measurements	Time(s)				
	0	1	0.8	0.4	0.2
1	214	386	341	273	242
2	214	387	346	273	243
3	213	386	342	277	243
4	213	390	345	277	243
5	213	389	344	274	240
<i>Average</i>	<i>213.4</i>	<i>387.6</i>	<i>343.6</i>	<i>274.8</i>	<i>242.2</i>

Table B.3 Flow times of BULK-sPS synthesized at a polymerization reaction time of 6 hrs.

Concentration (g/dl) Measurements	Time(s)				
	0	1	0.8	0.4	0.2
1	214	386	326	265	240
2	214	364	341	267	240
3	213	377	329	268	242
4	213	388	340	266	241
5	213	367	338	278	241
<i>Average</i>	<i>213.4</i>	<i>376.4</i>	<i>334.8</i>	<i>268.8</i>	<i>240.8</i>

Table B.4 Flow times of cPS.

Concentration (g/dl) Measurements	Time(s)				
	0	1	0.8	0.4	0.2
1	214	410	354	276	243
2	214	407	353	274	243
3	213	411	355	278	243
4	213	411	357	276	243
5	213	422	357	278	243
<i>Average</i>	<i>213.4</i>	<i>412.2</i>	<i>355.2</i>	<i>276.4</i>	<i>243</i>

Same calculation procedure given in Appendix A was applied in order to calculate relative (η_r) and specific (η_{sp}) viscosities of solutions. Then, reduced (η_{red}) and inherent (η_{inh}) viscosities were determined. Calculated viscosities of solutions are given in Tables B.5-B.8.

Table B.5 Calculated viscosities of BULK-sPS synthesized at a polymerization reaction time of 1.5 hrs.

Concentration (g/dl)	1	0.8	0.4	0.2
Viscosities				
η_r	1.641	1.499	1.232	1.117
η_{sp}	0.641	0.499	0.232	0.117
η_{red} (dl/g)	0.641	0.624	0.575	0.585
η_{inh} (dl/g)	0.495	0.506	0.517	0.553

* Average time values given in Table B.1 are used.

Table B.6 Calculated viscosities of BULK-sPS synthesized at a polymerization reaction time of 3 hrs.

Concentration (g/dl)	1	0.8	0.4	0.2
Viscosities				
η_r	1.816	1.610	1.287	1.134
η_{sp}	0.816	0.610	0.287	0.134
η_{red} (dl/g)	0.815	0.756	0.712	0.658
η_{inh} (dl/g)	0.596	0.590	0.626	0.617

* Average time values given in Table B.2 are used.

Table B.7 Calculated viscosities of BULK-sPS synthesized at a polymerization reaction time of 6 hrs.

Concentration (g/dl)	1	0.8	0.4	0.2
Viscosities				
η_r	1.763	1.568	1.259	1.128
η_{sp}	0.763	0.568	0.259	0.128
η_{red} (dl/g)	0.763	0.711	0.644	0.641
η_{inh} (dl/g)	0.567	0.562	0.572	0.603

* Average time values given in Table B.3 are used.

Table B.8 Calculated viscosities of cPS.

Concentration (g/dl)	1	0.8	0.4	0.2
Viscosities				
η_r	1.931	1.664	1.295	1.138
η_{sp}	0.931	0.664	0.295	0.138
η_{red} (dl/g)	0.930	0.822	0.732	0.676
η_{inh} (dl/g)	0.657	0.631	0.641	0.633

* Average time values given in Table B.4 are used.

Reduced and inherent viscosity values of polymer solutions as a function of concentration is plotted in Figures B.1-B.4.

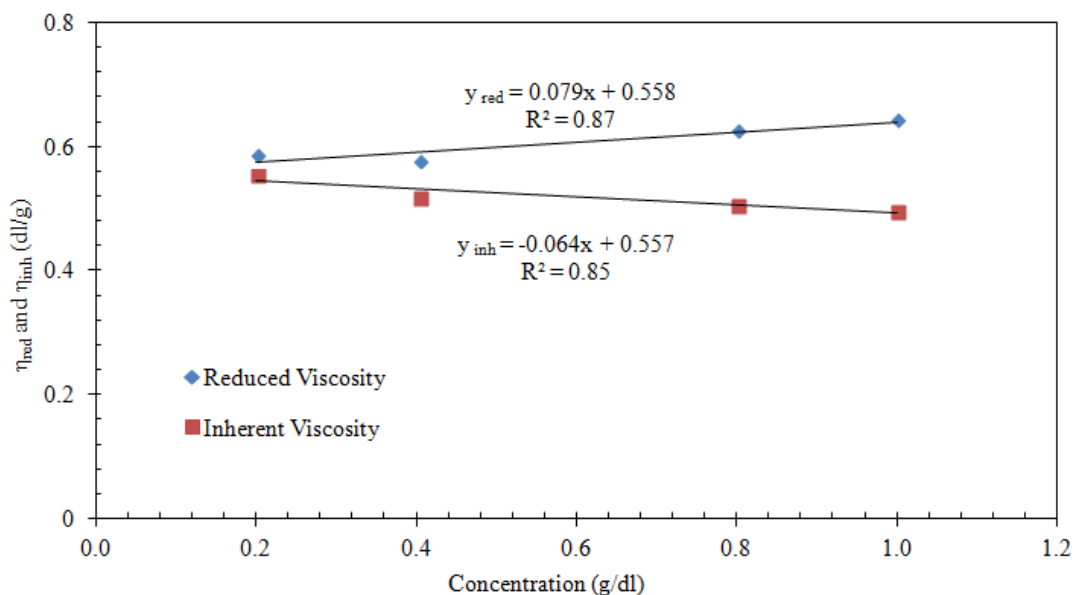


Figure B.1 Variation of reduced and inherent viscosities of BULK-sPS synthesized at a reaction time of 1.5 hrs with respect to concentration.

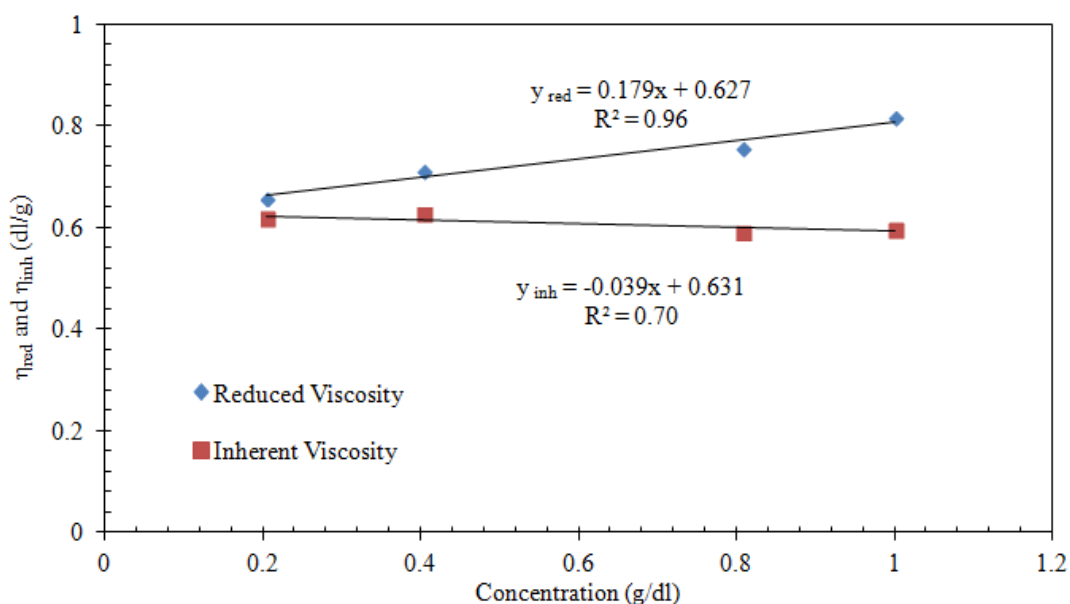


Figure B.2 Variation of reduced and inherent viscosities of BULK-sPS synthesized at a reaction time of 3 hrs with respect to concentration.

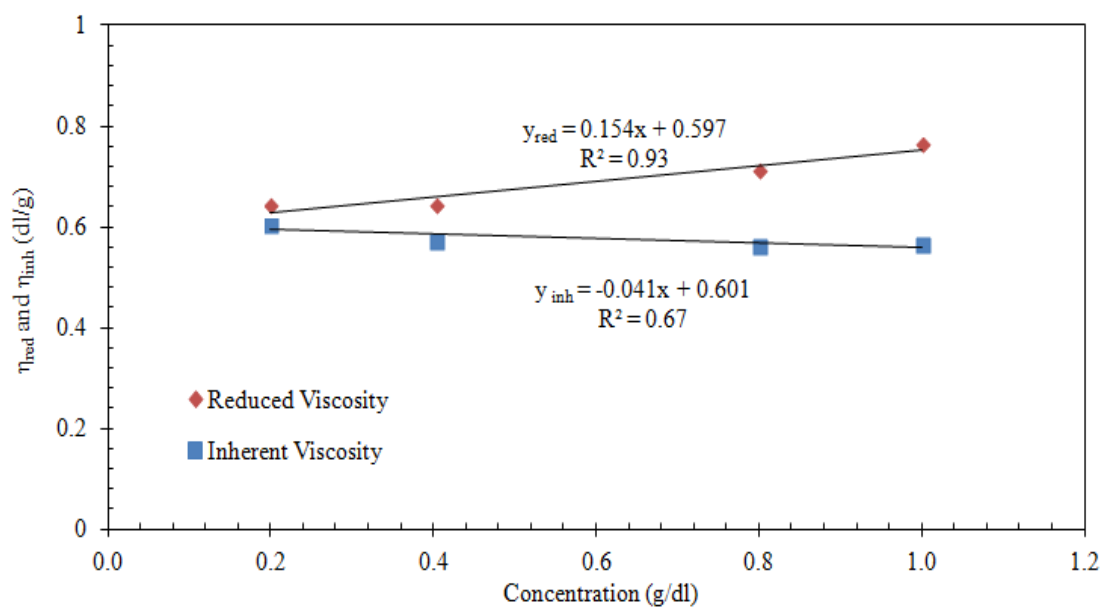


Figure B.3 Variation of reduced and inherent viscosities of BULK-sPS synthesized at reaction time of 6 hrs with respect to concentration.

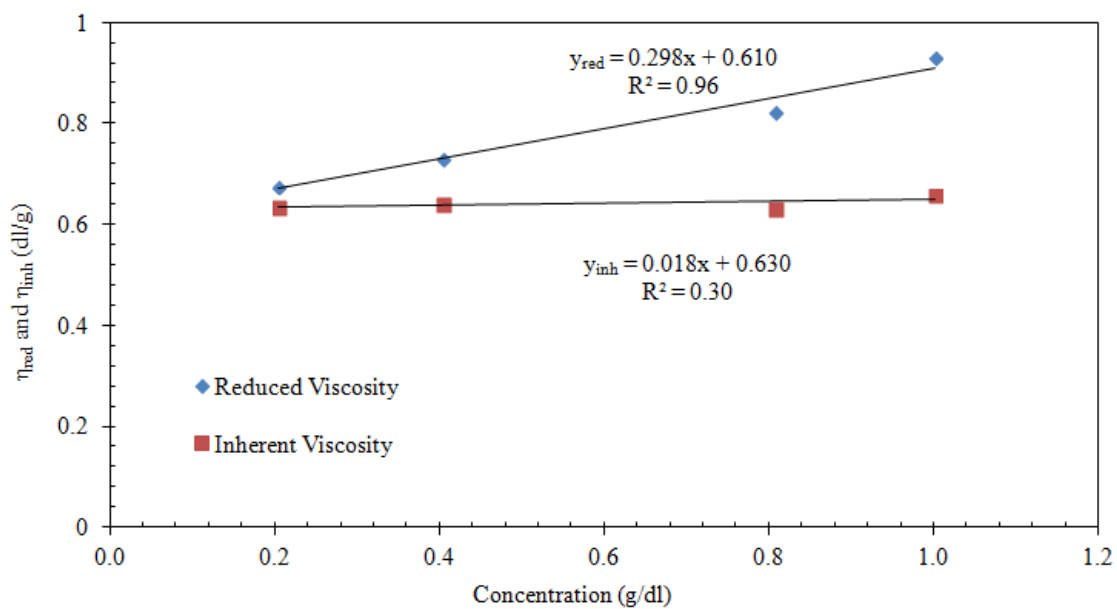


Figure B.4 Variation of cPS with respect to concentration.

Same procedure given in Appendix A was used in order to calculate intrinsic viscosity and then viscosity average molecular weight of BULK-sPS synthesized at different polymerization reaction time and cPS.

Flow times of synthesized PS (BULK-sPS) dissolved in toluene with respect to concentration are tabulated in Tables B.9–B.11.

Table B.9 Flow times of BULK-sPS synthesized using 0.03 mol/L initiator concentration.

Concentration (g/dl)	Time(s)				
	0	1	0.8	0.4	0.2
Measurements					
1	214	407	358	277	243
2	214	411	358	276	242
3	213	421	371	277	243
4	213	420	368	276	242
5	213	419	357	279	247
<i>Average</i>	<i>213.4</i>	<i>415.6</i>	<i>362.4</i>	<i>277</i>	<i>243.4</i>

Table B.10 Flow times of BULK-sPS synthesized using 0.02 mol/L initiator concentration.

Concentration (g/dl) Measurements	Time(s)				
	0	1	0.8	0.4	0.2
1	214	425	375	279	245
2	214	428	384	278	244
3	213	417	373	278	244
4	213	437	386	279	243
5	213	427	386	279	244
<i>Average</i>	<i>213.4</i>	<i>426.8</i>	<i>380.8</i>	<i>278.6</i>	<i>244</i>

Table B.11 Flow times of BULK-sPS synthesized using 0.01 mol/L initiator concentration.

Concentration (g/dl) Measurements	Time(s)				
	0	1	0.8	0.4	0.2
1	214	428	381	289	247
2	214	428	385	289	247
3	213	429	396	293	247
4	213	429	385	292	247
5	213	429	393	291	247
<i>Average</i>	<i>213.4</i>	<i>428.6</i>	<i>388</i>	<i>290.8</i>	<i>247</i>

Calculated viscosities are tabulated in Tables B.12-B.14.

Table B.12 Calculated viscosities of BULK-SPS synthesized using 0.03 mol/L initiator concentration.

Concentration (g/dl)	1	0.8	0.4	0.2
Viscosities				
η_r	1.947	1.698	1.298	1.140
η_{sp}	0.947	0.698	0.298	0.140
η_{red} (dl/g)	0.946	0.866	0.738	0.686
η_{inh} (dl/g)	0.665	0.657	0.646	0.641

* Average time values given in Table B.9 are used.

Table B.13 Calculated viscosities of BULK-SPS synthesized using 0.02 mol/L initiator concentration.

Concentration (g/dl)	1	0.8	0.4	0.2
Viscosities				
η_r	2	1.784	1.305	1.143
η_{sp}	1	0.784	0.305	0.143
η_{red} (dl/g)	1	0.973	0.758	0.699
η_{inh} (dl/g)	0.693	0.718	0.661	0.653

* Average time values given in Table B.10 are used.

Table B.14 Calculated viscosities of BULK-SPS synthesized using 0.01 mol/L initiator concentration.

<div style="display: flex; justify-content: space-between;"> Concentration (g/dl) Viscosities </div>	1	0.8	0.4	0.2
η_r	2.008	1.818	1.362	1.157
η_{sp}	1.008	0.818	0.362	0.157
η_{red} (dl/g)	1.007	1.013	0.899	0.768
η_{inh} (dl/g)	0.696	0.740	0.767	0.713

* Average time values given in Table B.11 are used.

Reduced and inherent viscosity of polymer solutions is plotted in Figures B.5-B.7.

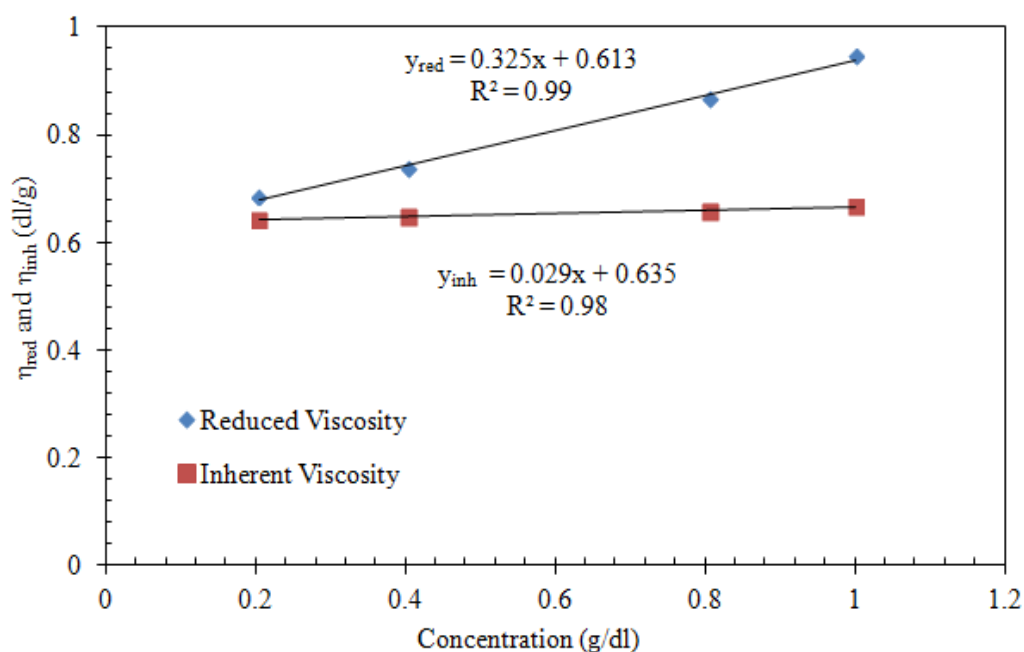


Figure B.5 Variation of reduced and inherent viscosities of BULK-sPS synthesized using 0.03 mol/L initiator concentration with respect to concentration.

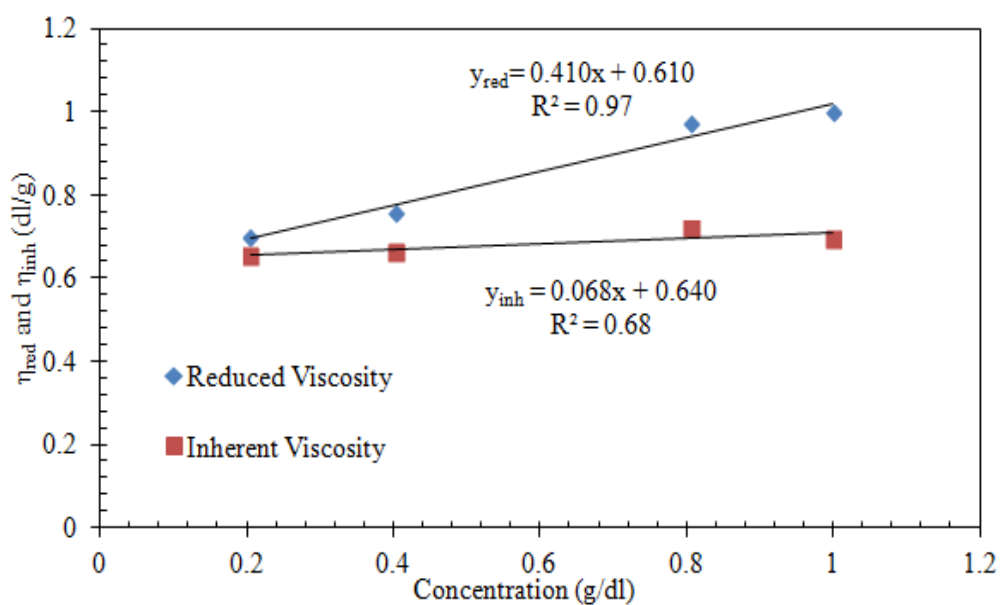


Figure B.6 Variation of reduced and inherent viscosities of BULK-sPS synthesized using 0.02 mol/L initiator concentration with respect to concentration.

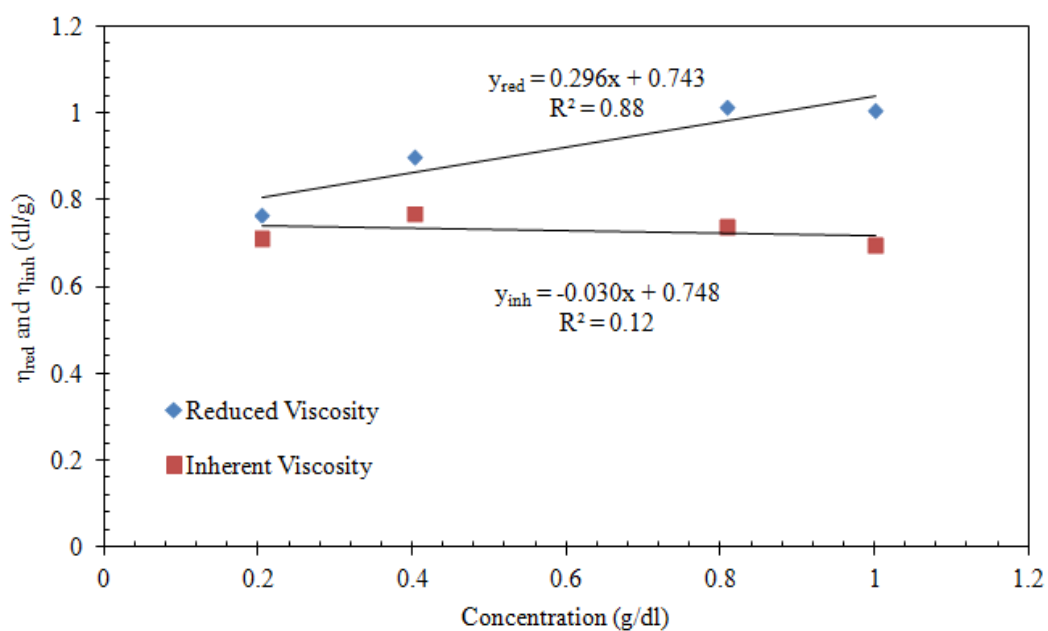


Figure B.7 Variation of reduced and inherent viscosities of BULK-sPS synthesized using 0.01 mol/L initiator concentration with respect to concentration.

Intrinsic viscosity and then viscosity average molecular weight of BULK-sPS synthesized using different AIBN concentrations were calculated with the help of Figures B.5-B.7 and Mark-Houwink-Sakurada equation.

APPENDIX C

MOLECULAR WEIGHT DISTRIBUTION CURVES

Molecular weight distribution curves of BULK-sPS synthesized using different initiator concentrations and cPS are given in Figures C.1 - C.4.

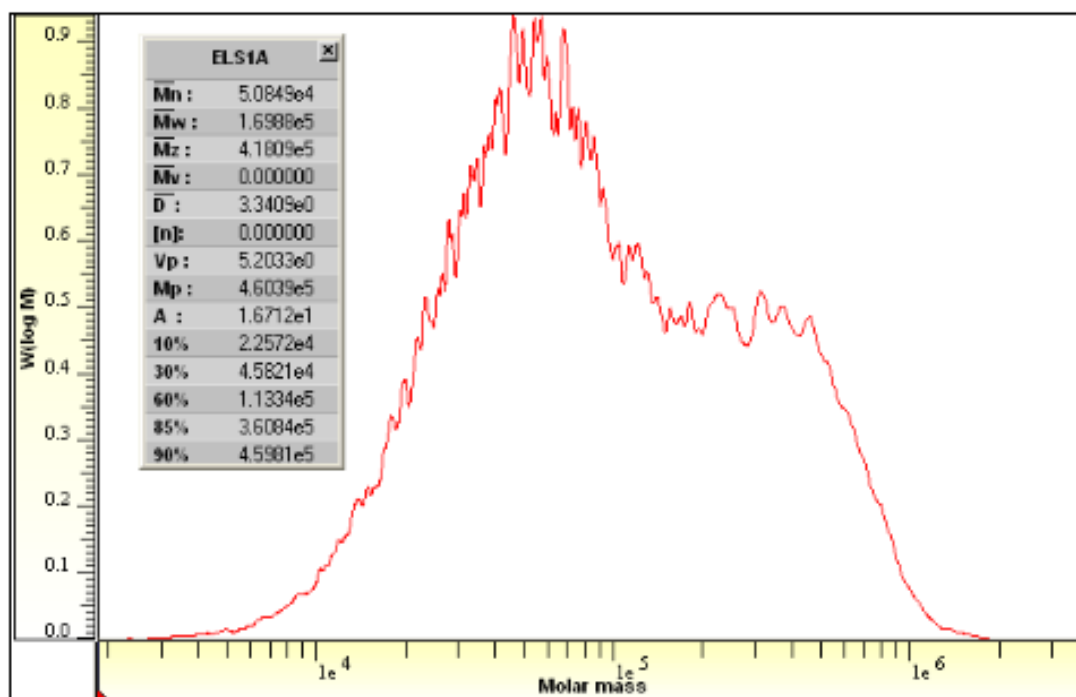


Figure C.1 Molecular weight distribution of BULK-sPS synthesized using an initiator concentration of 0.03 mol/L.

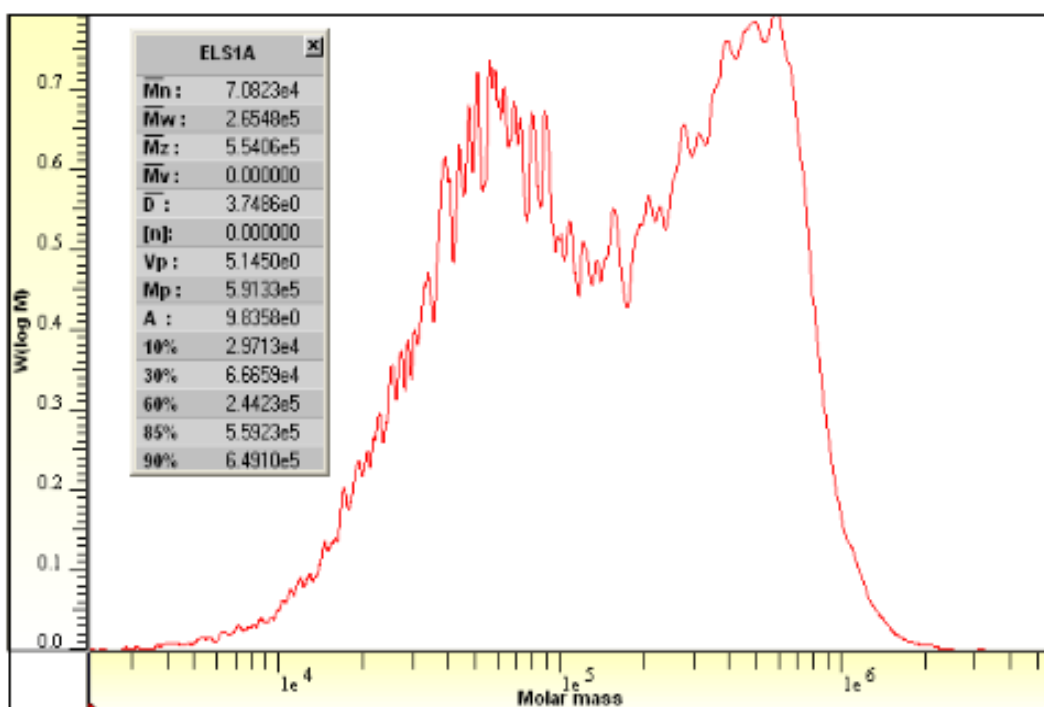


Figure C.2 Molecular weight distribution of BULK-sPS synthesized using an initiator concentration of 0.02 mol/L.

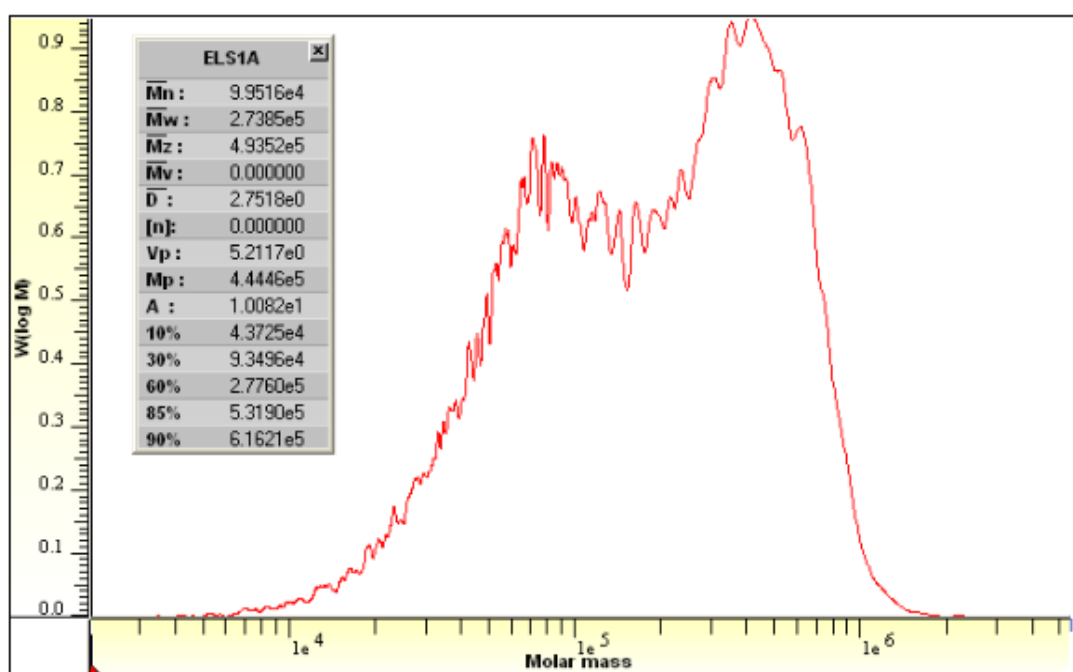


Figure C.3 Molecular weight distribution of BULK-sPS synthesized using an initiator concentration of 0.01 mol/L.

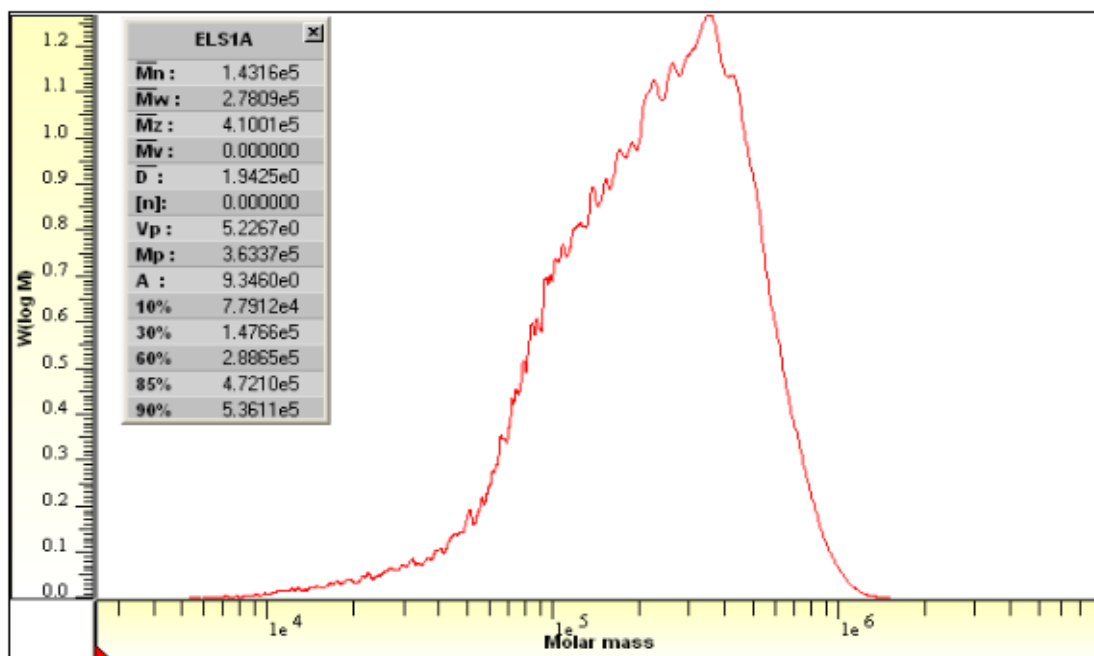


Figure C.4 Molecular weight distribution of cPS.

APPENDIX D

FTIR SPECTRA AND XRD RESULTS

FTIR spectra of polystyrene samples synthesized using the two different polymerization techniques are shown in Figures D.1-D.4 and FTIR spectrum of styrene monomer is given in Figure D.5.

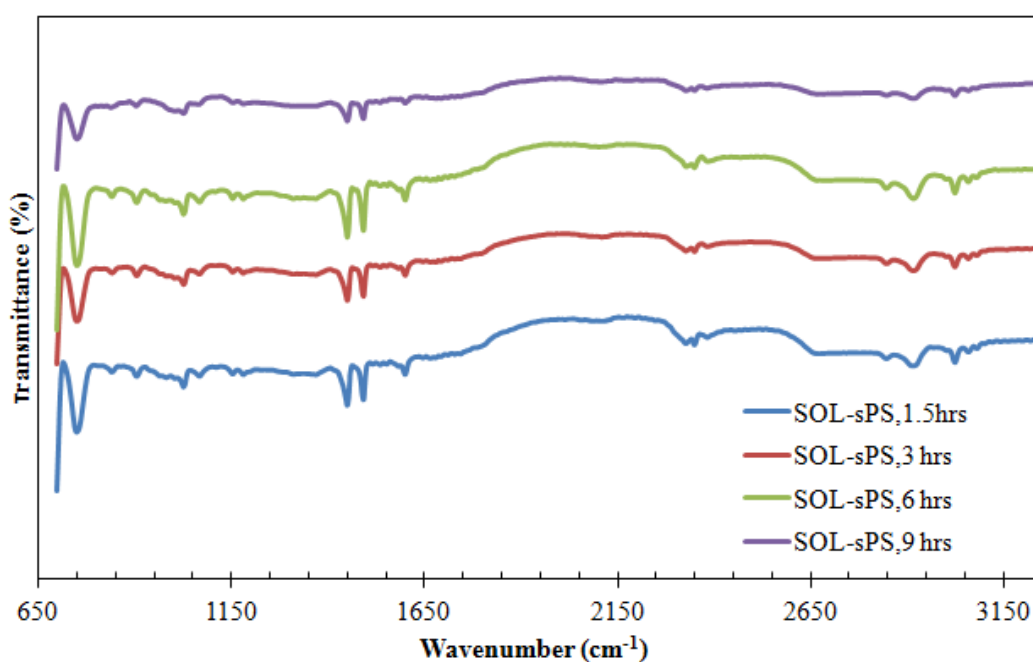


Figure D.1 FTIR spectra of SOL-sPS synthesized at different polymerization reaction times and temperature of 95 °C.

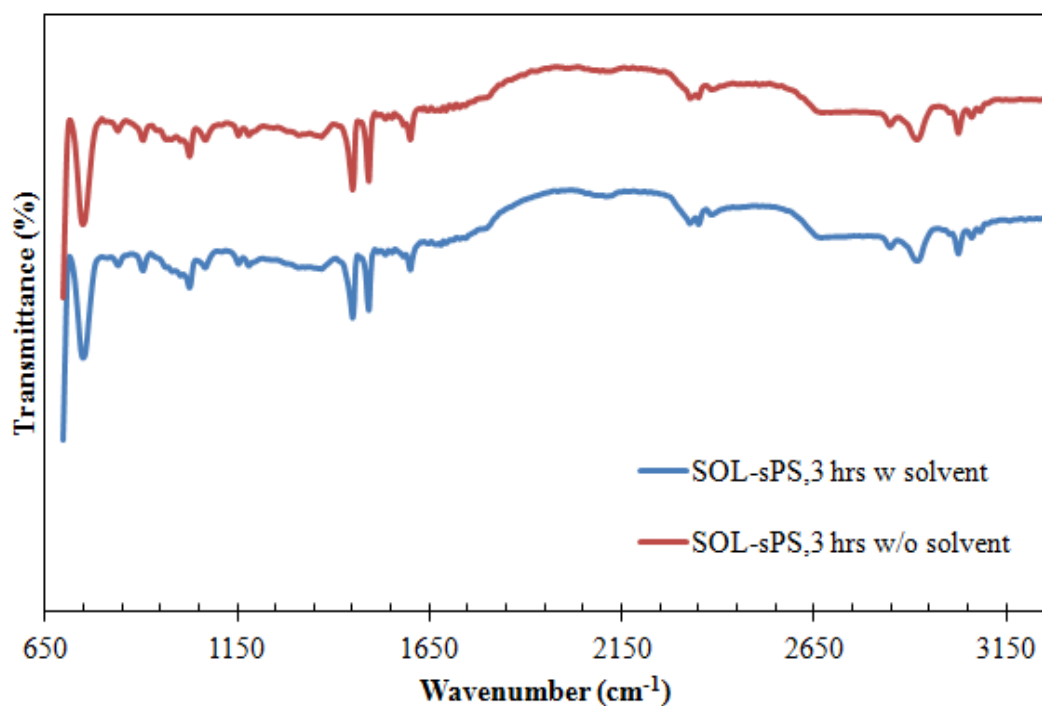


Figure D.2 FTIR spectra of SOL-sPS synthesized with and without solvent at 3 hrs polymerization reaction time and temperature of 95 °C.

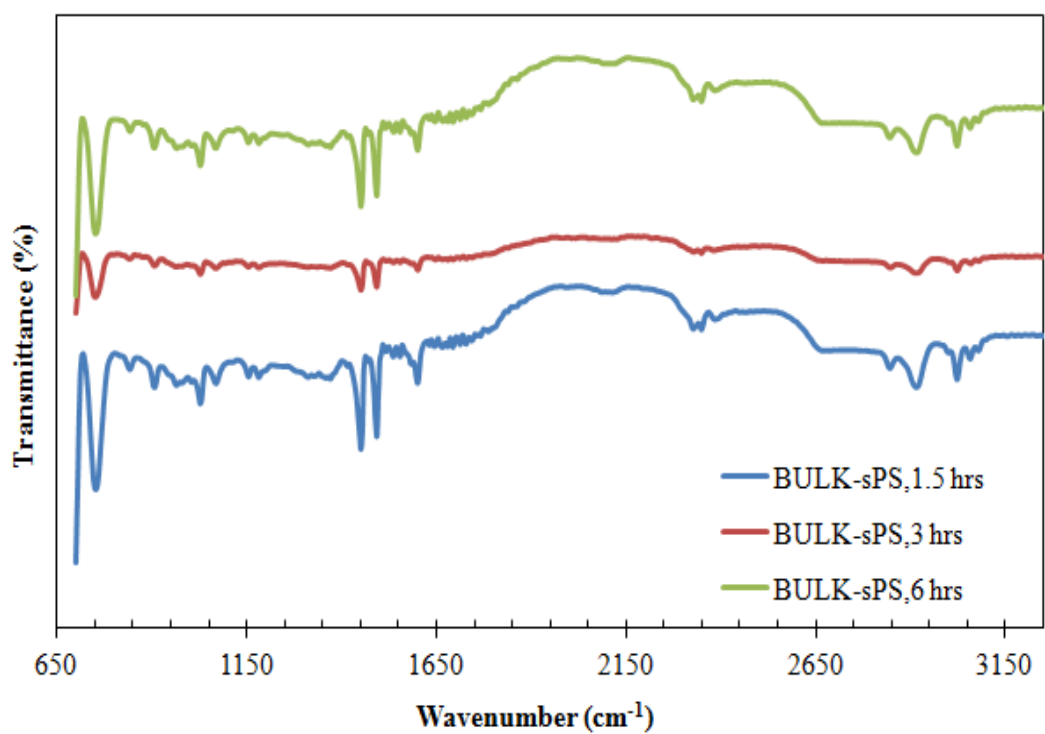


Figure D.3 FTIR spectra of BULK-sPS synthesized at different polymerization reaction times.

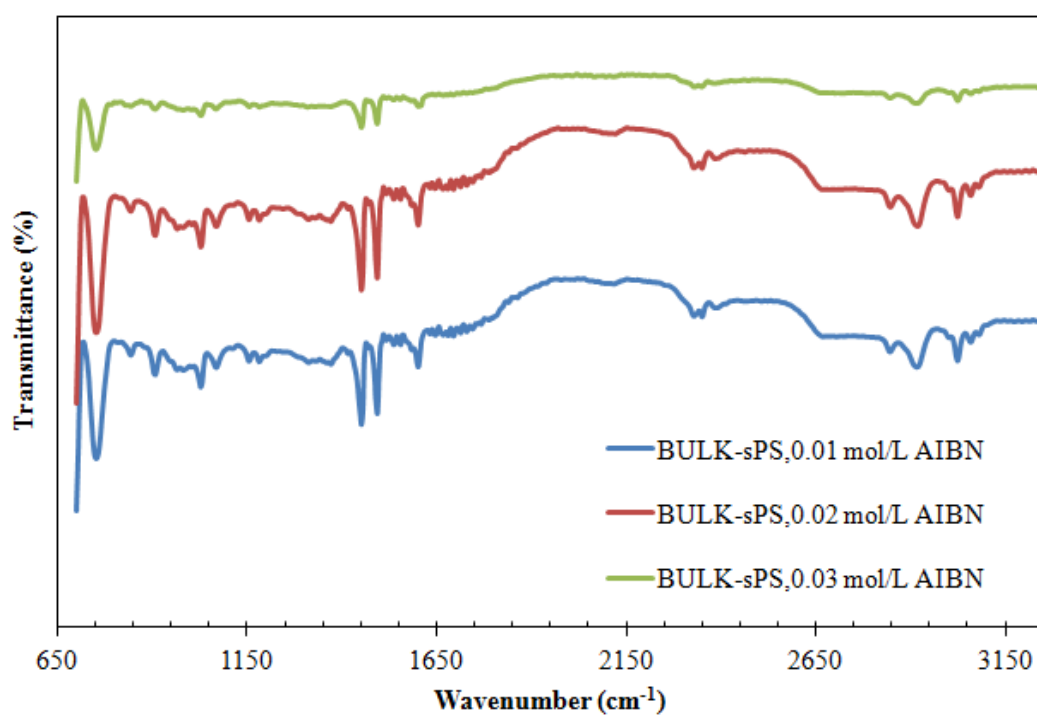


Figure D.4 FTIR spectra of BULK-sPS synthesized at different initiator (AIBN) concentrations.

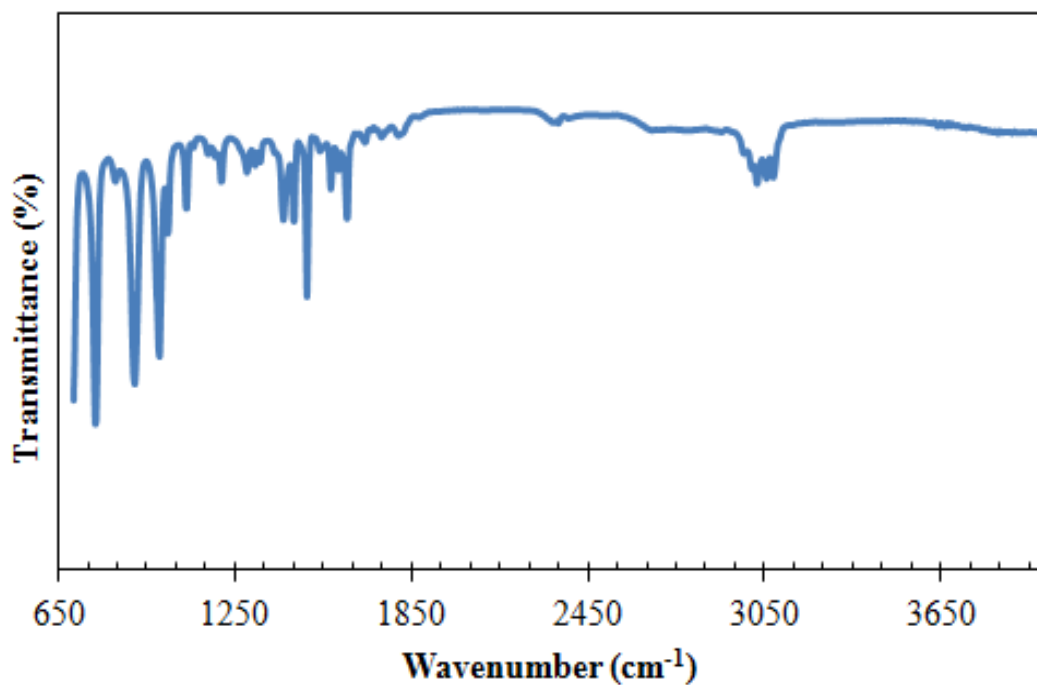


Figure D.5 FTIR spectrum of styrene monomer.

Figures D.6-D.9 represent XRD patterns of PS samples.

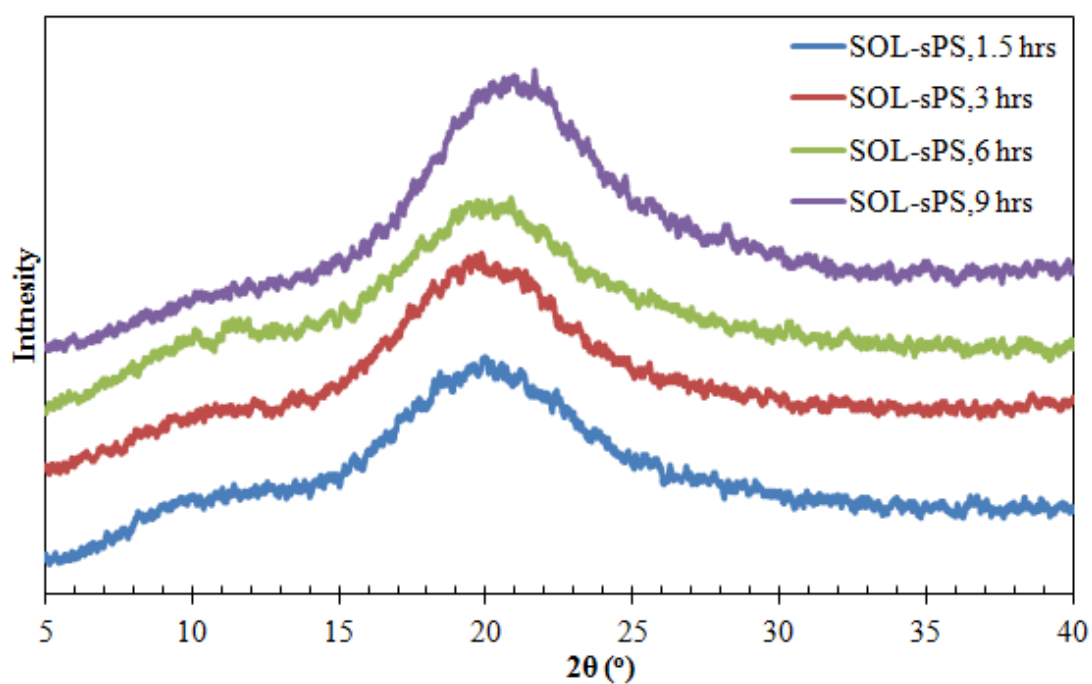


Figure D.6 XRD patterns of SOL-sPS synthesized at different polymerization reaction time and at temperature of 95 °C.

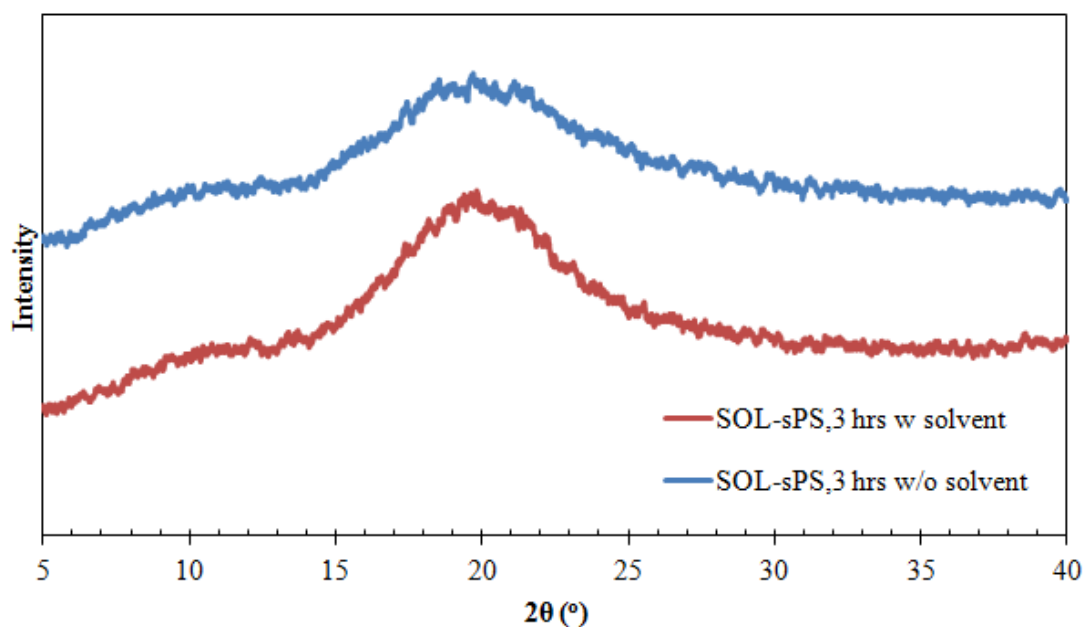


Figure D.7 XRD patterns of SOL-sPS synthesized with and without solvent at 3 hrs polymerization reaction time and at temperature of 95 °C.

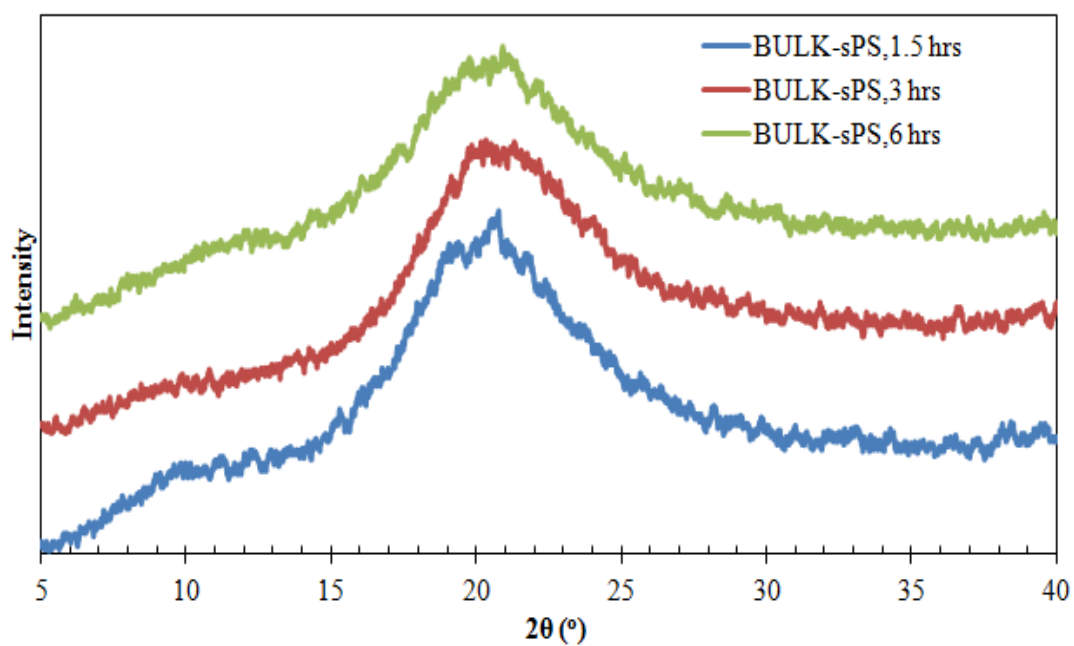


Figure D.8 XRD patterns of BULK-sPS synthesized at different polymerization reaction times.

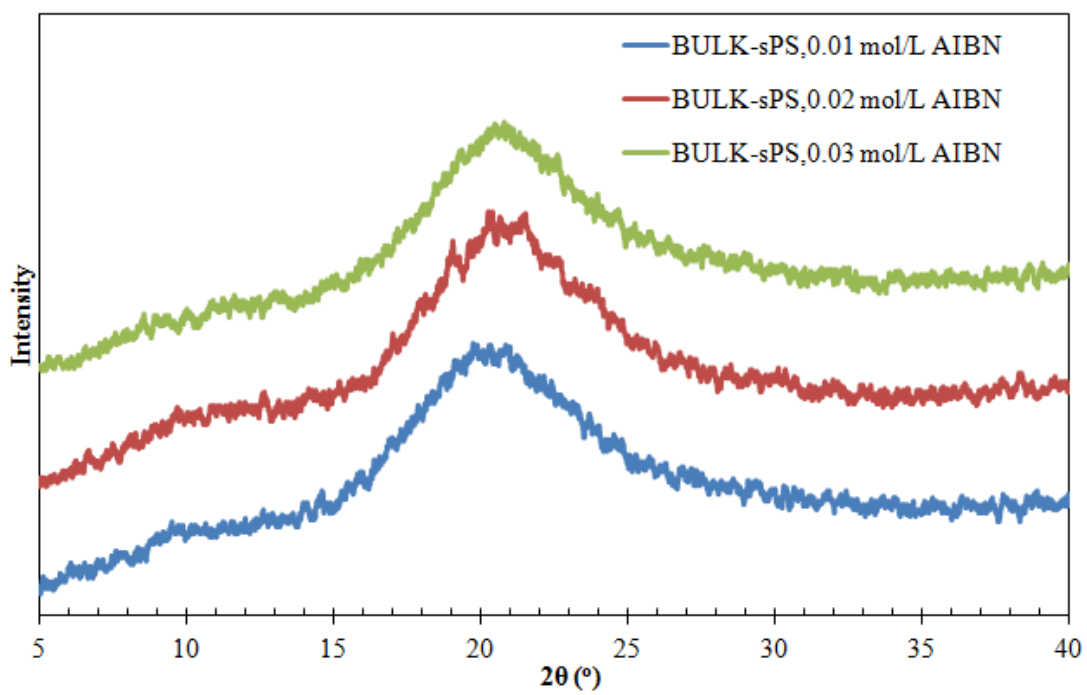


Figure D.9 XRD patterns of BULK-sPS synthesized at different initiator (AIBN) concentrations.

APPENDIX E

TENSILE AND IMPACT TEST RESULTS

Tables E.1 and E.2 show the tensile and impact test results of neat PS and PS-BNNT composites prepared in this study.

Table E.1 Tensile test results of neat PS and PS-BNNT composites.

Property Sample	Tensile Strength (MPa)	Young's Modulus (MPa)	Elongation at Break (%)
cPS	45.6 ± 1.7	1319 ± 130.4	5.4 ± 0.3
BULK-sPS	22.7 ± 2.9	1944 ± 85.6	2.0 ± 0.3
E-cPS	30.7 ± 4.4	1806 ± 108.7	3.8 ± 0.7
ME-PS	40.0 ± 4.2	1530 ± 182.0	4.4 ± 0.7
ME-PS + 0.5	45.4 ± 3.6	1318 ± 261.2	5.4 ± 0.8
ME-PS + 1.0	37.4 ± 4.3	1805 ± 176.5	3.7 ± 0.5
ME-PS + 3.0	36.5 ± 5.1	1451 ± 149.8	3.9 ± 0.7
ISP-PS + 0.5	32.5 ± 4.7	1803 ± 117.0	3.1 ± 0.4
E-cPS + 0.5	33.2 ± 3.9	1674 ± 92.1	3.6 ± 0.6

Table E.2 Impact strength values of neat PS and PS-BNNT composites.

Sample	Property	Impact Strength (kJ/m²)
cPS		6.7 ± 0.5
BULK-sPS		6.5 ± 0.2
E-cPS		10.8 ± 0.7
ME-PS		7.4 ± 0.5
ME-PS + 0.5		10.2 ± 1.0
ME-PS + 1.0		6.8 ± 0.2
ME-PS + 3.0		3.8 ± 1.0
ISP-PS + 0.5		4.4 ± 0.9
E-cPS + 0.5		6.5 ± 0.2

APPENDIX F

REPRESENTATIVE STRESS-STRAIN CURVES

Representative stress-strain curves of neat PS and PS-BNNT composites are shown in Figures F.1 - F.9.

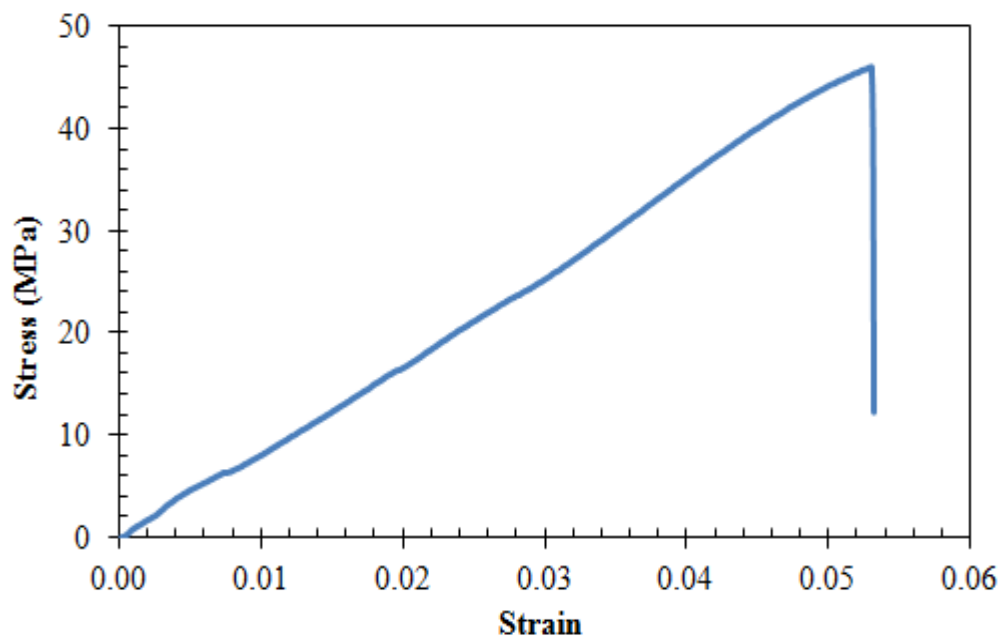


Figure F.1 Representative stress-strain curve for cPS.

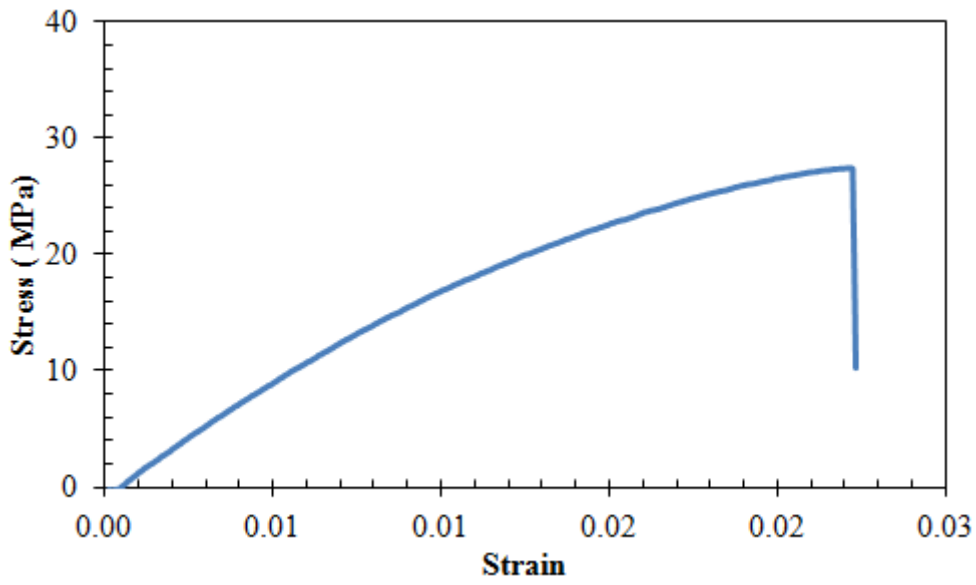


Figure F.2 Representative stress-strain curve for BULK-sPS.

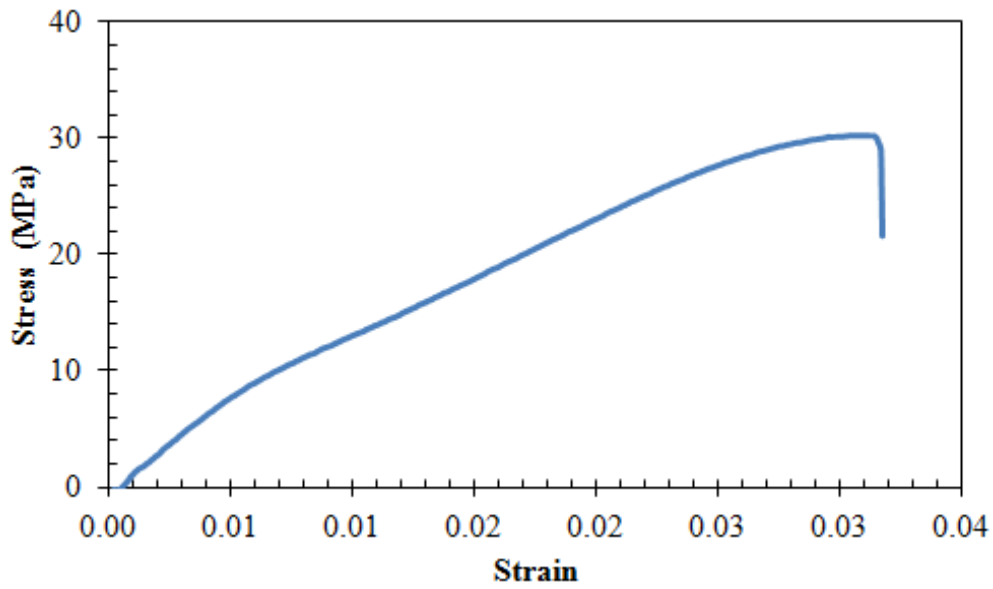


Figure F.3 Representative stress-strain curve for E-cPS.

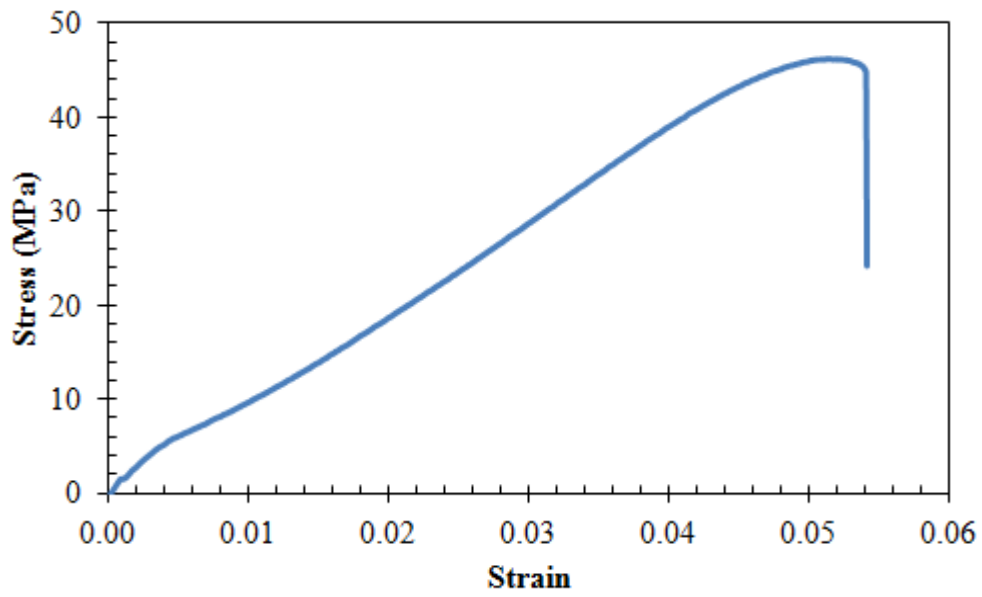


Figure F.4 Representative stress-strain curve for ME-PS.

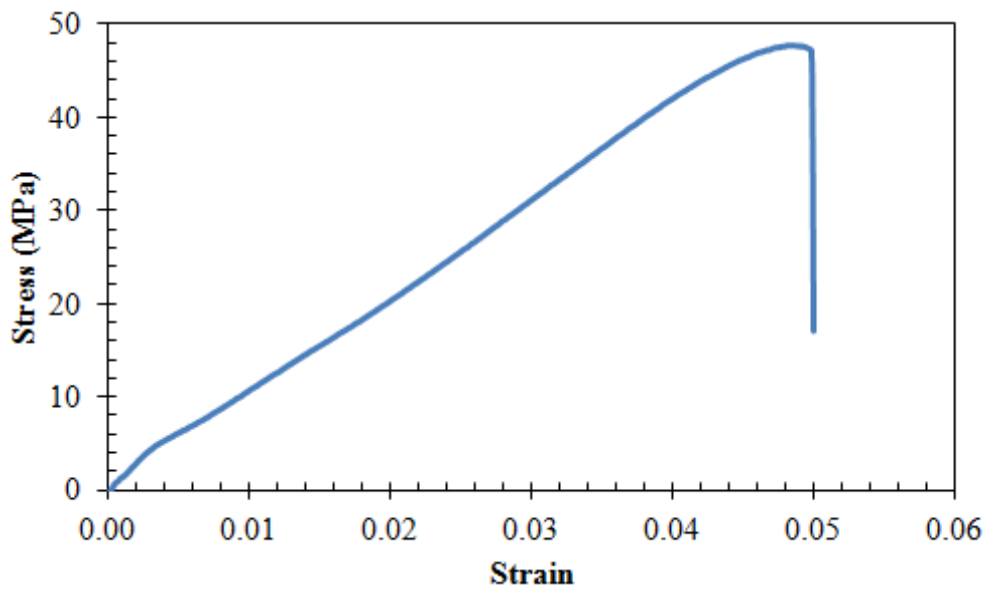


Figure F.5 Representative stress-strain curve for ME-PS+0.5.

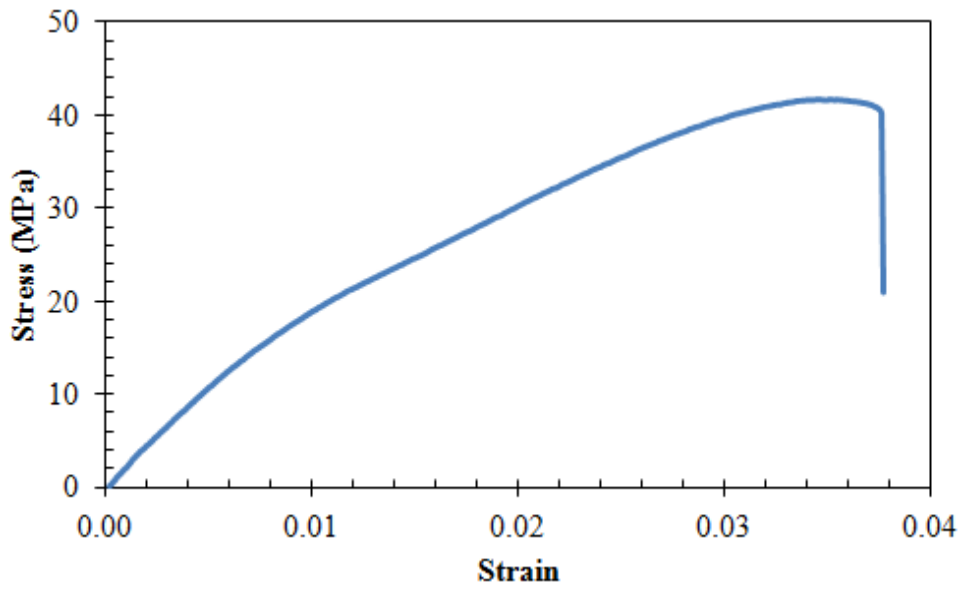


Figure F.6 Representative stress-strain curve for ME-PS+1.0.

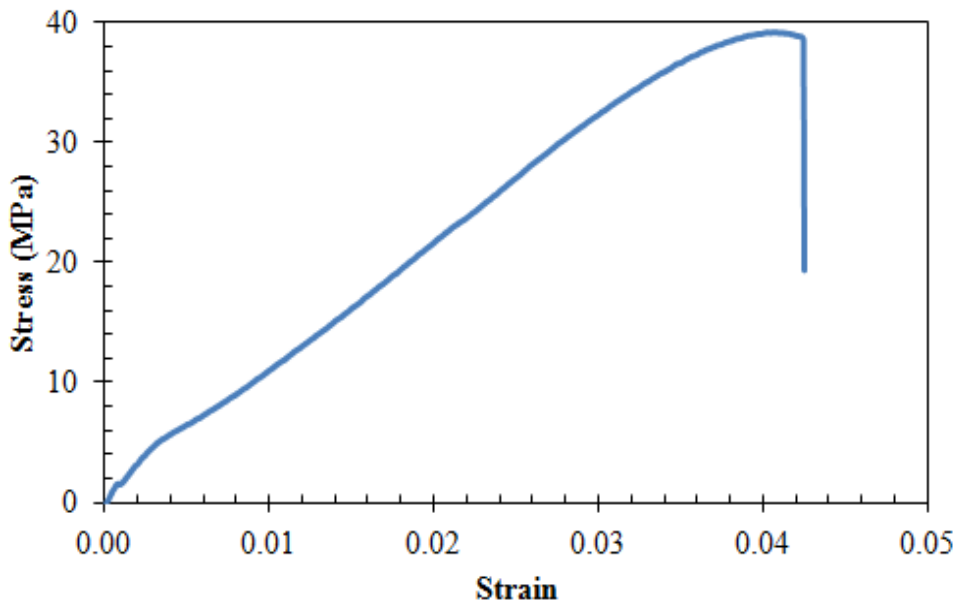


Figure F.7 Representative stress-strain curve for ME-PS+3.0.

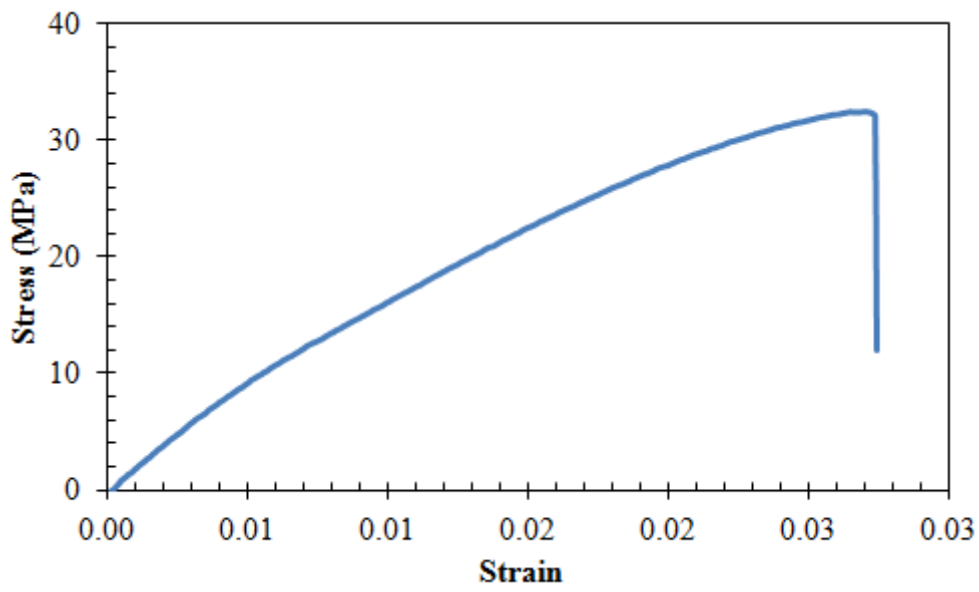


Figure F.8 Representative stress-strain curve for ISP-PS+0.5.

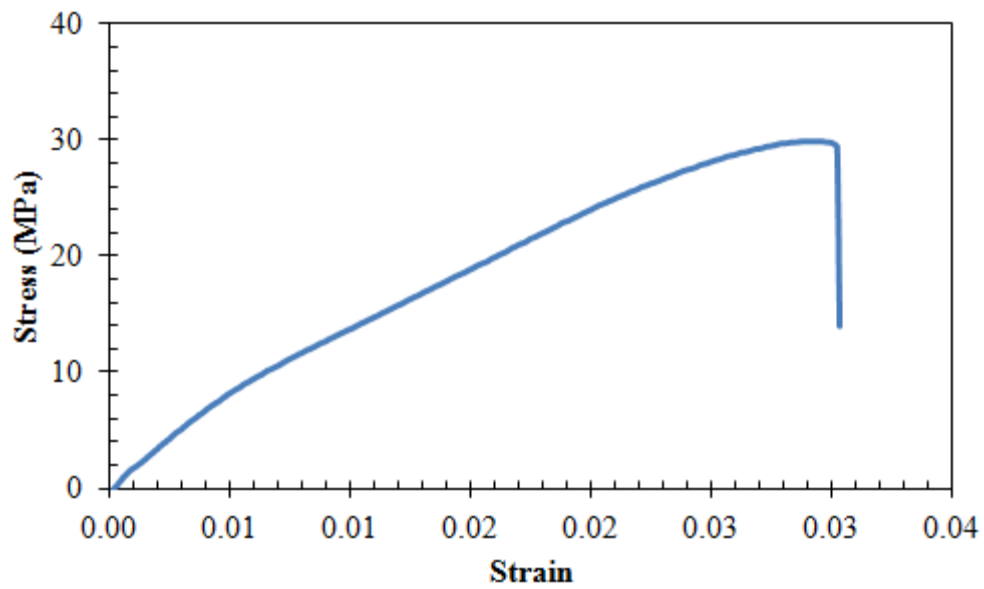


Figure F.9 Representative stress-strain curve for E-cPS+0.5.

APPENDIX G

DIFFERENTIAL SCANNING CALORIMETRY RESULTS

DSC thermogram of neat PS and PS-BNNT composites are shown in Figures G.1-G.9.

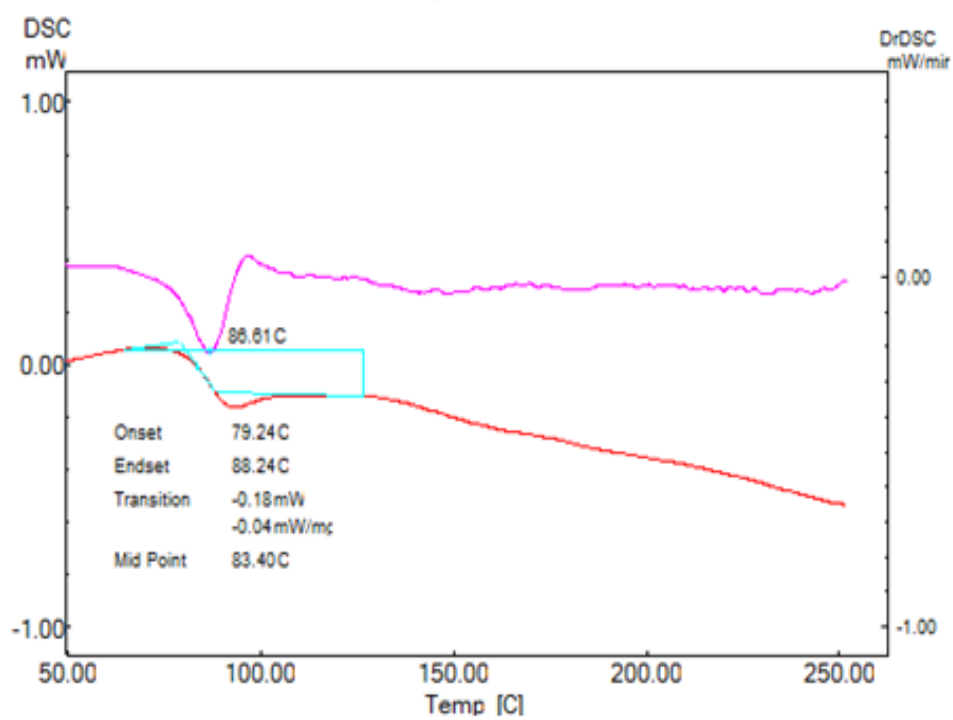


Figure G.1 DSC thermogram of cPS.

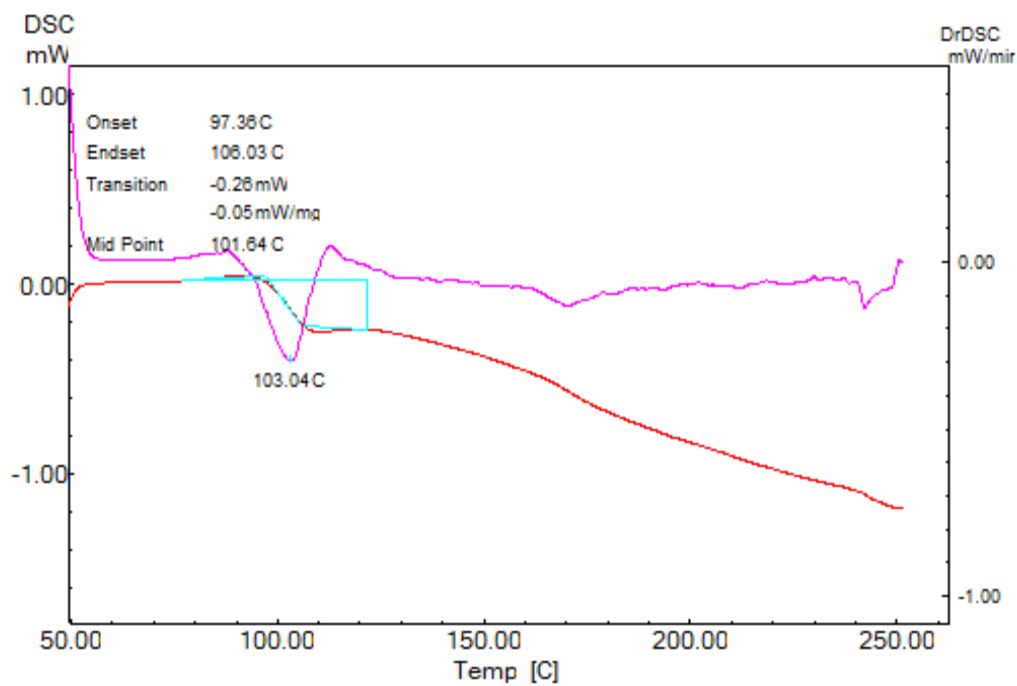


Figure G.2 DSC thermogram of BULK-sPS.

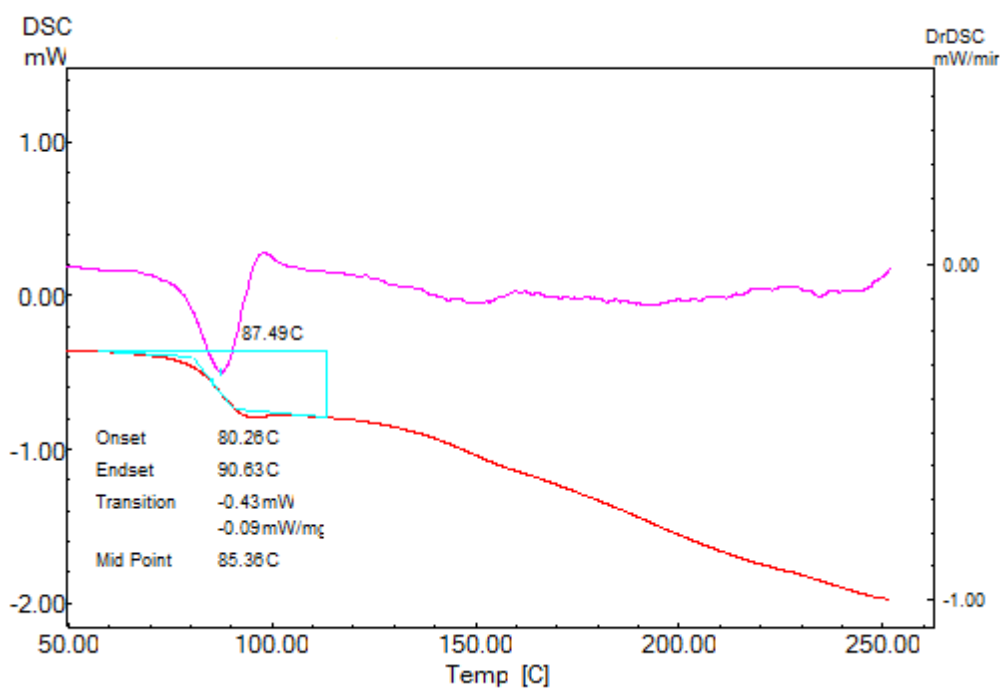


Figure G.3 DSC thermogram of E-cPS.

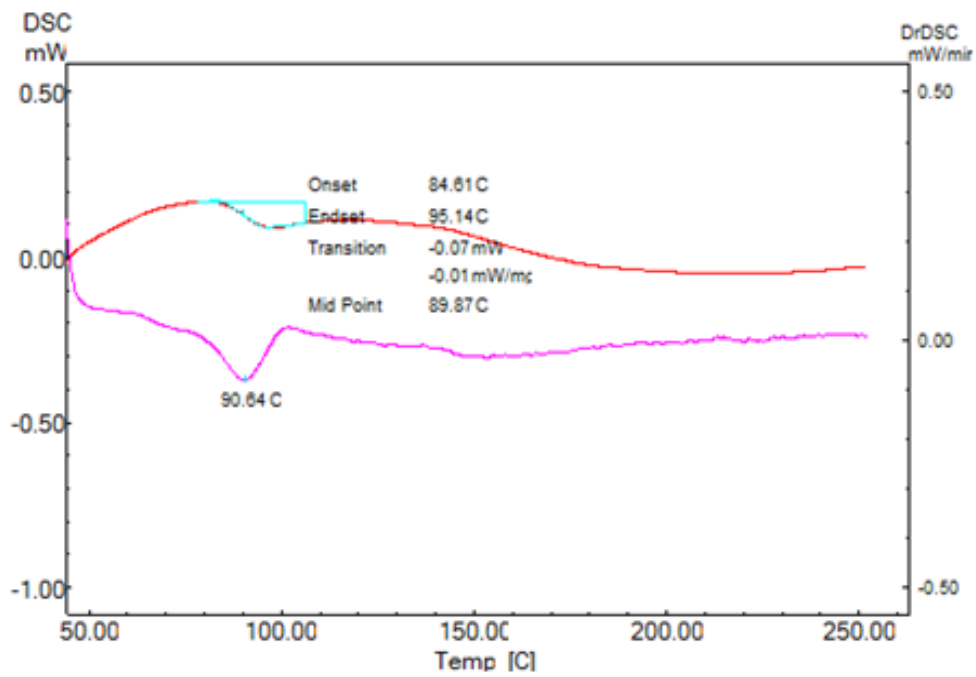


Figure G.4 DSC thermogram of ME-PS.

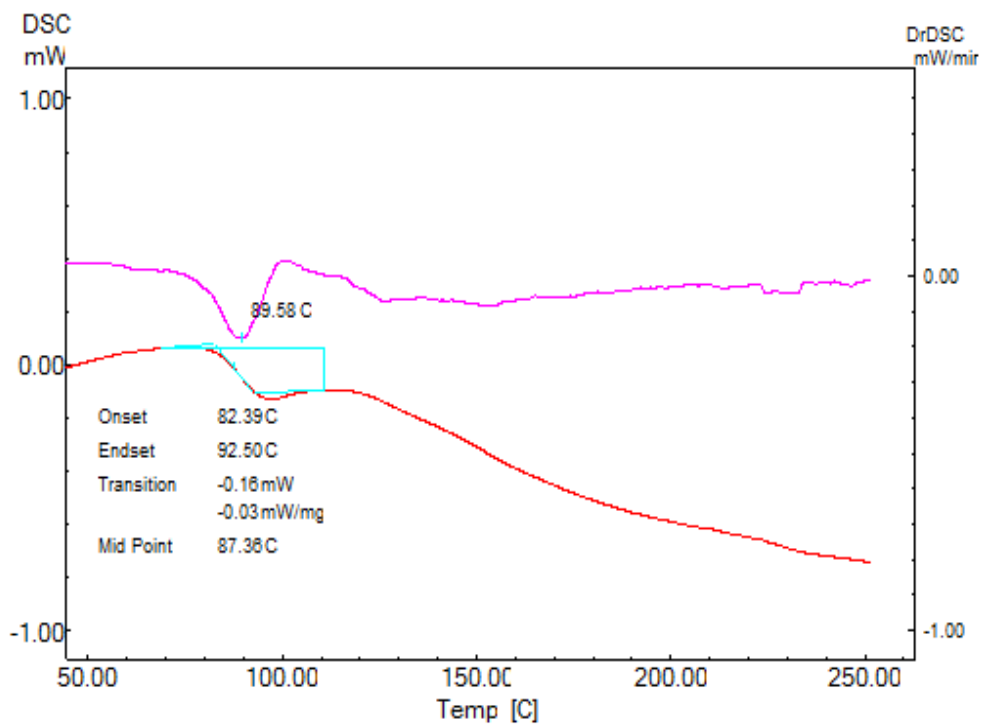


Figure G.5 DSC thermogram of ME-PS+0.5.

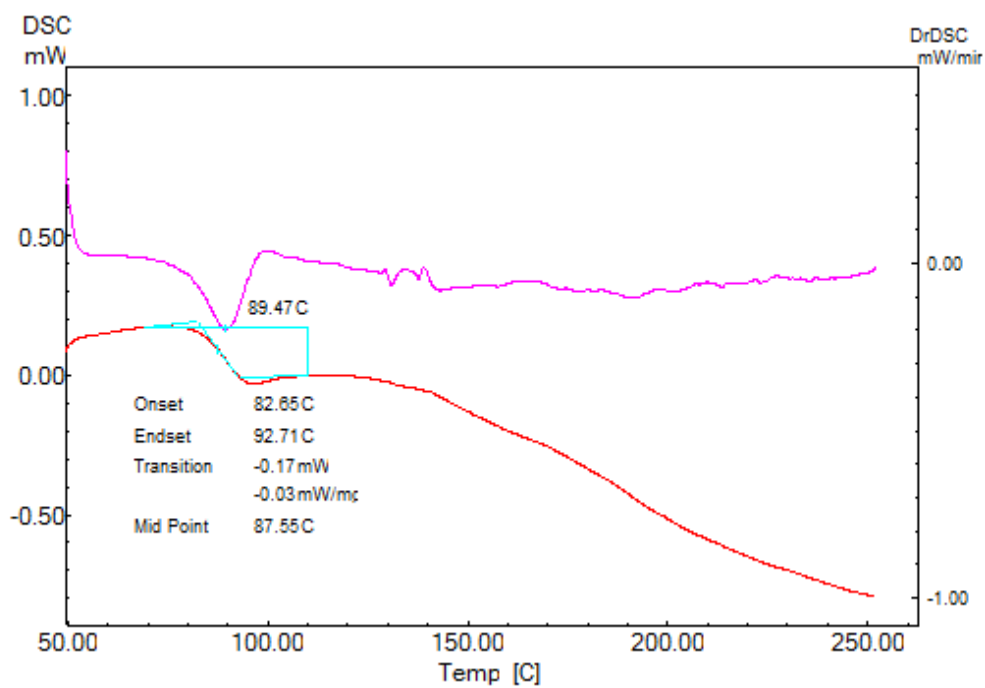


Figure G.6 DSC thermogram of ME-PS+1.0.

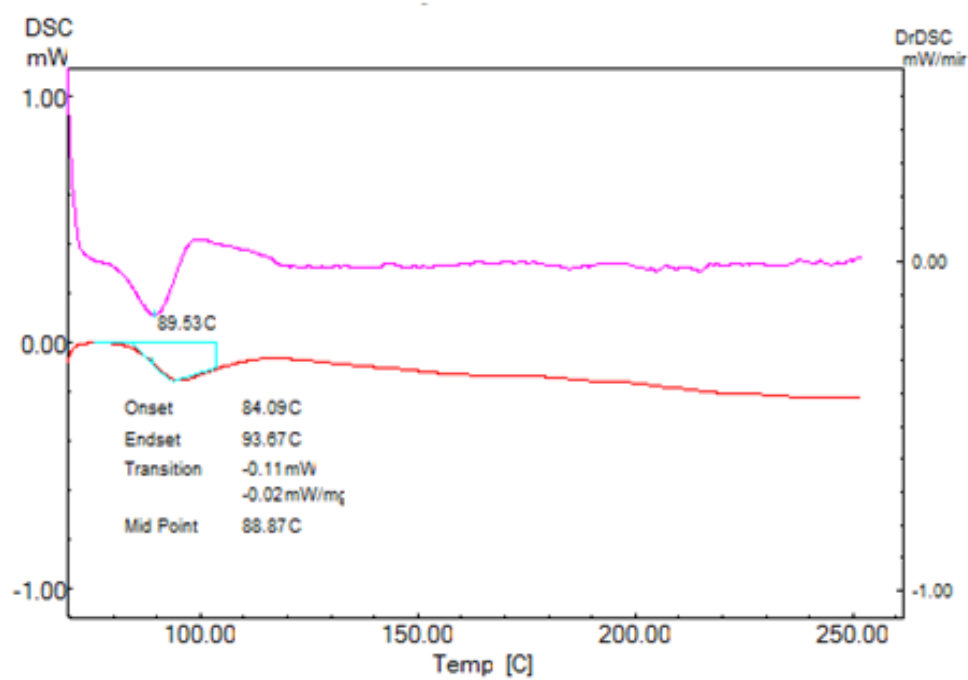


Figure G.7 DSC thermogram of ME-PS+3.0.

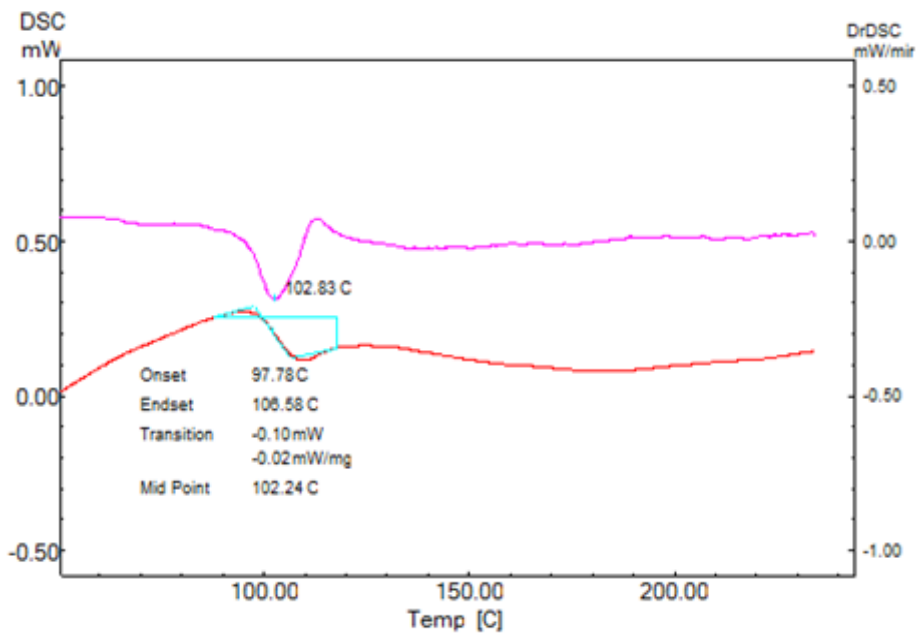


Figure G.8 DSC thermogram of ISP-PS+0.5.

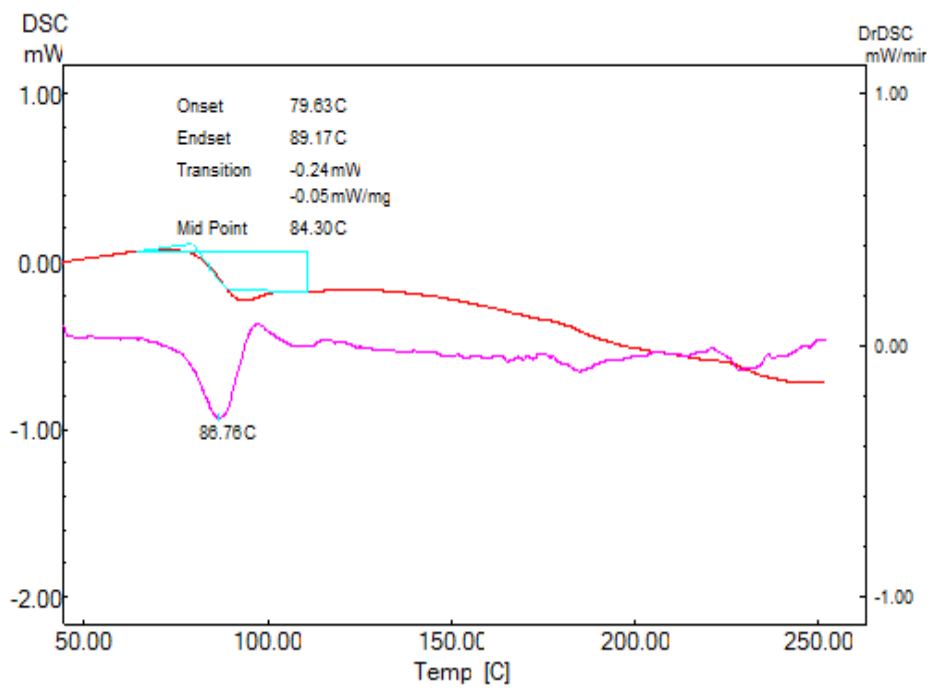


Figure G.9 DSC thermogram of E-cPS+0.5.